UNIVERSITÀ DEGLI STUDI DI TRIESTE

__XXVIII___CICLO DEL DOTTORATO DI RICERCA IN

ENVIRONMENTAL AND INDUSTRIAL FLUID MECHANICS

MEDITERRANEAN THERMOHALINE PROPERTIES AND LARGE-SCALE CLIMATIC PATTERNS

Settore scientifico-disciplinare: **GEO/12**

DOTTORANDO / A
LALEH SHABRANG

COORDINATORE
PROF. VINCENZO ARMENIO

SUPERVISORE DI TESI
PROF. MIROSLAV GACIC

ANNO ACCADEMICO 2014 / 2015

Abstract

The link between wintertime variations of the large-scale climatic indices and thermohaline properties of the Mediterranean Sea was studied using correlation coefficients and the difference of the patterns between positive and negative modes. North Atlantic Oscillation (NAO), East Atlantic (EA) pattern and Mediterranean Oscillation (MO) were considered as the climatic patterns.

Stronger heat loss in the Western Mediterranean during the negative NAO mode is associated with intensification of the winter convection, and consequently, the presence of the colder and saltier water in this sub-basin. Therefore, negative NAOI (North Atlantic Oscillation Index) provides a more suitable condition for the Western Mediterranean Deep Water Formation. On the other hand, lower temperature is revealed in the Eastern Mediterranean during NAOI+ due to the enhancement of heat loss. However, lower salinity in the eastern basin during the positive phase cannot be explained by the atmospheric forcing and it is probably due to the internal mechanisms. In addition, high NAOI is associated with less precipitation as well as lower sea level height in the major portion of the basin. However, some differences in the relationship between NAOI and oceanographic conditions in the Mediterranean sub-basins have also been evidenced. More specifically, the sea level in the North Ionian gyre is not influenced by NAO. Variations of temperature and salinity in the West Alboran Sea are opposite of what is observed in the rest of the Western Mediterranean. In addition, the warmer water in the eastern coasts of the Sicily during the NAOI+ is not related to the surface heat fluxes, and NAO reveals a weak impact on the upper layer temperature and salinity of the Adriatic Sea.

Unlike NAO which has the strong impact on the thermohaline characteristics of the entire basin, the influences of two other indices are limited to the smaller areas. In other words, the effects of EA is more evidenced in the western basin and MO reveals the strong impacts on the thermohaline properties of the Eastern Mediterranean. More specifically, positive EAI (East Atlantic Index) is associated with the warmer and lower salinity water in the Western Mediterranean while the negative mode is characterized by the stronger buoyancy loss due to the heat loss intensification and provides more favourable conditions for the Western Mediterranean

Deep Water Formation. Furthermore, during high MO stronger heat loss reduces the temperature of the eastern basin. However, due to additional impact of the internal oceanic processes, the effects of the climatic patterns on the salinity of the Eastern Mediterranean are not considerable.

Table of contents

List of Abbreviations:

4D-Var…….4-Dimensional Variational analysis

ADT…….Absolute Dynamic Topography

AGV…….Absolute Geostrophic Velocity

AMO……Atlantic Multi-decadal Oscillation

AW……...Atlantic Water

BiOS…….Bimodal Oscillating System

CCMP……...Cross-Calibrated, Multi-Platform

CIW……..Cretan Intermediate Water

CTD……..Conductivity-Temperature-Depth

DW……Deep Water

DWF……..Deep Water Formation

E……Evaporation

EA pattern…….East Atlantic pattern

EAI……East Atlantic Index

EA/WR…….East Atlantic/West Russian pattern

ECMWF……European Centre for Medium-Range Weather Forecasts

EMDWF……Eastern Mediterranean Deep Water Formation

EMED……Eastern Mediterranean

EMT……...Eastern Mediterranean Transient

EOF……Empirical Orthogonal Function

JFM……....January-February-March

LIW……Levantine Intermediate Water

MO…….....Mediterranean Oscillation

MOI……Mediterranean Oscillation Index

NAO…….....North Atlantic Oscillation

NAOI …… North Atlantic Oscillation Index

NEMO-OPA ….Nucleus for European Modelling of the Ocean-Ocean Parallelise

NetCDF……..Network Common Data Format

NH……..Northern Hemisphere

NIG…….North Ionian Gyre

NOAA…….National Oceanic and Atmospheric Administration

OA-SST……...Objective Analyses-Sea Surface Temperature

OGCM ……Ocean General Circulation Model

P……...Precipitation

PC……Principal Components

PNA…….Pacific/ North American

REMSS……Remote Sensing Systems

RPCA……...Rotated Principal Component Analysis

SAG…….South Adriatic Gyre

SAP……..South Adriatic Pit

SCAN……...Scandinavian pattern

SLP……...Sea Level Pressure

SST……...Sea Surface Temperature

TNH…….Tropical Northern Hemisphere

VAM……Variational Analysis Method

VOS XBT……Voluntary Observing Ship-eXpandable Bathythermograph

WMED……Western Mediterranean

Acknowledgement

I would like to express my special appreciation to my enthusiastic supervisor Prof. Miroslav Gačić. Working with him has been a wonderful experience not only for his tremendous academic support which has allowed me to grow as a research scientist, but also for his relaxed demeanor which made a good working relationship and impetus for me. I am also hugely appreciative to Giuseppe Civitarese, Milena Menna, Vedrana Kovacevic, and Vanessa Cardin for sharing their expertise in the ocean science so willingly.

A special thanks to my family who are the most important people in my world and I dedicate this thesis to them. Words cannot express how grateful I am to my mother, and father for all of the sacrifices that they've made on my behalf. Special mention goes to my beloved husband, Anton, for his unbelievable support in the moments when there was no one to answer my queries, and to my sisters and brothers who incented me to strive towards my goal. I would also like to thank all of my friends for all they've done and been for me.

Chapter 1

Introduction

Introduction

The physical properties and thermohaline circulation in the Mediterranean Sea are, to a large extent, affected by atmospheric factors. Meteorological patterns and weather circulation systems are generated by the fluctuations of the atmospheric characteristics which occur at different temporal scales such as days (storm systems), weeks (mid-winter warm-up or a mid-summer wet period), months (cold winters or hot summers), years (abnormal winters for several years in a row) and centuries (long-term climate change). Sometimes these patterns are forced by the fluctuations in the Sea Surface Temperature (SST) and tropical convection[1].

Teleconnection is identified by the linkage between climate anomalies occurring in widely separated (typically thousands of kilometers) regions of the globe. It is associated with a significant simultaneous positive or negative correlation between fluctuations in the atmospheric parameters at the distant parts of the world (Wallace and Gutzler, 1981). The irregular weather conditions and changes in the meteorological characteristics such as temperature, precipitation, the location and intensity of the jet stream and storm tracks, in the large scale, are highly affected by the teleconnection patterns.

Since the large-scale climate indices represent a synthesis of the various physical and meteorological conditions of the system, they are more helpful in the analysis of the variability of the meteorological parameters than any individual local variable. In this dissertation the impact of three prevailing climatic patterns, North Atlantic Oscillation (NAO), East Atlantic (EA) pattern, and Mediterranean Oscillation (MO), on the Mediterranean thermohaline properties is discussed. This introduction represents the background of the research including objectives and research questions, scope, basic structure, previous works which have been done so far on this topic, and the brief outline of the thesis.

Mediterranean Sea

- **Geography of the Mediterranean Sea**

The Mediterranean Sea is a semi-enclosed sea connected to the Atlantic Ocean on the west and bordered by Southern Europe and Anatolia on the north, North Africa on the south and the Levant

[1] *NOAA.NCEP.CPC*

on the east. It has the approximate area of 2.5 million km² and the average depth of 1500 m with the deepest point of 5267 m located in the Calypso Deep in the Ionian Sea. The longitudinal and latitudinal extensions of the Mediterranean are 3000 and 1500 km, respectively.

The connection between the Mediterranean and the Atlantic is through the Strait of Gibraltar while Dardanelles and the Bosporus connect the Mediterranean to the Sea of Marmara and the Black Sea, respectively. The Mediterranean Sea is connected to the Red Sea by the long man-made Suez Canal in the southeast. Two sub-basins of the Mediterranean of nearly equal size are:

1. Western Mediterranean (WMED):

   - On the west: Between Cape Trafalgar in Spain and Cape Spartel in Africa.
   - On the northeast: The Western Coast of Italy, the East extreme of the Island of Sicily and the North Coast of Sicily.
   - On the east: between Cape Lilibeo in the Western point of Sicily and Cape Bon in Tunisia through the Adventure Bank.

2. Eastern Mediterranean (EMED):

   - On the west: The Northeastern and Eastern limits of the Western Basin.
   - On the northeast: A line joining Kum Kale (26°11'E) and Cape Helles, the Western entrance to the Dardanelles.
   - On the southeast: The entrance of the Suez Canal.
   - On the east: The coasts of Syria, Israel, Lebanon, and the Gaza Strip.

The Mediterranean Sea is also divided into smaller areas, each with special properties. These subdivisions are defined as:

- The Strait of Gibraltar;
- The Alboran Sea, between Spain and Morocco;
- The Balearic Sea, between mainland Spain and its Balearic Islands;
- The Ligurian Sea between Corsica and Liguria (Italy);
- The Tyrrhenian Sea enclosed by Sardinia, the Italian peninsula and Sicily;
- The Ionian Sea between Italy, Albania and Greece;

– The Adriatic Sea between Italy, Slovenia, Croatia, Bosnia and Herzegovina, Montenegro and Albania;
– The Aegean Sea between Greece and Turkey;

The location of the Mediterranean Sea and its sub-basins is represented in the Fig. 1-1[2].

Figure 1- 1 the composite satellite image of the Mediterranean Sea

– **Mediterranean water masses and general circulation**

Semi-enclosed basins such as the Mediterranean often have limited water exchanges with the neighboring water bodies and consequently, the basin characteristics are, to some extent, independent and distinct from the adjacent areas.

Meteorological and oceanic conditions, in other words, air-sea water and heat exchanges; and the exchanges of water, salt, heat, and the other properties between the Mediterranean Sea and the

[2] *http://en.wikipedia.org/wiki/Mediterranean_Sea*

Atlantic Ocean, to a large extent, generate the basinwide thermohaline circulation as well as deep water formation in Mediterranean Sea (Tsimplis et. al., 2006). Various factors, such as topographic and coastal effects, multiple driving forces and internal dynamical processes induce a complex general circulation in the Mediterranean which is composed of the basin scale, sub-basin scale, and meso-scale spatial patterns.

There are some analogies and differences between internal thermohaline cells in the eastern and western Mediterranean, as well as between the entire Mediterranean and the global thermohaline circulation. The general vertical structure of the Mediterranean is formed by three different water masses in the different layers of the basin and can be described as follows:

Atlantic Water (AW), enters the Mediterranean through the Strait of Gibraltar and circulates in the whole basin. It migrates eastward and bifurcates into the multiple pathways, since the Mediterranean basin is the evaporation basin (negative estuary), the temperature and salinity (and, therefore, density) increase when it circulates towards the Levantine Sea. AW occupies the surface layer, of approximately 100-200 m thick. The temperature of AW is variable under the influence of the seasonal fluctuations while the salinity differs from 36.6 in the Alboran to 38.6 in the Ionian, and 38.9 in the Levantine Seas.

When AW reaches the Levantine Basin, it frequently gets involved in the convection processes during exceptionally cold winters and forms the Levantine Intermediate Water (LIW) in the northeast part of the basin. It then returns to the western basin (Robinson et al, 2001) and moving westward, the temperature and salinity of the LIW decrease. LIW occupies the depth of 300 to 800 m in the entire basin and its temperature changes from ~15.5 $^{\circ}$C in the Levantine, to ~14.5 $^{\circ}$C in the Ionian; and ~13 $^{\circ}$C in the Alboran Sea and salinity varies from ~39.1 in the Levantine, to ~38.8 in the Ionian and ~38.5 in the Alboran sub-basins.

Deep Water (DW) fills the layer from ~800 m to the bottom and it is characterized by lower salinity and temperature than LIW. Winter convection is responsible for the deep water formation. In the WMED, deep water is produced in the Gulf of Lion, and spreads into the basin, driving the thermohaline cell. Strong meso-scale processes exist around the sub-basin scale gyres in the Alboran and Balearic Seas. The composition of sub-basin scale gyres linked by sub-basin scale jets generates the basin scale circulation. Lower salinity water enters WMED from the Gibraltar Strait and EMED through the Sicily Strait. Western Mediterranean Deep Water (WMDW) is characterized by the temperature and salinity of ~12.8 ($^{\circ}$C) and ~38.4 respectively while the

Eastern Mediterranean Deep Water (EMDW) has the temperature of ~13.5 ° C and the salinity of ~38.7 (Lionello 2012).

Two main sources of the deep water formation in the EMED are the North Adriatic shelf area (Hendershott and Rizzoli, 1972) (through the winter cooling and mixing) and the South Adriatic Gyre (SAG) (via open-ocean convection in the centre of the South Adriatic Pit (SAP), (Gačić et al., 2002; Manca et al., 2002). The dense water formed in the South Adriatic Sea outflows the Ionian Sea through the Strait of Otranto.

- **Eastern Mediterranean Transient (EMT) and Adriatic-Ionian Bimodal Oscillating System (BiOS)**

In the early 1990s, a dramatic change happened in the location of dense water formation in the EMED. The Adriatic Sea was replaced by the Aegean Sea as a site of generation of dense water due to exceptional heat losses and winds (Josey, 2003). This phenomenon is called Eastern Mediterranean Transient, which influenced the circulation over the entire EMED and the North Ionian Sea where the circulation reversal from cyclonic to anticyclonic and vice versa occurs on decadal time scales.

In 1987 the circulation of North Ionian Gyre (NIG) changed from cyclonic to anticyclonic phase (Demirov and Pinardi, 2002). The passage from anticyclonic to cyclonic mode took place in 1997 (Larnicol et al., 2002; Pujol and Larnicol, 2005) associated with the EMT and the consequent vorticity transfer (Borzelli et al., 2009). The next reversal happened in 2006 when the gyre circulation changed from cyclonic to anticyclonic mode (Gačić et al., 2010). The decadal reversals of the circulation in the North Ionian Sea and its interaction with the South Adriatic Sea are known as Adriatic-Ionian Bimodal Oscillating System which has been the focus of attention of many studies in the recent years. During the anticyclonic mode, AW diverges into two branches after entering the Eastern basin through the strait of Sicily. One part of this colder and less-saline AW flows north-eastward into the North Ionian while the other branch moves toward the Levantine Sea, and, therefore, decreases the temperature and salinity of those areas. Conversely, in the cyclonic mode of BiOS AW spreads zonally to the Levantine Sea and then, to a less extent, turns cyclonically toward the North Ionian and therefore, passes the longer path and has enough time to be influenced by the LIW and Cretan Intermediate water (CIW), which are characterized by the higher temperature and salinity. The warmer and saltier water then enters the North Ionian and

consequently flows into the Adriatic Sea. Hence, depending on the origins of the water masses entering the Adriatic Sea, the thermohaline properties of the dense water generated in the South Adriatic, which spreads into the deep layer of the Ionian Sea and the circulation mode in the Ionian, changes (Civitarese et al., 2010). The schematic pattern of two modes of BiOS with the pathways of the different water masses is shown in the figure 1-2.

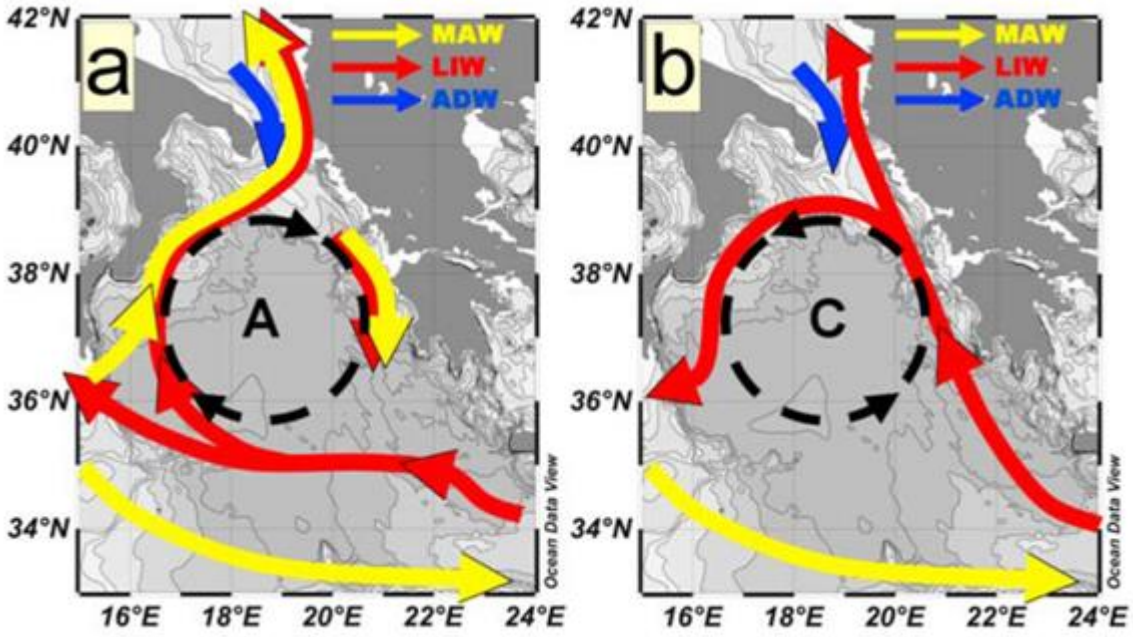

Figure 1- 2 Schematic image of BiOS at the a) anticyclonic and b) cyclonic mode. The yellow, red and blue arrows show the water streams of AW, LIW and Adriatic Deep Water, respectively (Gacic et al., 2010)

Large-scale climatic patterns

- **North Atlantic Oscillation (NAO)**

One of the most important large-scale climatic patterns in all seasons in the European continent and the Mediterranean Sea is North Atlantic Oscillation (Barnston and Livezey 1987). It was first identified by Sir Gilbert Walker in the 1920's. NAO is the dominant mode of the atmospheric variabilities over the North Atlantic Ocean. It affects the climate of Eastern North America, the North Atlantic and the Eurasian continent (Van Loon and Rogers, 1978; Wallace and Gutzler, 1981; Hurrell, 1995b, 1996; Kushnir, 1999). Although it is more prominent in winter time (when the ocean mixed layers are deep and much of the ocean uptake of gasses takes place), NAO forcing should be noted during the summer (Rogers, 1990).

NAO is defined by the north-south dipole anomalies in the surface pressure and geopotential height located over the Iceland (low pressure) and Azores (high pressure). The positive North Atlantic Oscillation Index (NAOI) is characterized by the intensification of both pressure centers and north-eastward deflection of the pressure gradient axis and the storm tracks. Furthermore, it reflects above normal precipitation in northern Europe and Scandinavia, and more than normal temperature over the eastern United States and North Europe. During NAOI+, dry conditions exist in southern and central Europe and below-average temperatures are established in Greenland and oftentimes across southern Europe and the Middle East.

Conversely, negative NAOI is associated with positive (resp. negative) pressure and geopotential height anomalies in the higher (resp. lower) latitudes and the zonal storm tracks. Moreover, the temperature and precipitation patterns are opposite of what is observed in the positive phase (Hurrell 1995), (see Fig. 1-3).

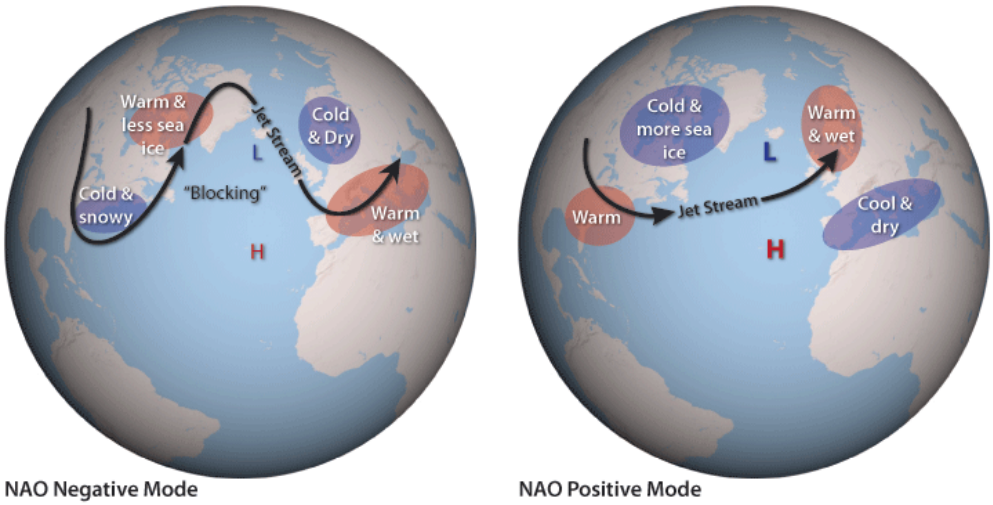

Figure 1- 3 Negative and positive NAO phases with the related patterns of temperature, precipitation and storm tracks (Source: https://www.climate.gov/news-features/understanding-climate/forensic-meteorology-solves-mystery-record-snows).

In the last 100 years the NAOI has exhibited considerable variability. The high positive NAOI associated with strong winds and above normal temperature was present over Europe from the beginning of the 20th century until the beginning of the 1930's (excepting the winter of 1916 and 1919), (e.g. Rogers, 1985). The decreasing trend and consequently below average temperature was observed from the early 1940s until the early 1970s in Europe during the winter (van Loon and Williams, 1976). NAOI sharply increased and remained in the high positive phase from 1980 until

the end of 2000's. This persistence of high NAO mode was the most pronounced ever recorded and was associated with warming in Northern Hemisphere surface temperatures over the last decades (Hurrell, 1995a, 1996; Wallace et al., 1995; and figure 1-4).

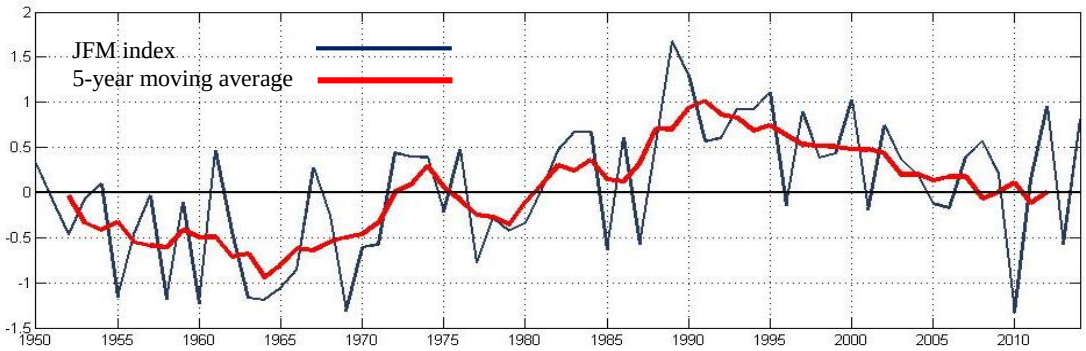

Figure 1- 4 time series of the JFM NAO index (blue) and the 5 years moving average (red) over the period 1950-2013.

– **East Atlantic (EA) pattern**

The second mode of low-frequency variability of the tropospheric circulation in the North Atlantic area is East Atlantic pattern. EA is defined as a north-south dipole of the anomaly centres, similar to the NAO structure but with the southeastward displacement of the centers. For this reason, the pattern is often referred to a southward shifted NAO. EA can be distinct from NAO by linkage of the low-pressure centre with the modulations of intensity and location of the subtropical ridge. During positive EAI (East Atlantic Index) Europe is characterized by above-average surface temperatures in all months while the below-normal temperature is exhibited over the southern U.S from January to May and in the north-central U.S. in the period from July to October. Moreover, the positive phase is associated with an increase in precipitation over northern Europe and Scandinavia and drier condition across southern Europe. The strong multi-decadal variability of the EA pattern was revealed during 1950-2004 with the negative phase prevailing during March of 1950-1976, and the positive phase occurring during March of 1977-2004. The strong and

persistent positive phase occurred over the period of 1997-2004[3](Wallace and Gutzler, 1981). Temporal variation of the JFM EAI is demonstrated in the Fig. 1-5.

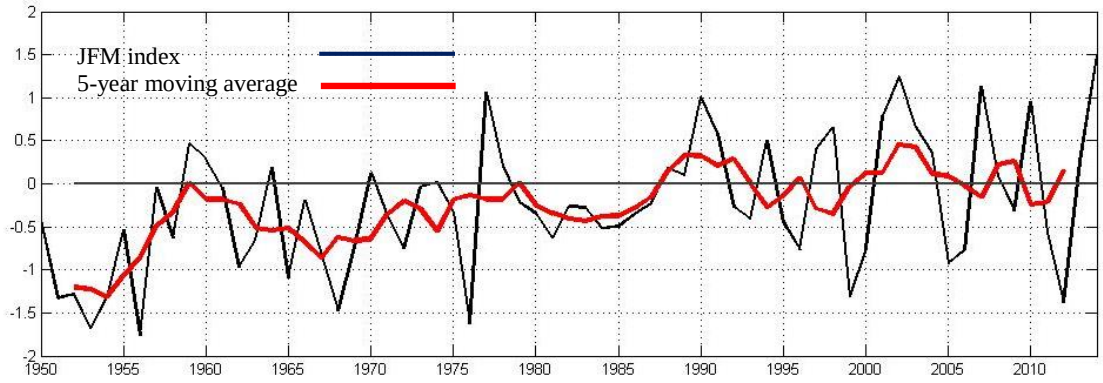

Figure 1- 5 time series of the JFM EAI (blue) and the 5 years moving average (red) over the period 1950-2013.

– **Mediterranean Oscillation (MO)**

Mediterranean Oscillation suggested by Conte et al. (1989), representing the dipole behavior of the atmosphere between the western and eastern Mediterranean, is recognized to be more relevant for the Mediterranean Sea. It is defined by the difference of some climate variables, such as pressure, temperature, precipitation, and circulation between two selected points in the eastern and western basins. This index has a strong influence on the turbulent fluxes and it is applied to illustrate the effects of the intra-basin sea level pressure (SLP) field on the turbulent parameters over the Mediterranean Sea (Papadopoulos et al. 2012b).

The first Mediterranean Oscillation Index (MOI) was defined by Conte et al (1989) as the difference of the standardized 500 hPa geopotential heights between Algiers (36.4°N, 3.1°E) and Cairo (30.1°N, 31.4°E). Palutikof (2003) used the sea level pressure difference between the northern frontier of Gibraltar (36.1°N, 5.3°W) and Lod Airport Israel (32.0°N, 34.5°E) to compute the second version of the MO index. The other MOI defined by the normalized sea level pressure difference between Marseille and Jerusalem is more appropriate for the Central Mediterranean and is highly correlated with the total precipitation and frequency of rainy days in Italy (Brunetti et al.,

[3] *http://www.cpc.ncep.noaa.gov/data/teledoc/ea.shtml*

2002). Papadopoulos et al. (2012b) presented the index based on the pressure centers located in the south of France (45°N, 5°E) and Levantine Sea (35°N, 30°E) in the NW-SE direction which reflects the more realistic dipole pressure pattern. Another definition of MOI is obtained by the principal component (PC) of the first mode of normalized sea level pressure anomalies across the extended Mediterranean region (Suselj and Bergant, 2006; Gomis et al., 2006). Figure 1-6 shows the time-series of the wintertime MOI and the 5-year moving average.

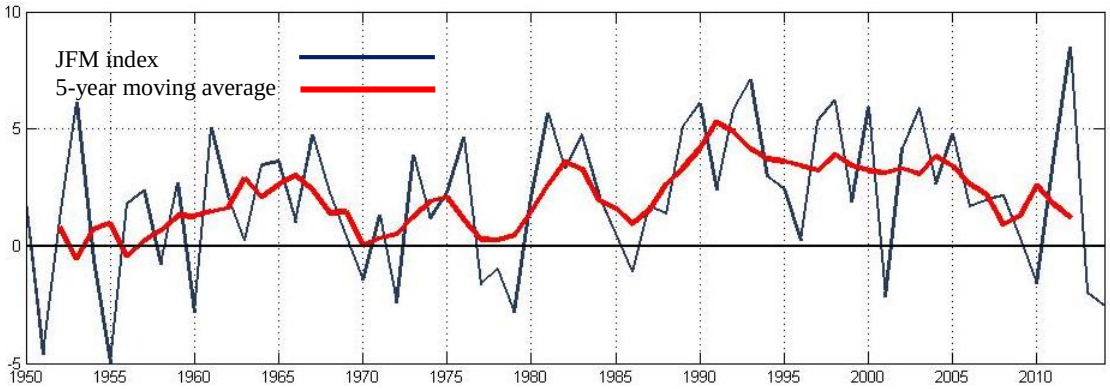

Figure 1- 6 time series of the JFM MOI (blue) and the 5 years moving average (red) over the period 1950-2013.

It should be noted that NAO and EA are considered to be independent modes of atmospheric variability according to an orthogonal analysis done at the National Oceanic and Atmospheric Administration Climate Prediction Center (NOAA/CPC) while MO may reflect the combination of some independent climatic modes on the Mediterranean Sea (Papadopoulos et al. 2012c). The correlation coefficients between these 3 indices during the winter period, summarized in Table 1-1, reveals the fact that there is rather high correlation between NAOI and MOI, but the EAI is uncorrelated with 2 other climatic modes.

Table 1-1. Correlation coefficients between the winter (JFM) climatic indices. Bold font indicates the statistically significant coefficient at 99% confidence level.

Index 1	Index 2	Correlation coefficient
NAOI	MOI	**0.54**
NAOI	EAI	0.15
EAI	MOI	-0.1

Background of study

The Mediterranean Sea is one of the regions highly affected by climate change (Giorgi, 2006; Rosenzweig et al., 2007; Giorgi and Lionello, 2008). Numerous studies have been conducted regarding variations in processes relevant for the climate of the Mediterranean region. A large number of these works considered the influences of NAO modes on the sea circulation and the physical and thermohaline properties. However, despite its effect on the inter-annual variations of the climate variables (e.g. air temperature, sea surface temperature, wind and heat fluxes) EA pattern is not so well known. In fact EA sometimes is found to be more dominant than NAO or at least as important as the NAO. It has been shown that the changes in the jet stream cannot be only explained in terms of NAO but the EA pattern is also required to provide a good description of the jet stream variation (Woollings et al. 2010). Furthermore, only a few studies in the recent years have focused on the effects of the MO.

The consistent temperature changes in the WMED and the North Atlantic, evidenced from the recent 50-year Mediterranean climatology, correspond to the anomalies of the air-sea heat flux and are strongly correlated to NAOI (Rixen et al., 2005). Generally, it has been shown that positive NAOI provides warmer conditions over the northern areas and cooler conditions over the southern parts of the Mediterranean and the opposite pattern is revealed in the negative phase (Xoplaki, 2002; Trigo et al., 2002b 2006; Xoplaki 2002; Toreti et al., 2010; Giorgi and Lionello 2008; Pettenuzzo et al. 2010). This suggests that the Mediterranean region might be especially vulnerable to global change. However, these studies mostly focus on the western and eastern basin averages and the spatial distributions and the response of the Mediterranean sub-regions have not been considered.

In addition, the EA pattern can explain the variability of the air temperature in the WMED (Saenz et al., 2001) and in the Italian Peninsula (Toreti et al., 2010). Skliris et al. (2011) linked the rise in temperature in the period 1985–2008 to the changes in the horizontal heat advection and an increasing warming of the Atlantic inflow. Their analysis showed that the inter-annual variation of the net heat flux (mostly due to the latent heat flux) is out of phase with SST increase. The first EOF (Empirical orthogonal function) mode of the SST time series is highly correlated to the EAI and the Atlantic Multi-decadal Oscillation (AMO) index while the low and non-significant correlation of SST and NAOI with the opposite signs is observed in the eastern and western basins. The increase of the second EOF mode of the SST anomaly in the western basin from 1973 to the

late 1980s is associated with a long-term increase of the NAOI and inflowing the warmer AW. In the eastern basin, the rise in SST is slower. Although this work has presented an interesting explanation of the warming trend in the Mediterranean basin, it didn't consider the role of wind forcing in the SST variation.

Using NCEP/NCAR and ARPERA datasets, Josey et al., (2011) considered the influences of the first four modes of atmospheric variability, NAO, EA, Scandinavian pattern (SCAN), and East Atlantic/ West Russian pattern (EA/WR), on air-sea heat exchange in the full Mediterranean basin as well as in the eastern and western sub-basins. They showed the dominance of the winter anomalies on the annual mean heat fluxes. Moreover, they demonstrated the small effect of the NAO on the winter mean heat budget in the full basin and the major impact of the EA and EA/WR mode on both eastern and western sab-basins. In contrast to EA, EA/WR generates a dipole of heat fluxes with the opposite signs on two sab-basins. It has also a strong impact on the Aegean Sea and it is connected to the deep water formation in this region. They also showed that SCAN mode does not reveal any considerable impact on the basin.

The atmospheric circulation patterns responsible for the winter heat loss at four sites of the intermediate and deep water formation in the Mediterranean were studied by Papadopoulos et al. in 2012c. They found an SLP pattern dominated by an anticyclone over northwestern Europe and a weaker cyclone to the southeast associated with strong heat loss in these areas. The pattern reflects the combined effect of different atmospheric modes of variability (NAO, EA, EA/WR, SCAN, with the North Sea–Caspian pattern and MOI). The strong events of heat loss are related to the intensity and location of the centres of the SLP patterns, SLP gradients, and the resulted northerlies, which transfer the cold and dry air over these areas as well as latent and sensible heat flux components.

In oceanography, the wind stress field, or the work done by the wind, is regarded as the driving source for the oceanic surface layer motion. In other words, the parameter usually used to study the wind forcing on the sea is wind stress, which is defined by the horizontal force of the wind on the sea surface and represents the vertical transfer of the horizontal momentum which is transformed from the atmosphere to the sea. One of the major factors in reinforcing the cyclonic circulation and in contributing to deep water formation (DWF) in the sea is the wind stress vorticity (Herbaut et al., 1997; Josey et al, 2011). Since there are several sites of deep water formation in

the Mediterranean, it is necessary to clarify spatial and temporal behaviors of the wind stress vorticity variations attributable to the climate indices.

The importance of the wind stress vorticity in the sea circulation has been demonstrated in many studies. For the first time, Vignudelli et al. (1999) related the circulation of the northern part of the WMED to the wintertime NAOI. They showed that the seasonal and inter-annual variabilities of the current in the Corsica Channel are the main components of the circulation of the Northern Basin and correspond to the cold and dry or warm and wet air masses driven from the NAO mode. They concluded that the major forcing of the current variations come from the NAO induced air-sea exchanges, which affect oceanic processes such as deep water formation.

The mechanisms responsible for the open-ocean deep convection (deep water formation in the ocean) have been the subject of many recent studies. These processes take place in the small number of locations such as Mediterranean, Labrador, and Irminger seas. Pickart et al. in 2003, related the convection in the Irminger Sea to a low-level atmospheric jet (Greenland tip jet) associated with elevated heat flux and strong wind stress curl. They also showed that the deep convection occurs in the periods characterized by the high NAOI. However, the convection mechanism in this area is different from the one in the Mediterranean Sea. The main wind events generating the deep convection in Mediterranean, such as mistral and tramontane, are northerly and they are less frequent and more persistent (Schott et al., 1996). Furthermore, in Mediterranean, a single cyclonic gyre develops directly underneath the forcing region where the deepest convection takes place (Madec et al., 2003).

Pandžić and Likso (2005) classified 11 wind field patterns over the eastern coast of the Adriatic Sea and found the strong relation between these mesoscale wind patterns and large-scale (regional) atmospheric conditions. The Icelandic cyclone and the Azores anticyclone (two controlling pressure centres of NAO) appeared as important large scale factors affecting the wind configurations of the Eastern Adriatic Sea. Due to the main contribution of the Adriatic Sea in Eastern Mediterranean Deep Water formation (EMDWF), it is worthwhile to analyze the influence of wind forcing on the circulation in this region and its relation to the climate patterns.

According to deCastro et al. (2008), the main upwelling anomaly variability along the entire western coast of the Iberian Peninsula during the upwelling season, (July to October) is significantly out of phase with EAI. This implies the relevance of the upwelling in this area to EA. However, NAO is considered to be the second most influential atmospheric mode. The focus of

this study is on the warm periods of the year while it will be interesting to explore the connection between upwelling in this area and the climate patterns during winter, considering wind and salinity variation.

The variability of the Mediterranean water budgets in relation to NAO has been the subject of many studies. Wintertime precipitation has appeared to be out of phase with NAOI over the large area of the western and northern Mediterranean (Ulbrich et al., 1999; Trigo et al., 2004, 2006; Turkes and Erlat, 2003; Giorgi and Lionello, 2008). Josey (2003) investigated the variability of the heat and freshwater forcing of the EMED and its impacts on deep water formation. He showed the major contribution of the thermal effects to the increase in density of the surface waters during the winter and proposed that though the heat anomalies in this region are not related to NAO they can be associated with the negative mode of the EA pattern. However, some other studies suggested that NAO can be a major contributor to the bimodal behavior of the Aegean Sea in the formation of the dense water. (Zervakis et al., 2004, Josey et al., 2011; and Papadopoulos et al., 2012c).

In 2011, Mariotti and Dell'Aquila presented research on the decadal climate variability of the Mediterranean Sea and concluded that NAO is responsible for more than 25% - 30% of the variance of the decadal wintertime precipitation over a region spanning parts of Spain, Marocco, Southern France, Italy and the Balkans. It has been shown that the variation in the precipitation is due to modulating of SLP by NAO and reorganizing large-scale moisture fluxes into the region (Mariotti and Arkin, 2007).

Criado-Aldeanueva and Soto-Navarro in 2013 analyzed the correlation of precipitation (P), evaporation (E), and net heat flux with the different MO indices in the inter-annual to inter-decadal scale. They concluded that the PC paradigm can demonstrate more efficiently, the influence of the large scale atmospheric pattern in the annual scale while the station base index shows low correlations in the smaller scales. However, during the winter, all indices have the high ability to represent the atmospheric forcing.

The influence of the climate indices (NAOI and MOI) on the long-term variability of the heat and water fluxes in the Mediterranean has been studied by Criado-Aldeanueva et al. in 2014(a). The results demonstrated the correlation between atmospheric forcing and water and heat budgets at the inter-annual and inter-decadal scales. With the switch from low to the high mode of the indices from the mid-1960s to the late 1980s, the mean precipitation in the basin decreased. Since

the eastern and western basins have different behavior in precipitation (P) and evaporation (E), the water deficit (E-P) is not well correlated with the indices. Both indices have the similar effects on P and E-P while MOI is more efficient to indicate the inter-decadal variations of E and net heat flux which is explained by the relatively steady MO centre and its influence on the most of the Mediterranean Sea during the year.

The impact of atmospheric forcing on the Mediterranean heat and freshwater was studied by Criado-Aldeanueva et al. (2014b). They correlated the inter-annual to interdecadal precipitation, evaporation, freshwater budget (E-P) and net heat flux with the climate indices such as NAOI, EAI, and MOI. In addition, they determined the cause-effect relationships between the indices by performing a composite analysis to highlight the differences between the positive and negative phases of climatic modes. The results showed the similar influence of the NAO and MO on the Mediterranean but with the higher correlation of all variables on the annual basis, especially in the negative phase which is associated with more precipitation and with the positive anomaly of the evaporation, particularly in the Levantine Sea. The effects of the EA pattern on the precipitation over the basin were found to be not significant, but they showed the strong influence of the EA on the evaporation and heat losses over the winter period. Moreover, they concluded that since MO is not independent from the other modes, it can be a powerful tool for monitoring the atmospheric impacts over the basin.

Having relatively small spatial scales, EMED responses very quickly to the atmospheric forcing (Malanotte-Rizzoli, 2003), which can influence the variations of the deep water formation (Castellari et al., 2000). In the recent decades, numerous studies have been conducted focusing on the variations of the circulations and the thermohaline properties in the EMED.

In 2002 Demirov and Pinardi used the ocean circulation model to study the inter-annual variability of the Mediterranean Sea circulation in the period of 1988 to 1993. A drastic change in the Northern Hemisphere (NH) decadal scale atmospheric regimes occurred at the end of the 1980's due to the significant change of the NAO mode from negative to positive and the intensification of the positive phase. At the same time, the overall kinetic energy in the WMED weakened and the structure of circulation in the EMED changed. The simulations showed the increase of the anticyclonic activities with different intensities at the South Ionian Sea and the area of the mid-Mediterranean Jet in that period which are in a good agreement with observations. They suggested that the propagation of AW and LIW, the transport of salinity content of the Levantine

waters toward the Aegean and the Adriatic Sea and the intensification of the deep water formation in the Aegean Sea, can be related to the high values of the NAOI during this period.

Borzelli et al. in 2009 showed that the change in the circulation of NIG from anticyclonic to cyclonic in 1997, which took place in the relaxation stage of EMT, was associated with the strong interaction between the Ionian and Aegean Seas and the northward spreading of the Aegean waters along the eastern Ionian flank. Moreover, the presence of the anticyclonic wind vorticity showed that wind forcing cannot explain the circulation reversal. Therefore, they suggested that the circulation reversal can be determined by the baroclinic vorticity production.

In 2011, Gačić et al. described the effects of BiOS on the thermohaline properties of the Levantine and Cretan Seas. Their results demonstrated the intensification of the AW flow in the cyclonic phase of BiOS. Moreover, the variability of the sea level height in the North Ionian is out of phase with the Aegean and Levantine Seas. They also showed that the intensity of the AW inflow determines the salinity content of the Levantine Basin and moreover, the salinity of the Ionian Sea is out of phase with the one in the Levantine Sea at the surface and with the deep water salinity of the Aegean Sea at the deep layer. It suggests the rapid transfer of the surface salinity variations through winter deep convection. The relation between the change of the salinity in the Levantine and Cretan Seas and the inversion of the Ionian Circulation (BiOS) implies that the preconditioning for EMT is driven by internal processes. Furthermore, EMT is potentially recurrent and cannot be an isolated phenomenon. These results suggest to proceed the research by exploring the possible impact of the climatic patterns on the sea surface height of the North Ionian as well as the salinity of the EMED.

In 2013, Gačić et al. found that the high salinity in the Levantine basin could potentially be a pre-conditioning of EMT. They estimated the travel time of about 25 years for LIW in order to reach the WMED (deep mixed layers of the Algero-Provencal sub-basin). In addition, they showed that about 60% of the salt content increment in the bottom layer of the WMED is due to the extra salt input from EMED. Furthermore, the last cyclonic phase of BiOS occurred in 2011 but it was unexpectedly changed to anticyclonic circulation. Gačić et al. (2014) related the sudden reversal of the Ionian circulation to the extreme winter in 2012, which caused a strong deep water formation process. The inflow of the produced dense water in the Ionian changed the bottom pressure gradient and consequently the circulation of the NIG.

The estimated rate of the Mediterranean sea level rise over the twentieth century is 1.1–1.3 mm/year (Marcos and Tsimplis, 2008), while it is 1.7 mm/ year at the global scale over the same period (Solomon et al. 2007). The impacts of the long-term sea level rise can be modified or reduced by the regional sea level variability in different time-scales. The regional sea level variability in the Mediterranean Sea is strongly related to the barotropic effects of the atmosphere forcing, in terms of atmospheric pressure and wind, which can mainly correspond to the climate systems (especially winter NAO), (e.g. Gomis et al., 2008).

Tsimplis and Josey in 2001 studied the variability of the sea level in the Mediterranean Sea and its linkage with NAO through the changes in the atmospheric pressure anomalies and water budget (precipitation and evaporation). The high positive NAOI during the 1960's to 1990's is associated with the reduction in the Mediterranean Sea level which highlights the effects of the atmospheric forcing on the characteristics of the ocean. In addition, the change in the freshwater flux in the basin during the 90's (characterized by the high positive NAO mode) is suggested to be connected to the occurrence of the EMT. This study, however, explored the general impact of NAO on the Mediterranean Sea level and the regional impacts of NAO have not been reflected.

In addition, Tsimplis and Rixen (2002) showed the connection between the sea level change in the Adriatic and Aegean Sea's and NAO. They concluded that heating cannot be the only factor affecting on the steric height. However, the different response of each sub-basin of the EMED to the various forcings complicates the dependency of the sea level on the various mechanisms. In agreement with Tsimplis and Rixen, Criado-Aldeanueva et al. in 2008 showed that the sea level variations are not only the function of steric effects (∼55% which is comparable to that reported for the global ocean) but they are also driven by the mass-induced component. They estimated the average trend of 2.1±0.6 mm/year for the whole Mediterranean with the high value in the Levantine and south of Crete (10±1 mm/year) and more moderate trend in the Adriatic and Alboran Seas. Sea level decreases in the Algerian basin, between the Balearic Islands and the African coasts and, particularly, in the Ionian basin with the negative trends of −10±0.8 mm/year mainly due to the mass-induced contribution or circulation changes (it was explained later by BiOS mechanism).

Tsimplis and Shaw (2008) showed that the correlation between NAOI and sea level in the Adriatic Sea and EMED remains significant after removing the direct effects of the pressure and wind. Therefore, in addition to the external forces, the changes in the steric properties of the water

(the thermosteric and halosteric components) can also determine the inter-annual variability of the sea level (Köhl, 2014).

The numerical analysis of the spatial and temporal sea level extremes variability in the Mediterranean Sea and the Atlantic Ocean coasts, by Tsimplis and Shaw (2010), showed the larger extreme values over Atlantic than the Mediterranean. The sea level extremes are directly affected by the atmospheric forcing as the winter values are well correlated with NAOI and MOI in the coastal Atlantic area adjacent to the Mediterranean, WMED, and the Adriatic Sea.

Tsimplis, et al., (2013) analyzed the variations of sea level and water mass in the Mediterranean over the period 1993–2011 and their relation to the NAO modes. They showed that the increase of the oceanic mass in the basin leads to the sea level rise with the linear trend of 3.0 ± 0.5 mm/yr. This variability is explained by the change of atmospheric pressure and consequent change of the wind configurations corresponding to the wintertime NAO modes. The atmospheric pressure and wind forcing are the factors responsible for the Mediterranean mass distribution. However, there is also a third unresolved contribution which can be due to the change in the oceanic baroclinic circulations caused by the wind in the Atlantic Ocean. The average steric signal in the Mediterranean is not affected by NAO, while the local atmospheric forcing can influence the steric properties in some areas such as the Adriatic and Aegean Sea's (Tsimplis and Rixen, 2002).

Since atmospheric conditions are considered important in affecting the circulation in the Mediterranean Sea (in terms of the wind forcing and heat and water exchanges), the improvement of our knowledge of the connection between large-scale climate indices and the circulation variability in the entire basin and each specific area in the Mediterranean is thought to be essential to get a better understanding of the Mediterranean circulation and its response to climate change.

In spite of the numerous studies concentrated on the oceanography of the Mediterranean Sea, the influences of the climate patterns and meteorological conditions on the variation of the sea level height, circulation, thermohaline properties, water mass transport and all basin characteristics, there still remain many open questions to study. Many studies have focused on the variation of these parameters on the entire basin while the regional effects of atmospheric conditions have not been much considered. Moreover, the influence of EA and MO on the characteristics of the basin is not well studied.

The purpose of this research is to explain different responses of the Mediterranean Sea and its sub-regions to three prevailing climatic modes in the Mediterranean basin and to try to address the

relative importance of each climate pattern in different sub-basins, the influence of external forcing on deep water formation sites and the possible role of internal processes, as well as the mechanisms responsible for the long-term variability of the circulation in some sub-regions of the basin.

The structure of this dissertation is as follows: In chapter 2 the data sets and methods used for the analysis are described. The variation of the characteristics of the Mediterranean basin and its sub-regions associated with the large-scale climatic indices (NAOI, EAI, and MOI) are presented and discussed in chapter 3. Finally in chapter 4, the main results of the study are summarized and the conclusions will be obtained.

Chapter 2

Data and methods

Data and methods

The possible response of the Mediterranean basin characteristics in terms of the changes in the buoyancy or thermohaline properties, circulation patterns and air-sea heat and water exchanges to low frequency variability of the atmospheric forcing is investigated in this work. For this purpose, calculating the correlation coefficients, the time series of the climate indices were compared with the physical and oceanic parameters for each grid point of the entire Mediterranean basin and the spatial distributions were obtained. Temperature, salinity, wind stress vorticity, sea level height, water budgets (P, E, and E-P) and heat and buoyancy fluxes have been considered. The domain of study consists of the Mediterranean Area between 7˚W – 37˚E and 29˚N - 48˚N, show below in Figure 2-1.

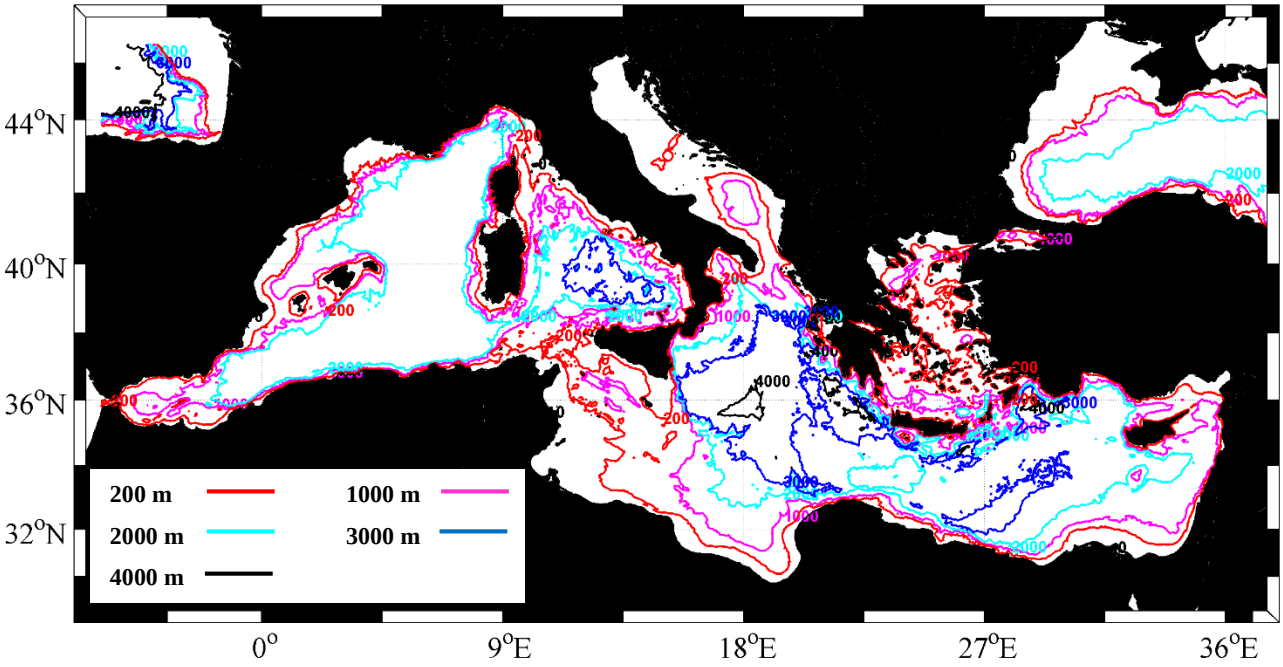

Figure 2- 1 Domain of study, Mediterranean Sea. Contours indicate the bathymetry of the basin.

Due to the fact that the winter periods dominate the annual signal for the air-sea exchanges (Josey, 2003), the monthly time-series were found to be uncorrelated or low-correlated with the climate indices (figures are not shown). Therefore, the focus of this work is on the winter periods from January to March (hereafter referred to JFM).

Furthermore, in order to assess the influence of the large-scale climate patterns on the Mediterranean oceanography, the spatial distributions of the average of the physical and oceanic parameters over the winter months (JFM) were estimated separately for the years characterized by the positive and negative phases of the large-scale climatic patterns. The spatial patterns and strength of the fields in the both modes of each index were then studied and compared.

The climate indices implemented in this work are NAOI and EAI which represent the first and second leading modes of the low-frequency atmosphere variability in the North Atlantic region (Rogers1990; Krichak et al. 2002). Moreover, the impacts of the MO on the basin characteristics are also taken into considerations.

2-1 Climatic indices

The monthly NAO and EA indices used in this work were obtained from the National Weather service, Climate Prediction Center of NOAA (National Oceanic and Atmospheric Administration). The procedures used to identify the indices is the Rotated Principal Component Analysis (RPCA) (Barnston and Livezey, 1987). This technique is applied to the monthly anomalies of the geopotential height at the 500-mb pressure level in the analysis region between 20°N and 90°N from January 1950 to December 2000. The monthly averages and standard deviations of the geopotential height in the period of 1950 to 2000 have been used to standardize the anomalies. To calculate the leading rotated modes, first, the leading modes of the unrotated EOFs of the standardized monthly height anomalies are obtained in the three-month period centered on each month and then, a varimax rotation is applied to the leading unrotated modes. The variability of the structure and amplitude of the teleconnection patterns in relation to the annual cycle of the extratropical atmospheric circulation can be well described in this analysis. Moreover, the better continuity of the time series from one month to the next is provided by three-month centered calculations. This method also yields the more robust results by increasing the number of fields used to calculate the monthly modes and it is superior to grid-point-based analyses, typically determined from one-point correlation maps, in that the teleconnection patterns in the RPCA

approach are identified based on the entire flow field, and not just from height anomalies at selected locations[4].

In addition to NAOI and EAI, we included MOI, which is the high interest for the Mediterranean region. Following Papadopoulos et al. (2012b) the index was obtained from the anomaly of SLP difference between South France (5E, 45N) and the Levantine Sea (30E, 35N). SLP from NCEP/NCAR re-analysis dataset (Kalnay et al. 1996) is used to calculate the index.

2-2 Potential temperature and salinity

The monthly mean time-series of the Mediterranean Sea Physics Reanalysis sea water potential temperature and salinity obtained from OGCM (Ocean General Circulation Model), NEMO-OPA (Nucleus for European Modelling of the Ocean-Ocean Parallelise) version 3.2 (Madec et al 1998), are used in order to study the influence of climate indices on the temperature and salinity of the basin. The model is primitive equation in spherical coordinates implemented in the Mediterranean basin and the extension into Atlantic (6° W – 36.25 ° E; 30.187° N – 45.937° N) with the horizontal grid resolution of $\frac{1}{16}^{\circ} \times \frac{1}{16}^{\circ}$ (approximately 6-7 km) and the 72 unevenly spaced vertical levels (Oddo et al., 2009) which cover from the surface to the depth of 5500 m. The data is available for the time period of 1987 to 2012[5].

Using the momentum, water and heat fluxes calculated from 6-h, 0.75° horizontal-resolution ERA-Interim reanalysis fields from the European Centre for Medium-Range Weather Forecasts (ECMWF), the model predict the surface temperature (Tonani et al., 2008). In addition, 6-h, 0.75° horizontal-resolution ERA-Interim precipitation data, as well as evaporation derived from the latent heat flux and monthly mean runoff datasets, were used to compute the water balance by the model. A variational data assimilation scheme (OceanVAR) were used to assimilate the following data: Sea level anomaly, sea surface temperature, in situ temperature profiles by VOS XBTs (Voluntary Observing Ship-eXpandable Bathythermograph), in situ temperature and salinity profiles by Argo floats, and in situ temperature and salinity profiles from CTD (Conductivity-

[4] *(http://www.cpc.ncep.noaa.gov/data/teledoc/nao.shtml)*
[5] *http://www.myocean.eu*

Temperature-Depth). Satellite OA-SST (Objective Analyses-Sea Surface Temperature) data is used for the correction of surface heat fluxes with the relaxation constant of 60 W/m2K1. Temperature and Salinity computed from in-situ data sampled before 1987 (PRE-TREANSIENTclimatology) from SeaDataNet FP6 project, have been used to initialize the reanalysis. First January 1985 has been set as the initial time of the model as well as the satellite and in situ data assimilation. Considering 2 years of spin-up, the data is available from 1987.

Using the described data (Mediterranean Sea Physics Reanalysis), vertically averaged fields of the temperature and salinity from the sea surface to the 150 m, 150 m to 400 m and 400 m to bottom have been calculated and defined respectively as the surface layer, intermediate layer and deep layer. Then the spatial distributions of the correlation coefficients between wintertime temperature and salinity and NAOI, EAI and MOI have been computed for the upper and intermediate layers. Furthermore, the average of JFM upper layer temperature and salinity for the periods characterized by the positive and negative climate indices were calculated and compared.

2-3 Heat and buoyancy fluxes, evaporation and precipitation rates

ERA-Interim dataset (January 1979 to December 2014) obtained from the European Centre for Medium-Range Weather Forecasts (ECMWF) is used to calculate the monthly net heat flux (Q_{net}) through Eq. 2-1. ERA-Interim is produced by the data assimilation system based on a 2006 release of the IFS (Cy31r2). The system includes a 4-Dimensional Variational analysis (4D-Var) with a 12-hour analysis window. The data is available from 1979 to 2014 with the spatial resolution of 0.125 degree in the both longitude and latitude directions. Synoptic monthly average values forecasted from 0 UTC, 12 UTC for the time step 3, 6, 9 and 12 hours were downloaded and used to calculate the monthly mean time-series of the heat flux components and the net heat flux according to the Eq. 2-1:

$$Q_{net} = SW + LW + LH + SH \qquad (Wm^{-2}) \qquad (2\text{-}1)$$

where SW and LW are solar and thermal radiation, respectively, LH is the latent heat flux and SH is sensible heat flux.

The ERA-Interim reanalysis datasets of the evaporation and precipitation over the entire Mediterranean released by ECMWF dataset (1979-2014; $0.125^{\circ} \times 0.125^{\circ}$) were used to analyze the relation between the climate indices and major water budget components. This data-set is more in agreement with the satellite retrievals relative to the some other sources of data (e.g. ERA-40) due to an improvement in representation of wind speed field. The positive values indicate the downward heat and water fluxes (heat gain by the sea and precipitation) and the negative sign demonstrates the surface heat loss and evaporation.

In addition, using the ERA-Interim reanalysis datasets, the net buoyancy flux and the thermal and haline components were estimated from the Eq. 2-2:

$$B_0 = g\alpha Q_{net}/(\rho C_p) + g\beta PS_0 - g\beta ES_0 \qquad (2\text{-}2)$$

where $B_0(m^2 s^{-3})$ is the net buoyancy flux and the terms on the right hand side are thermal buoyancy flux, precipitation buoyancy flux and evaporation buoyancy flux, respectively. *g (9.8 ms^{-2})* is the gravity acceleration, $\alpha(2.1\times10^{-4\circ}C^{-1})$ is the effective thermal expansion coefficient $(-\rho^{-1}\frac{\partial\rho}{\partial T})$, $Q_{net}(Wm^{-2})$ is the net heat flux, $\rho(1029 kgm^{-3})$ is the ocean density, $C_p(3.8\times10^{+3} Jkg^{-1}K^{-1})$ is the specific heat of water, $\beta(7.6\times10^{-4})$ is the effective haline contraction coefficient $(-\rho^{-1}\frac{\partial\rho}{\partial S})$, *E* and *P (*$ms^{-1}$*)* are the rate of evaporation and precipitation, respectively and $S_0(38.5)$ is the reference salinity (Cronin and Sprintall, 2001). The positive sign indicates the buoyancy gain by sea.

2-4 Wind components

The wind products used in this study were the 6-hourly high-resolution (0.25 degree) gridded Cross-Calibrated, Multi-Platform (CCMP) ocean surface wind velocity. The level 3.0, first-look version 1.1 downloaded from the NASA Physical Oceanography DAAC for the period July 1987 – December 2011 (Atlas et al., 2009) with the Network Common Data Format (NetCDF) were used to analyze the wind patterns.

These products were created using an enhanced Variational Analysis Method (VAM) to combine wind measurements derived from all available Remote Sensing Systems (REMSS) cross-calibrated such as SSM/I, SSMIS, AMSR-E, TRMM TMI, QuikSCAT, SeaWinds and WindSat. A cross-calibrated sea-surface emissivity model function is used to improve the consistency between wind speed retrievals from microwave radiometers (i.e., SSM/I, SSMIS, AMSR, TMI, and WindSat) and those from scatterometers (i.e., QuikSCAT and SeaWinds). Using VAM, the data is combined with the available conventional ship and buoy data, ECMWF ERA-40 Reanalysis are used as the prior information from 1987 to 1998, and the ECMWF Operational analysis is used from January 1999 onward. The data is referenced to a height of 10 meters[6].

The enhanced high-spatial resolution time averages of CCMP winds account the dataset to be extremely useful in explanation and evaluation of air – sea interaction and atmospheric processes and climatology of the ocean and atmosphere.

The CCMP were used to quantify the vertical component of the wind-stress curl $[\text{curl}\ \tau]_z$ over the Mediterranean Sea:

$$\left[curl\tau\right]_z = \frac{\partial \tau_y}{\partial x} - \frac{\partial \tau_x}{\partial y}; \left(\tau_y, \tau_x\right) = \rho C_D \left(u_w, v_w\right) U_{10} \qquad (2\text{-}3)$$

where (τ_x, τ_y) are the wind-stress components, ρ (1.22 kg/m^3) is the density of air, (u_w, v_w) and U_{10} are the components and the magnitude of the wind speed at 10 meters, respectively, and C_D is the drag coefficient which has been obtained according to Yelland and Taylor (1996).

$$C_D = (0.29 + \frac{3.1}{U_{10}} + \frac{7.7}{U_{10}^2}) \times 10^{-3} \qquad 3\frac{m}{s} \le |U_{10}| \le 6\frac{m}{s} \qquad (2\text{-}4)$$

$$C_D = (0.6 + 0.07U_{10}) \times 10^{-3} \qquad 6\frac{m}{s} \le |U_{10}| \le 26\frac{m}{s}$$

In order to relate the variations of the wind stress vorticity to the climate indices, first the spatial distributions of the correlation coefficient between time-series were calculated over the winter periods. Also, the average of the wind stress magnitude and vorticity were estimated separately for the periods associated with the positive and negative NAO, EA and MO modes. In addition, the spatial average of the JFM wind stress curl over the main sites of the deep water formation in the

[6] *http://podaac.jpl.nasa.gov/datasetlist?ids=Collections&values=CCMP*

Mediterranean basin (South Adriatic Sea, Gulf of Lion, Aegean Sea and Levantine Sea) were calculated and the scatter diagrams with the JFM climate indices were obtained.

2-5 Absolute Dynamic Topography and absolute geostrophic velocities

The altimeter products and the surface geostrophic current components over the Mediterranean region were obtained from the gridded (1/8º Mercator projection grid) Ssalto/Duacs weekly, multi-mission, delayed time (quality controlled) products from AVISO (SSALTO/DUACS users handbook 2014). The altimeter data contains the satellite surface heights above geoid or absolute dynamic topography (ADT) acquired from the sum of sea level anomaly and mean dynamic topography, estimated by Rio et al. (2014), over the period of 1993-2012. Absolute geostrophic velocity (AGV) data, derived from ADT through geostrophic balance equations, was downloaded for the 1992-2014 period. The delayed time products used in this work were based on two satellites (Jason-2/Altika or Jason-2/Cryosat or Jason-2/Envisat or Jason-1/Envisat or Topex-Poseidon / ERS) with the same ground track. This data series was homogeneous all along the available time period, thanks to a stable sampling. The monthly mean relative vorticity (ζ) of the AGV data was evaluated as the vertical component of the velocity field curl (Pedlosky, 1987):

$$\zeta = \frac{\partial v_g}{\partial x} - \frac{\partial u_g}{\partial y} \tag{2-5}$$

where u_g,v_g *(cm/s)* are the components of the AGV.

2-6 Long-term variability of the South Adriatic circulation in relation to NAO

The work proceeded with the study of the inter-annual variability of the SAG intensity, i.e. the vorticity of the flow field in the South Adriatic, to relate it to the vorticity inputs, and then possibly to a large-scale climatic regime (NAOI has been considered).

The 6 hourly wind stress curl estimated from CCMP using Eq. (2-3) was firstly time-averaged over monthly periods and finally spatially-averaged in the SAG.

Monthly means of the geostrophic current vorticity fields were spatially averaged in the region of the SAG and in the northern Ionian. Time series of these spatially averaged parameters were filtered using a 13-months moving average, in order to remove the seasonal and intra-annual variations and focus on the inter-annual fluctuations. The low-pass procedure consists of a zero-phase forward and backward digital infinite impulse response filtering, with a symmetric Hanning window (Yan et al., 2004) of 13-points (months).

The vorticity equation was analysed in order to evaluate the importance of various sources of current vorticity. Following Ezer and Mellor (1994) and Schwab and Beletsky (2003) current vorticity equation can be written as:

$$\frac{\partial \zeta}{\partial t} + v.\nabla\zeta = -curl(\frac{A}{D}) - div(fv) - \frac{1}{\rho_0} curl(\frac{1}{D}\nabla\Phi) + curl(\frac{\tau_s}{\rho_0 D}) - curl(\frac{\tau_b}{\rho_0 D}) \qquad (2\text{-}6)$$

where ζ is current vorticity, the terms on the left are vorticity tendency and advection, respectively, *A* is diffusion, *D* is total water depth, ρ_0 is the reference density, Φ is the potential energy, *f* is Coriolis parameter, v is current velocity, and τ_s and τ_b are wind-stress and bottom stress, respectively. Since we assume the predominance of the barotropic flow, the internal pressure gradient (the third term on the right) can be ignored. We also neglect the bottom stress.

If we separate the current velocity into geostrophic (V_g) and ageostrophic (V_a) parts and consider the non-divergence of the geostrophic current, we will have:

$$V = V_g + V_a \; ; \; \zeta = \zeta_g + \zeta_a \qquad (2\text{-}7)$$

$$div(fV) = f(\frac{\partial u_a}{\partial x} + \frac{\partial v_a}{\partial y}) = \frac{f}{D}(\frac{dh}{dt}) \qquad (2\text{-}8)$$

where *h* is the depth of water. Replacing the equations 2-7 and 2-8 in equation 2-6 and neglecting the diffusion A as well as bottom stress and divergence ($\frac{f}{D}(\frac{dh}{dt})$ which is two orders of magnitude smaller than rate of change of the vorticity) implies:

$$\frac{\partial(\zeta_g + \zeta_a)}{\partial t} = -(V_g + V_a).\nabla(\zeta_g + \zeta_a) + \frac{1}{\rho D} curl(\tau_s) \qquad (2\text{-}9)$$

Since $\frac{|V_a|}{|V_g|} = \frac{|\zeta_a|}{|\zeta_g|} \sim O(Ro) = O(\frac{U}{fL}) = 10^{-2}$ ($U \sim 10^{-1}\frac{m}{s}, L \sim 10^5 m, f \sim 10^{-4} s^{-1}$), the ageostrophic parts vanish and finally we obtain the current vorticity equation:

$$\frac{\partial \zeta_g}{\partial t} = -V_g.\nabla(\zeta_g) + \frac{1}{\rho D} curl(\tau_s) \qquad (2\text{-}10)$$

which shows that the variation of the geostraphic current vorticity can be explained in terms of the wind stress vorticity as well as vorticity advection from the neighbouring areas.

Chapter 3

Results and discussions

Results and discussions

The impacts of the large-scale climate patterns on characteristics of the Mediterranean basin over the winter periods are analyzed in this chapter. The circulation in the Mediterranean is induced by the wind forcing, water exchanges through different straits and the buoyancy variations related to the heat and water fluxes (Robinson et al. 2001). Therefore, the variation of these parameters and their relation to the climate patterns are studied. The NAOI, EAI pattern and MOI are considered as the most important indices. The analysis has been done using the correlation coefficients as well as the averages in the positive and negative climatic modes.

The Mediterranean area between 7° W – 37° E and 29° N - 48° N is defined as the study domain.

3-1- Relationship between NAO and the oceanography of the Mediterranean Sea

The correlation coefficient between wintertime NAOI, and temperature and salinity in the upper and intermediate layers of the whole basin were calculated over the winter periods and the spatial distributions are shown in the figure 3-1. The JFM temperature and salinity in the upper layer is affected immediately by the climate index (lag = 0) while in the intermediate layer they are lagging the JFM index by approximately one year due to the delayed response of the intermediate layer to the external forcing.

In general, the upper layer temperature in the WMED and the eastern coasts of Sicily is positively correlated with the winter NAOI while it is out of phase with the index in the EMED (fig. 3-1a). This dipole structure was also shown in different studies (e.g. Trigo et al., 2002; Skliris et al., 2011). In addition, the significant negative correlation coefficient between JFM NAOI and salinity is observed in the upper layer of WMED and the Levantine Sea (fig. 3-1b). Therefore, in the western basin, a high NAOI is associated with the warmer and less saline water, which can be related to the more stable water column and the absence or weakening of the vertical mixing.

In the intermediate layer, both temperature and salinity maintain the same patterns as the upper layer (with about 1-year phase lag) but with the lower correlations especially in WMED.

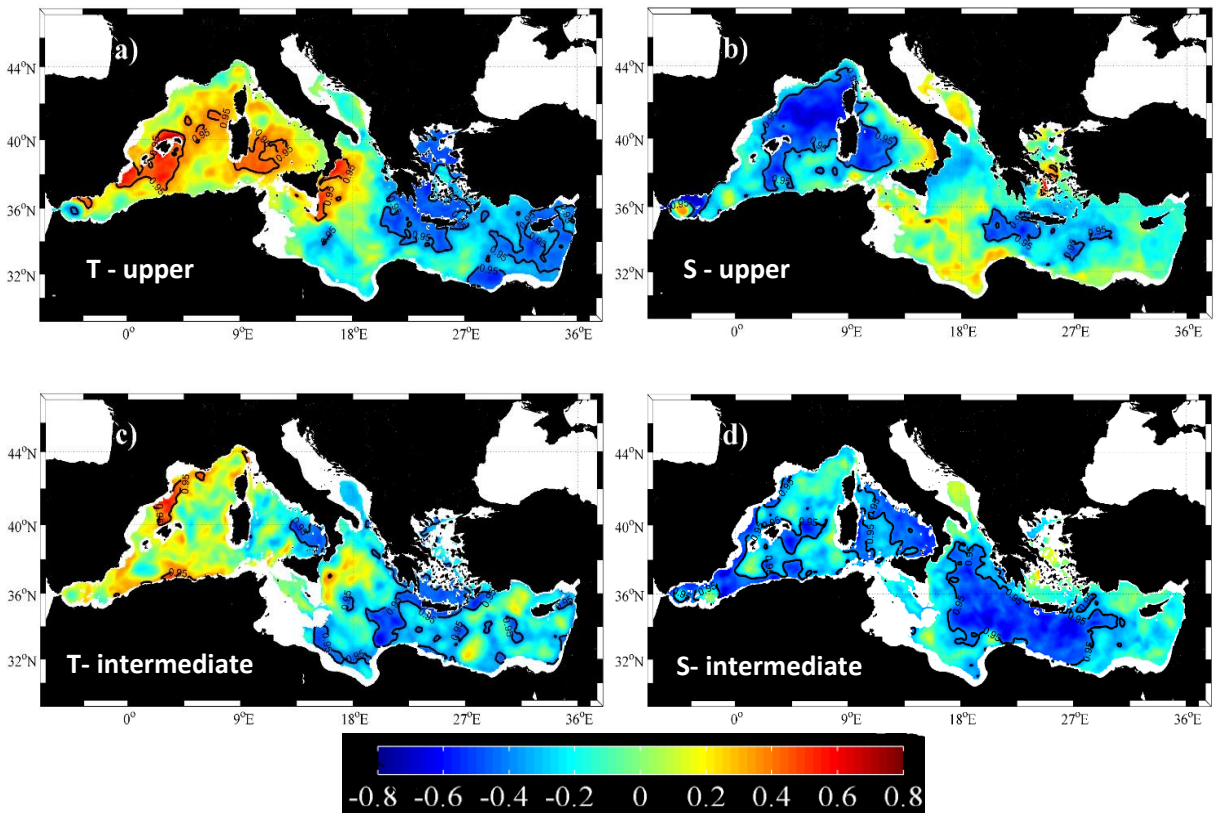

Figure 3- 1 Spatial distribution of the correlation coefficient between JFM NAOI with a) JFM upper layer temperature, b) JFM upper layer salinity, c) JFM intermediate temperature (lag =1 year), and d) JFM intermediate salinity (lag =1 year). The bold black line indicates the isoline of the 95% significance.

Variability of the sea temperature is due to several factors including air-sea heat fluxes and the local ocean processes such as vertical mixing and horizontal advection (Skliris et al. 2011).

The interaction between air and sea in terms of the surface heat fluxes plays a fundamental role in temperature change and, consequently, buoyancy variations, which can lead to the formation of the dense water. Since the dominant components of the net heat exchanges during the winter are latent heat loss and, to a lesser extent, sensible heat loss (Josey 2003), the correlation between wintertime NAOI and net heat flux, latent and sensible heat fluxes are estimated. The downward direction (from the atmosphere to the sea) is defined as positive values. The distribution maps of the correlation coefficients are presented in the figure 3-2. In the period from January to March, the net heat flux (Q_{net}) is significantly in phase with the NAOI in the western basin. The positive anomaly of Q_{net} during the NAOI+ is also demonstrated in other studies (Josey et. al., 2011). The correlation between NAOI and latent heat flux reveals the pattern similar as the one for Q_{net} but

with the lower value of the correlation coefficients. Latent heat is the predominant component determining the net heat exchanges, although according to the Fig. 3-2 both latent and sensible heat fluxes reveal the positive correlation with NAOI in the northwestern basin.

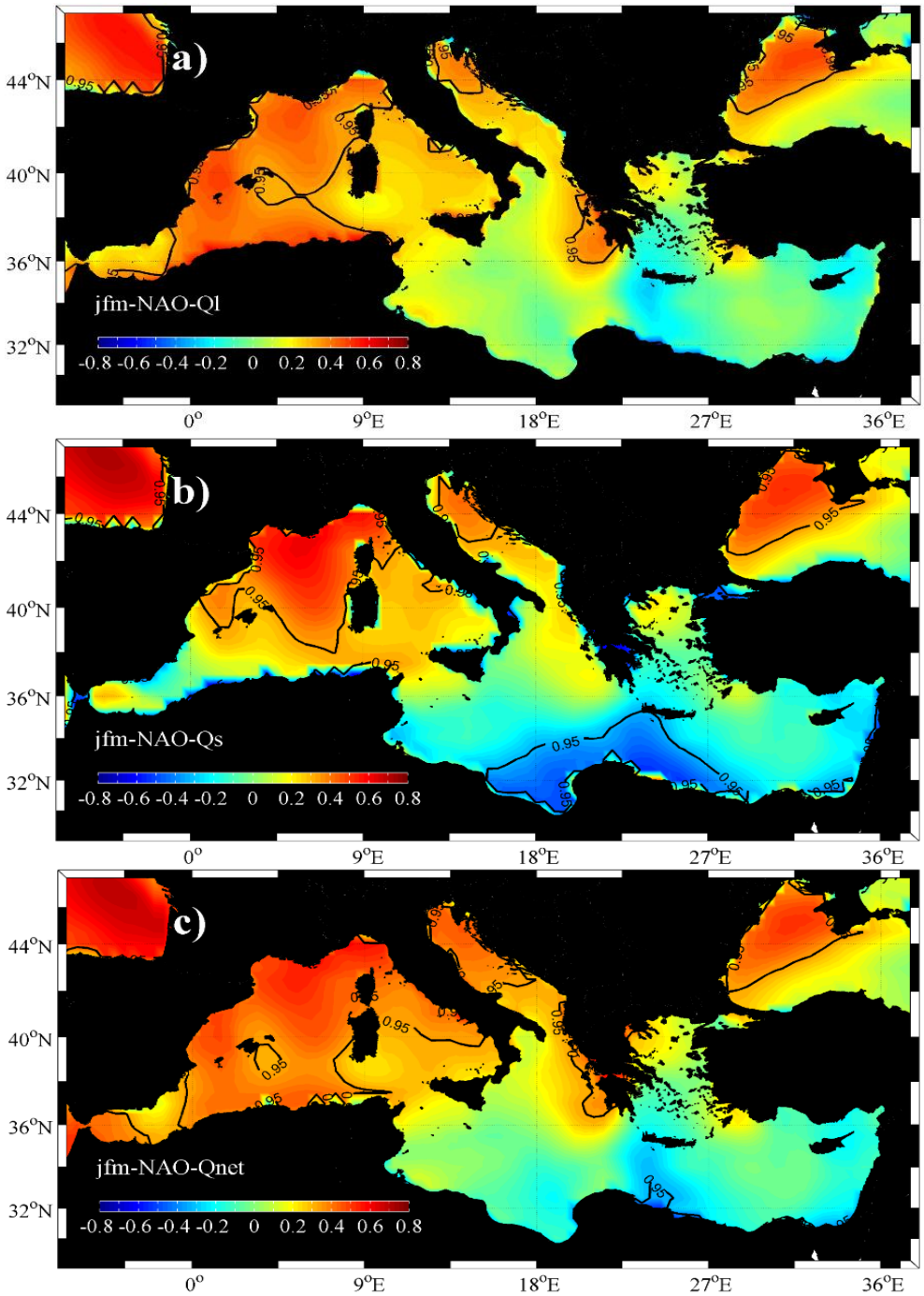

Figure 3- 2 Spatial distribution of the correlation coefficient between JFM NAOI and a) latent heat flux, b) sensible heat flux, c) net heat flux. The bold black line indicates the isoline of the 95% significance.

The average wintertime (JFM) upper layer temperature and salinity anomaly and the net heat flux are calculated for the periods associated with positive and negative NAO modes and shown in the figure 3-3. Since the positive mode of NAO is dominant during the period of study (see Fig. 1-4), we first considered those winter months (JFM) characterized by negative mode of this index to calculate the averages during NAOI-. Then, in order to have the time-series with the same statistical value, we calculated the NAO+ averages considering the winter months corresponded to the highest positive mode of NAO with the same length of time-series as those for NAO- periods. The years used in the calculations representing the periods associated with the positive and negative phases of NAO are indicated in the table 3-1.

Table 3- 1 list of years characterized by positive and negative NAO modes used for calculating the averages and corresponded NAOI

NAOI +					
Year	1989	1990	1993	1995	2000
Index value	1.67	1.30	0.92	1.11	1.02
NAOI -					
Year	1996	2001	2005	2006	2010
Index value	-0.14	-0.19	-0.12	-0.17	-1.32

A high NAOI is associated with a higher than normal temperature and a lower than normal salinity in the western basin (fig. 3-3a and 3-3c). Conversely, the negative anomaly of temperature and positive anomaly of salinity are observed in WMED over the periods characterized by the negative NAOI. This shows that during the positive NAO phase, higher heat flux gives rise to the temperature increase which increases the stability of the water column and consequently, lower salinity in the upper layer. Conversely, the lower heat budget during the negative phase implies the lower temperature and higher salinity associated with the stronger vertical mixing.

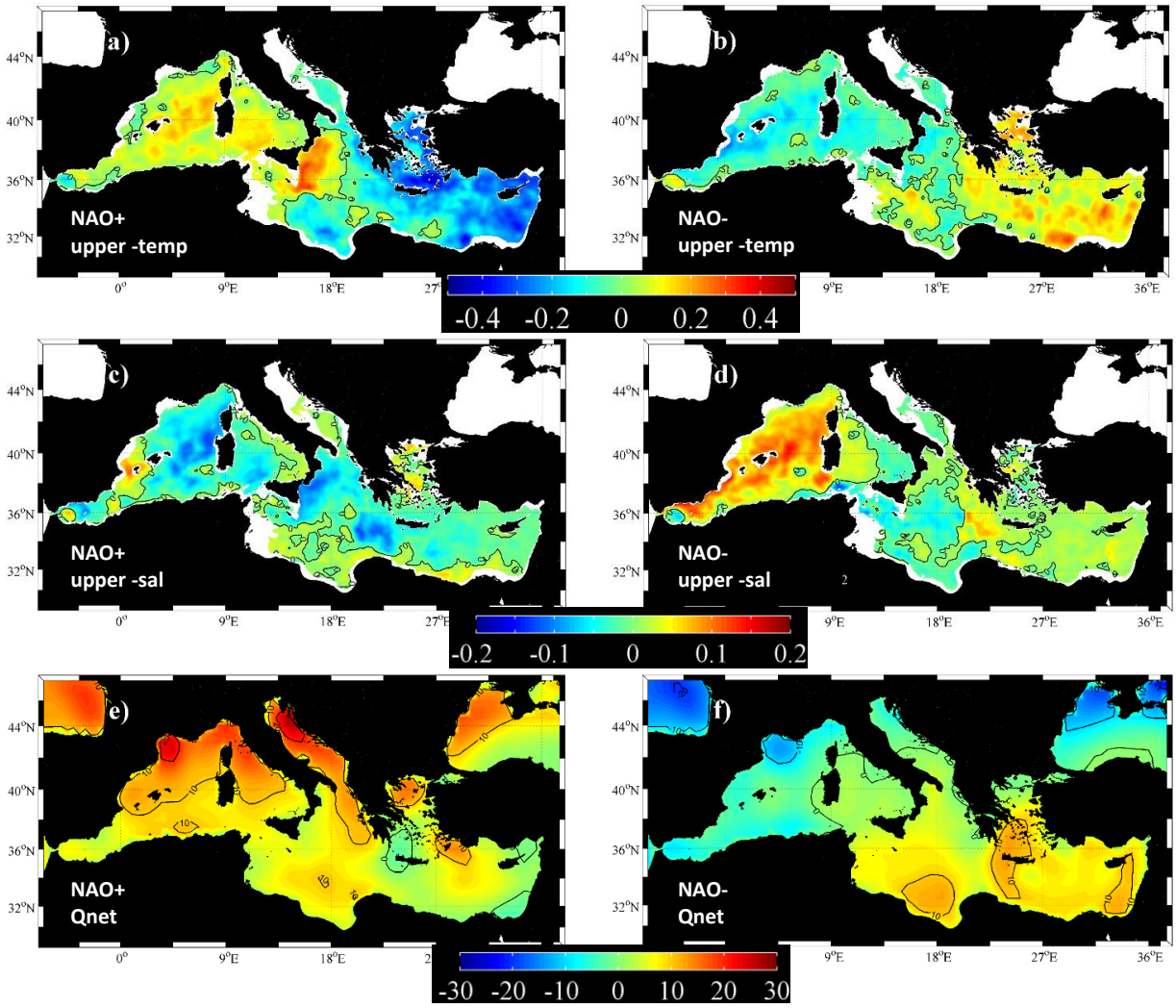

Figure 3- 3 Spatial distribution of the mean JFM a) temperature anomaly ($^{\circ}C$) during NAOI+, b) temperature anomaly ($^{\circ}C$) during NAOI-, c) salinity anomaly during NAOI+, d) salinity anomaly during NAOI-, e) net heat flux (Wm-2) anomaly during NAOI+, f) net heat flux (Wm-2) anomaly during NAOI-. The black contours show the isoline of 0.

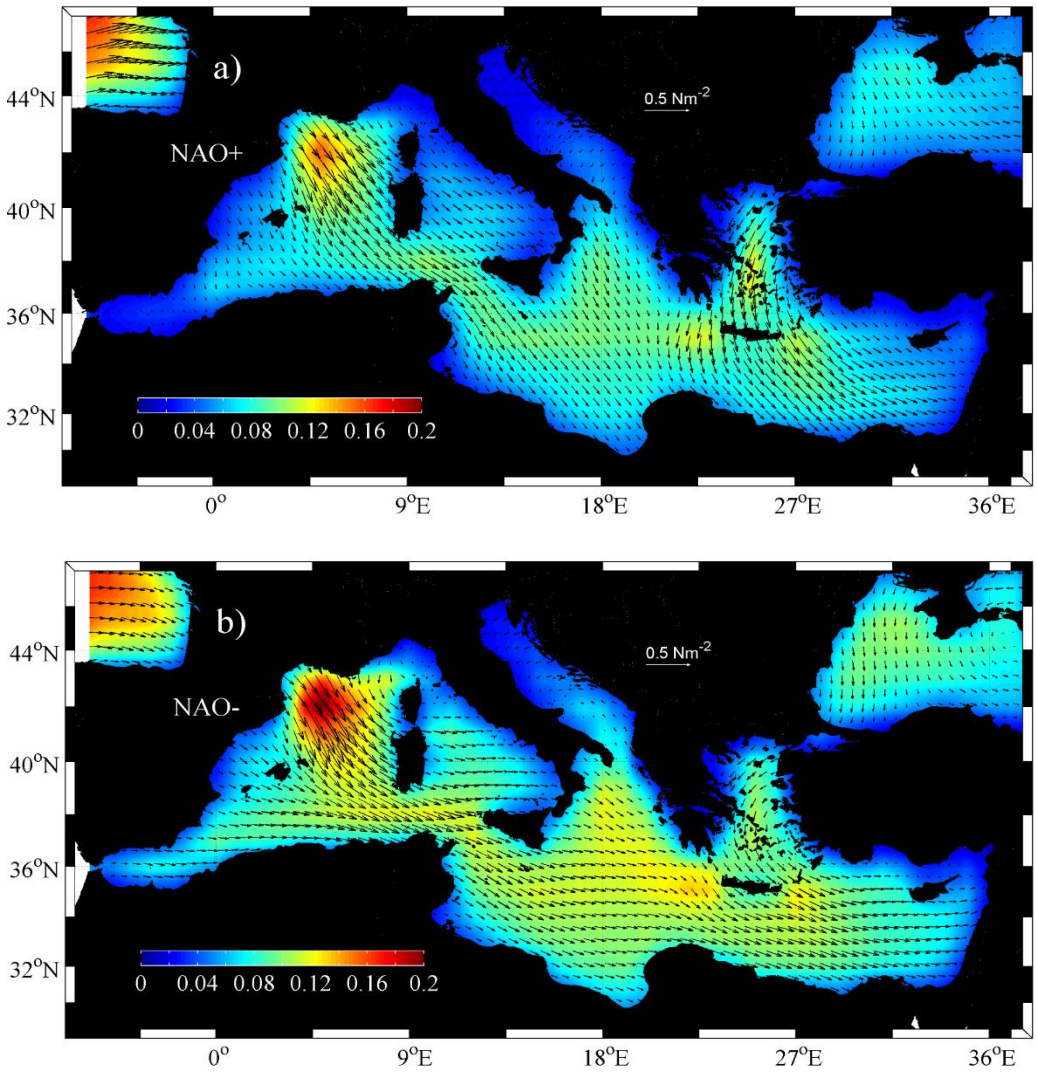

Figure 3- 4 Spatial distribution of the mean JFM wind-stress magnitude (colours; Nm^{-2}) and wind-stress vectors (arrows; Nm^{-2}) in the positive NAO phase (a) and negative NAO phase (b), 1988-2011.

The average of the wind magnitude and wind configuration for the periods characterized by the positive and negative index are demonstrated in the figure 3-4. According to this figure, although the wind direction is more northerly during the NAOI+, the wind speed is stronger all over the basin during the negative mode. The strongest wind magnitude is observed over the Gulf of Lion, which is significantly intensified in the NAOI- periods. The atmospheric pressure patterns confirm this configuration of the wind during two modes of NAO. This supports the idea that the negative mode of NAO is characterized by a more favorable condition for the winter convection and the formation of the WMDW because of stronger heat loss in NAOI-.

According to the vorticity equation (see Eq. 2-10) the important factors responsible for the sea circulation variability are the atmospheric forcing (through the wind stress vorticity) and the internal oceanic processes (advection from the neighboring areas). Therefore, it is worthwhile to study the variation of the wind forcing in response to the climate patterns. Using equations 2-3 and 2-4 (see chapter 2), the components of the wind stress vorticity were estimated and then the correlation coefficients between JFM NAOI and wind speed and vorticity were calculated. The spatial pattern of the correlations is demonstrated in the figure 3-5. The wind vorticity over the WMED, Adriatic Sea, Aegean Sea and generally those parts of the basin located in the latitudes higher than 36 $^{\circ}$ N, are more affected by NAO. Negative correlation is dominant in these areas as the result of the enhancement of the Azores high pressure over the Mediterranean region and the consequent changes in the wind patterns which produce the lower vorticity during the high NAOI periods. More specifically, depending on the phase of NAO, the pressure gradient over the North Atlantic changes in magnitude and orientation, which causes the differences in the speed and direction of winds in mid-latitudes (Lamb and Peppler, 1987). Therefore, in order to assess the influence of the NAO phases on the wind-stress velocity and vorticity in the basin, the average spatial distributions of wind velocities field over the winter months, from January to March, and of the relative wind-stress curl were estimated separately for the years characterized by the positive and negative phases of the JFM NAOI. Then, the average speed and direction of the wind and the strength of the vorticity in two wintertime NAO phases were studied and compared. These spatial distributions are shown in the figure 3-6.

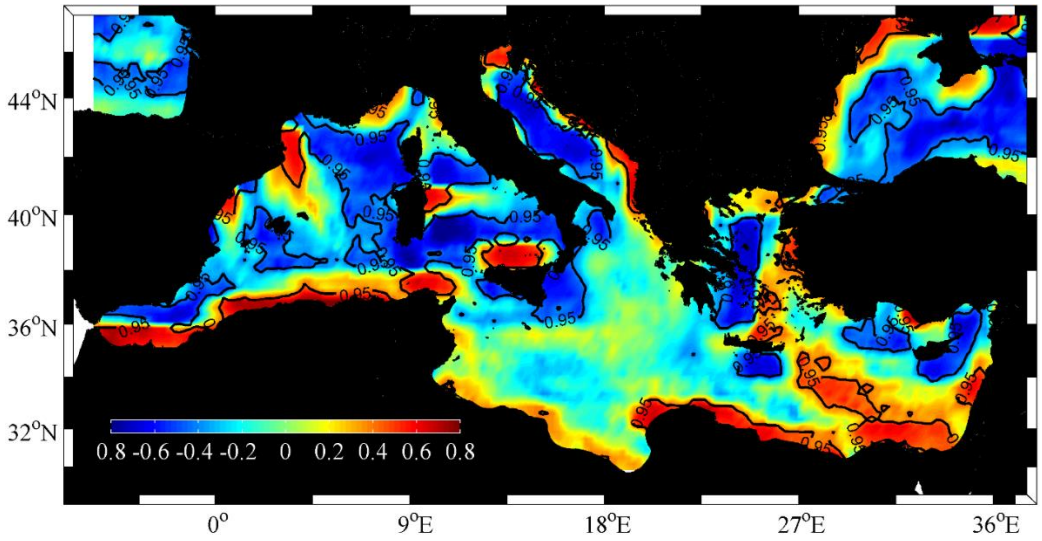

Figure 3- 5 Spatial distribution of the correlation coefficient between JFM NAOI and the wind stress curl. The bold black line indicates the isoline of the 95% significance.

During the positive NAO phase, north-westerlies are dominant in southern Europe and the Mediterranean Sea due to the intensification of the Icelandic Low as well as of the Azores High. Conversely, in the negative phase, the stronger westerlies are observed in these regions (in agreement with Jerez et al., 2013). The difference between wind configuration and circulation over the different sub-basins of the Mediterranean during the positive and negative periods of the NAOI will be discussed later, separately.

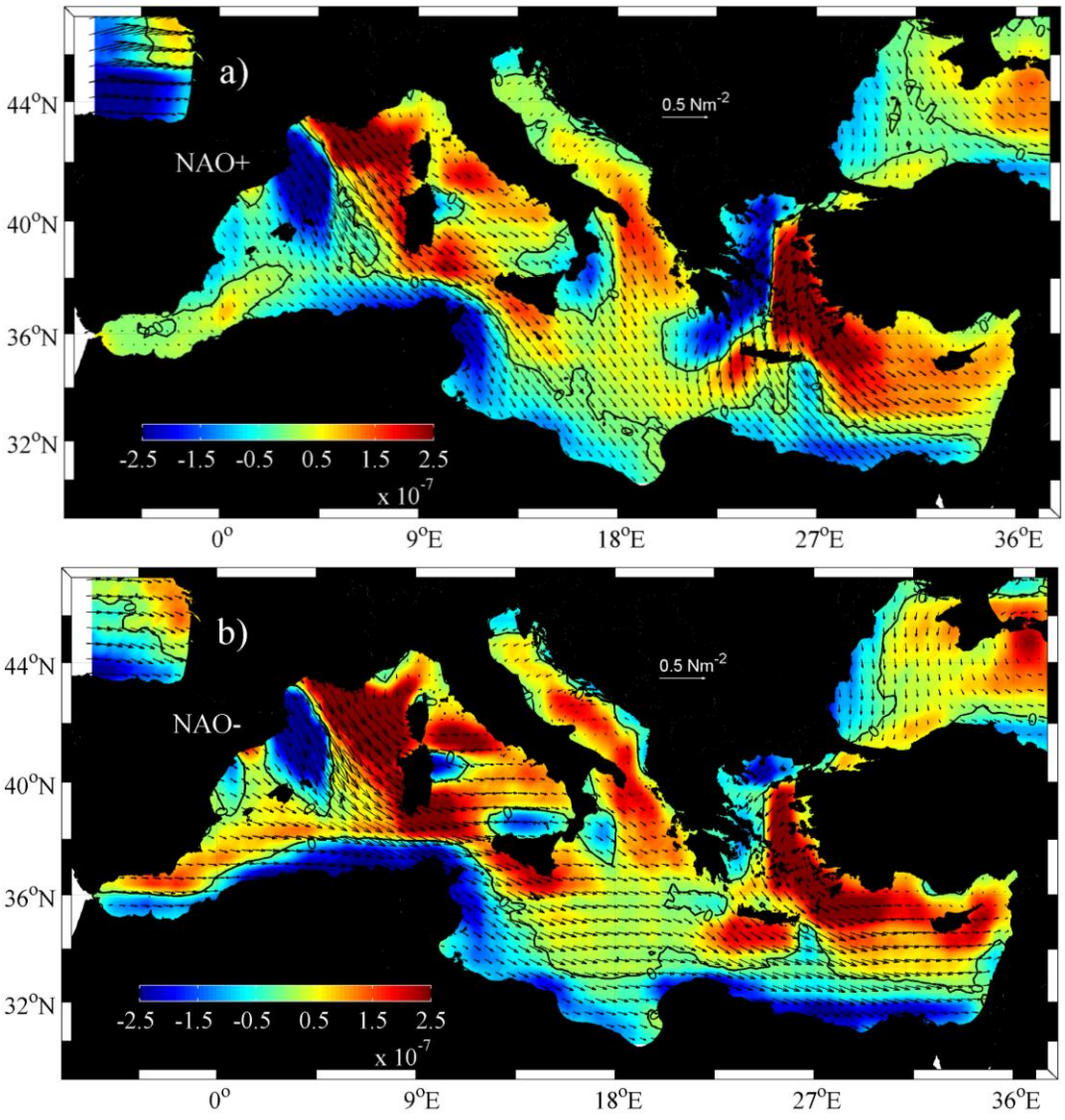

Figure 3- 6 Spatial distribution of the mean JFM wind-stress vorticity (colours; Nm-3) and wind-stress vectors (arrows; Nm-2) in the positive NAO phase (a) and negative NAO phase (b), 1988-2011.

The scatter plots calculated from the average of JFM wind stress curl and NAOI in the main sites of DWF (the averaging areas are presented with the polygons in the figure 3-7) show that vorticity over the South Adriatic Sea, Gulf of Lion and Aegean Sea (see fig. 3-8 a, b and c) are inversely proportional to the NAOI. In other words, the curl of wind stress in these regions is out of phase with the index. In contrast, in the Levantine Sea, the vorticity intensifies during the NAOI+ and the negative NAOI is associated with the weaker wind stress curl. The scatter plot of the winter-time wind stress vorticity and NAOI (fig 3-8d) shows the lower slope.

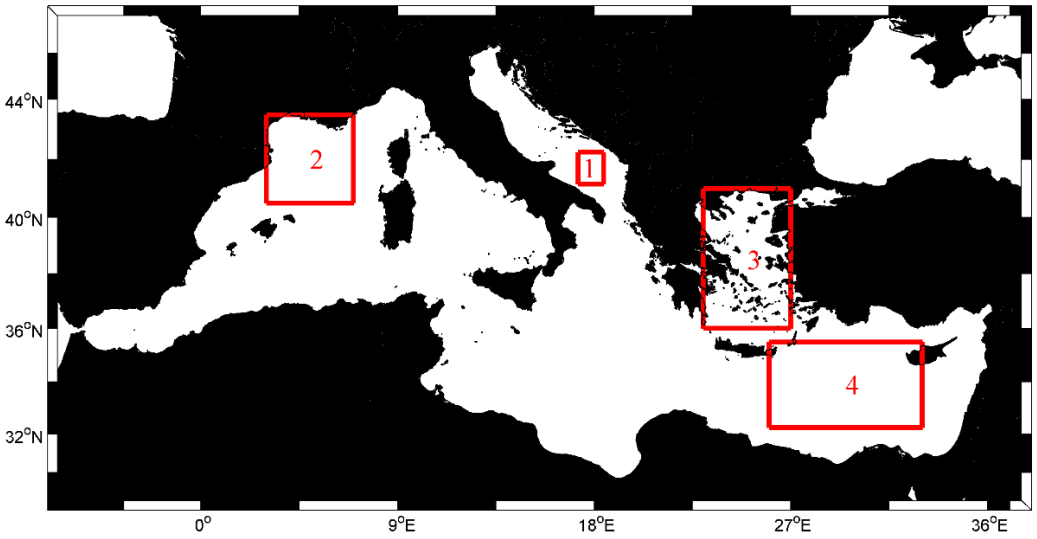

Figure 3- 7 Geography of the Mediterranean Sea. The red polygons show the areas used to estimate the averages in Figure 3-8. Polygons 1, 2, 3 and 4 indicate the areas used for averaging over the South Adriatic Sea, Gulf of Lion, Aegean Sea and Levantine Sea, respectively.

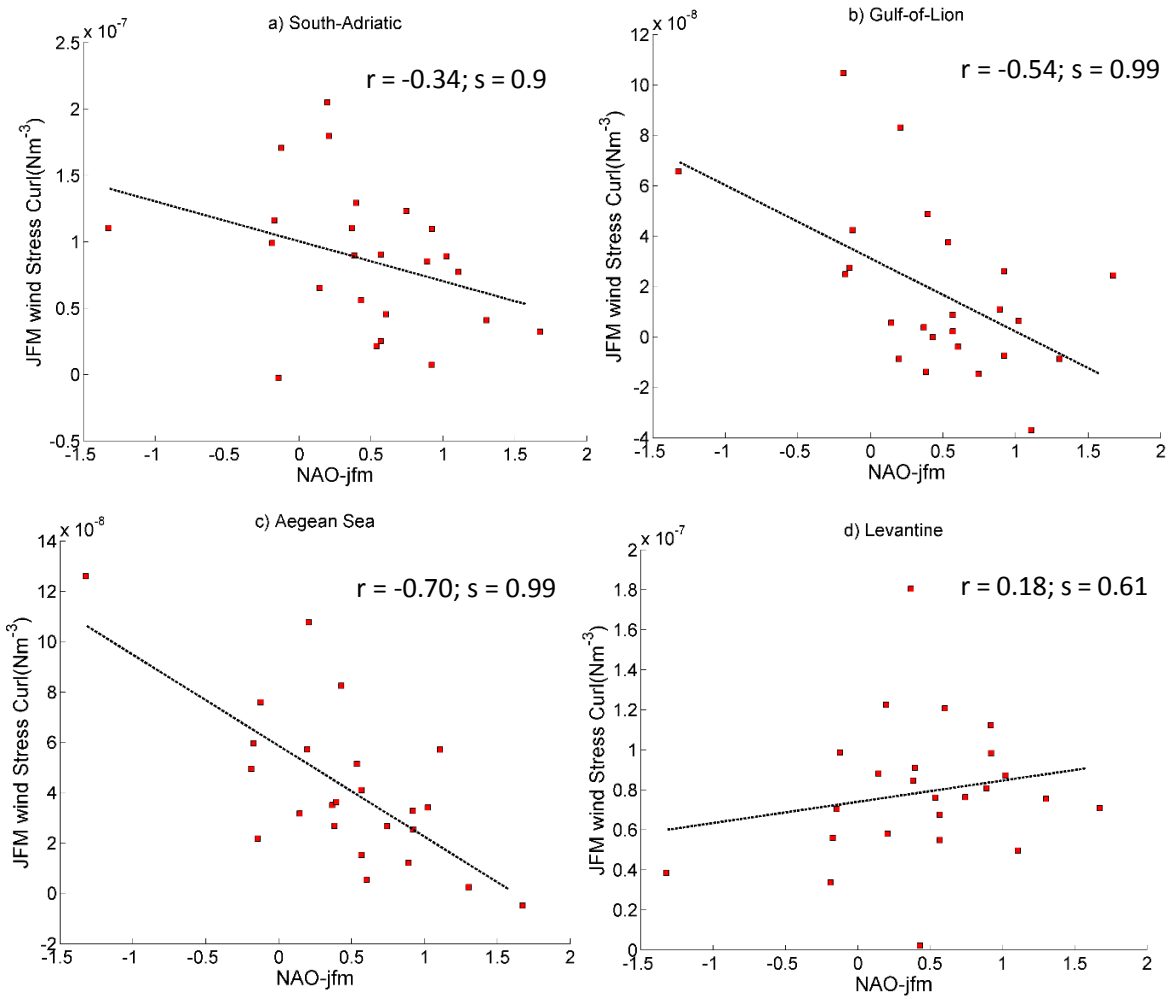

Figure 3- 8 Scatter plots of the wintertime NAOI and the average of the wind stress curl in a) South Adriatic Sea, b) Gulf of Lion, c) Aegean Sea and d) Levantine Sea (sea fig. 3-7 for the averaging areas).

The other factor determining the Mediterranean thermohaline properties, circulation, and formation of dense water, is air-sea water fluxes and exchange of water between the Mediterranean and Atlantic Ocean (Tsimplis et. al., 2006). Variability of the inflow and outflow through the Strait of Gibraltar can be determined to a large extent by the long-term changes in the freshwater deficit (E-P). The Mediterranean Sea is characterized by the negative water budget due to the excess of evaporation over the freshwater input. This can be compensated by the inflow of the relatively warm and fresh AW in the upper layer of the Mediterranean and the outflow of the relatively cool and saltier deep water to the Atlantic Ocean. Large evaporation, especially during the winter, takes place under the influence of the dry and cold northerly winds. Moreover, many studies have shown

the large decrease in the precipitation trend in the Mediterranean region (e.g. Giorgi 2002; Luterbacher et al. 2006). The main source of water in the atmospheric hydrologic cycle in the Mediterranean Sea is the difference between evaporation and precipitation (E-P) (Mariotti et al. 2002). In order to get a better understanding of the processes responsible for the variations of the water budget over the region, it is necessary to take into account the components of the water budget and the impacts of the atmospheric forcing on these components.

For this purpose, the correlation coefficients between the time-series of the wintertime NAOI and E, P and E-P are estimated and the spatial distributions are plotted. These spatial patterns are demonstrated in figure 3-9. The figure shows the low anti-correlation between wintertime evaporation and NAOI in the western basin, North Adriatic and the eastern coasts of the North Ionian Sea, which might be related to the stronger northerlies during the negative phase. In addition, winter precipitation is highly out of phase with this index in those areas of the basin located in the higher latitudes (see Fig. 3-9b). More specifically, NAOI- is associated with the precipitation increase in the major portion of the WMED as well as in the Adriatic, North Ionian and Aegean Seas. This can be explained by the increase of cyclonic activities in these regions due to the weakening of Azores high pressure. However, the precipitation rate over the Balearic Sea doesn't reveal any differences between the two NAO modes, which might be related to the permanent presence of anticyclonic (or weak cyclonic) atmospheric circulation in this area (see Fig. 3-6).

The different fresh water forcing in the western and eastern basin results in the different relative contributions of E and P to the net freshwater fluxes. In the Gulf of Lion, NAOI+ is associated with the strong reduction of P while in the eastern basin, particularly the Levantine basin and the South Aegean Sea the stronger evaporation rate is evidenced which can reinforce the net evaporation during the positive mode (see Fig. 3-10).

These results imply that during the winters characterized by the negative NAOI, the increase in the freshwater input to the areas to the west and the north of the central Mediterranean may reduce the surface buoyancy loss and possibly deep–intermediate water formation. The results are very close to those obtained by Romanou et al. (2010), although there are small differences in the spatial pattern which can be related to the differences in the time periods.

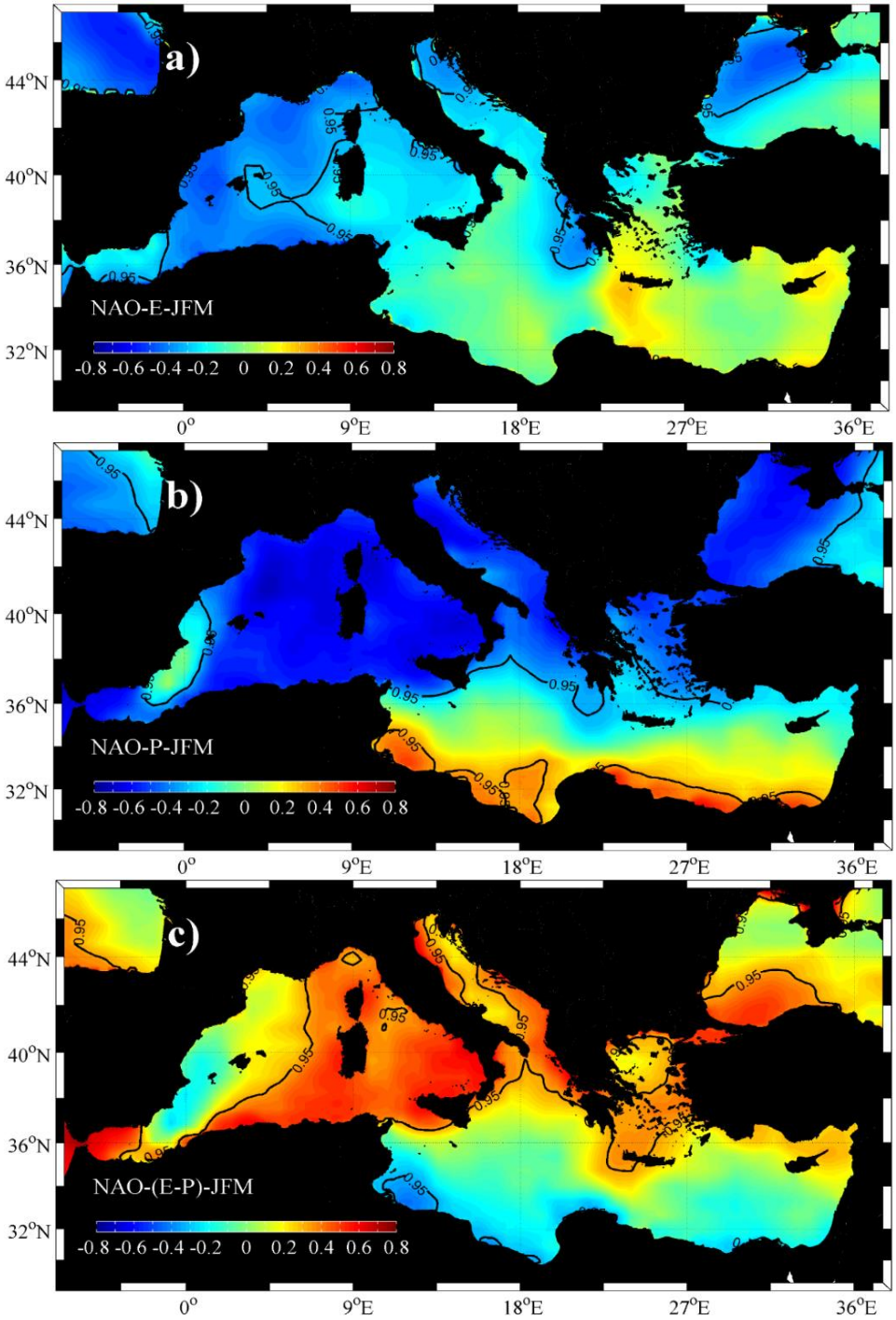

Figure 3- 9 Spatial distribution of the correlation coefficient between JFM NAOI and a) evaporation, b) precipitation and c) evaporation-precipitation. The bold black line indicates the isoline of the 95% significance.

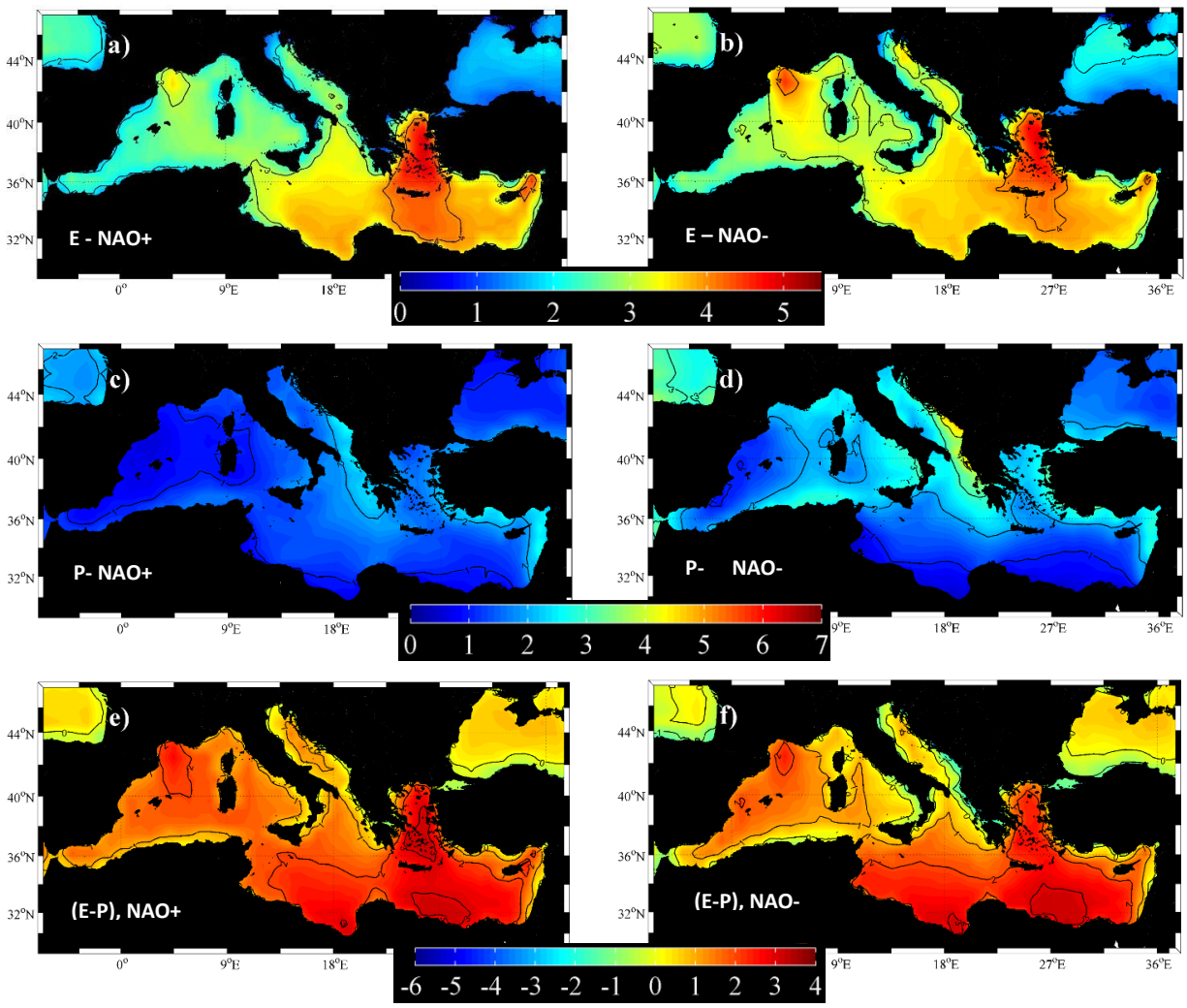

Figure 3- 10 Spatial distribution of the mean JFM a) evaporation during NAOI+, b) evaporation during NAOI-, c) precipitation during NAOI+, d) precipitation during NAOI-, e) net evaporation during NAOI+, f) net evaporation during NAOI- (mm/day). The black contours show the isolines with the interval of 2 mm/day.

The thermohaline circulation of the Mediterranean is partially driven by the buoyancy flux due to freshwater and heat exchanges and the resulting density variations (Robinson et al. 2001). The cooling increases the density of the surface water and decreases the buoyancy. In addition, the buoyancy will be reduced by the increasing the salinity due to the evaporation. Therefore, by reducing the temperature or increasing the salinity, the water is made denser and sinks to the deeper layer. Conversely, heating and precipitation give rise to the buoyancy increase of the water.

The contribution of the heat and water fluxes to the buoyancy of the water is shown in Eq. 2-2 (see chapter 2). Distribution of the correlation coefficients between JFM NAOI and net buoyancy

flux as well as thermal, evaporation and precipitation components are shown in the Fig. 3-11. The positive values represent the downward direction or buoyancy gain. The figures show the significant positive correlation between net buoyancy flux and NAOI in the WMED and North Adriatic Sea. Higher evaporation and heat loss associated with the NAOI- in the northwest of the basin increase the buoyancy loss in this mode. The same conditions during the NAOI+ reduce the buoyancy in the eastern basin. On the other hand, the higher precipitation in the WMED during the negative mode increases the buoyancy but the thermal effect is dominant and so, the net buoyancy is in phase with the index.

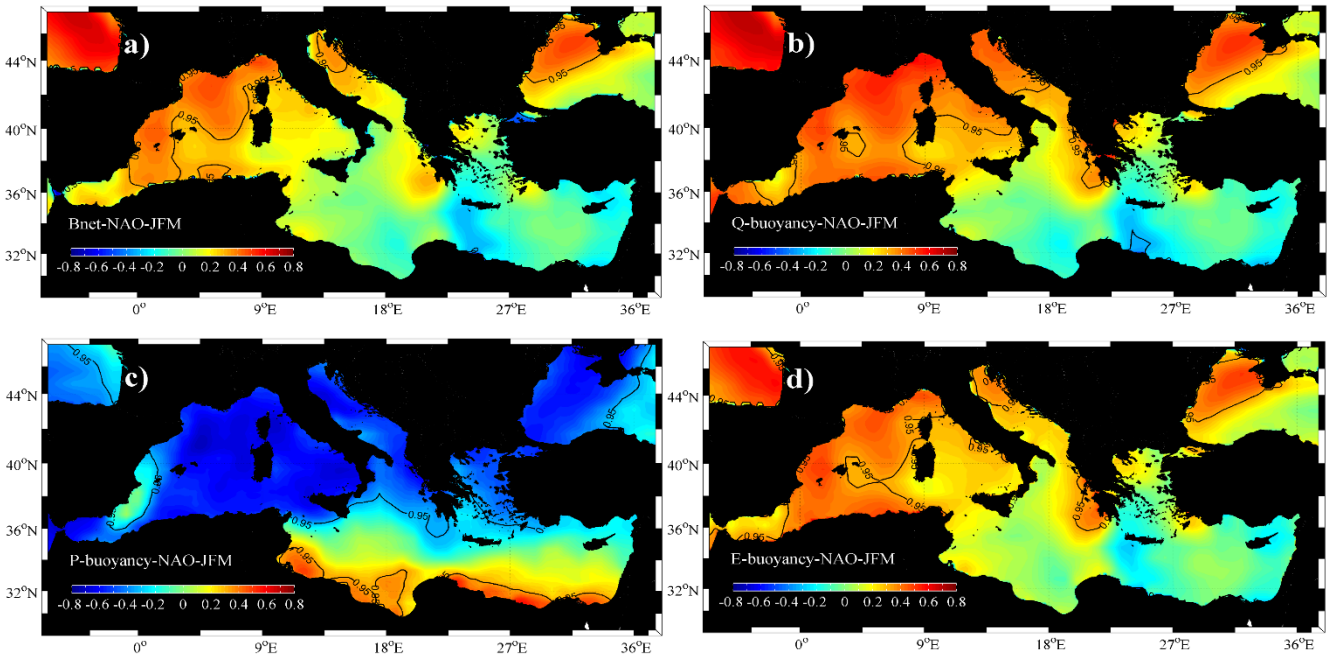

Figure 3- 11 Spatial distribution of the correlation coefficient between JFM NAOI and a) net buoyancy flux, b) thermal buoyancy flux, c) precipitation buoyancy flux and d) evaporation buoyancy flux. The bold black line indicates the isoline of the 95% significance.

Oceanic processes, in terms of the steric and mass variations and atmospheric changes through the pressure and wind configuration, are the forcing parameters responsible for the sea level variations (Tsimplis et al., 2011). Since the atmospheric pressure and wind configuration are highly influenced by the climate indices, correlation coefficient between JFM NAOI, and sea level height is estimated in order to assess the impact of the climate pattern on the sea level (Figure 3-12). In agreement with the other studies (e.g. Tsimplis and Shaw, 2008) sea level height is out of phase with NAOI. The higher atmospheric pressure associated with the positive mode reduces the

sea level over the basin. However, NIG and the meso-scale anticyclonic features such as Mersa-Matruh, Ierapetra and Algerian gyres and African current seem to be unaffected by the index. This implies that internal mechanisms and meso-scale processes are responsible for the circulation of the gyres and the variation of the sea level in these areas. In the rest of the basin, particularly in the Adriatic and the Aegean Sea and in the south of Sicily, the sea level is strongly influenced by this climate pattern.

The negative anomaly of the sea level is observed during the positive phase, while the NAOI- is associated with the above normal sea level height. The impact of NAO on the sea level height of the central and Eastern Mediterranean is more pronounced than that of western basin (see Fig. 3-13).

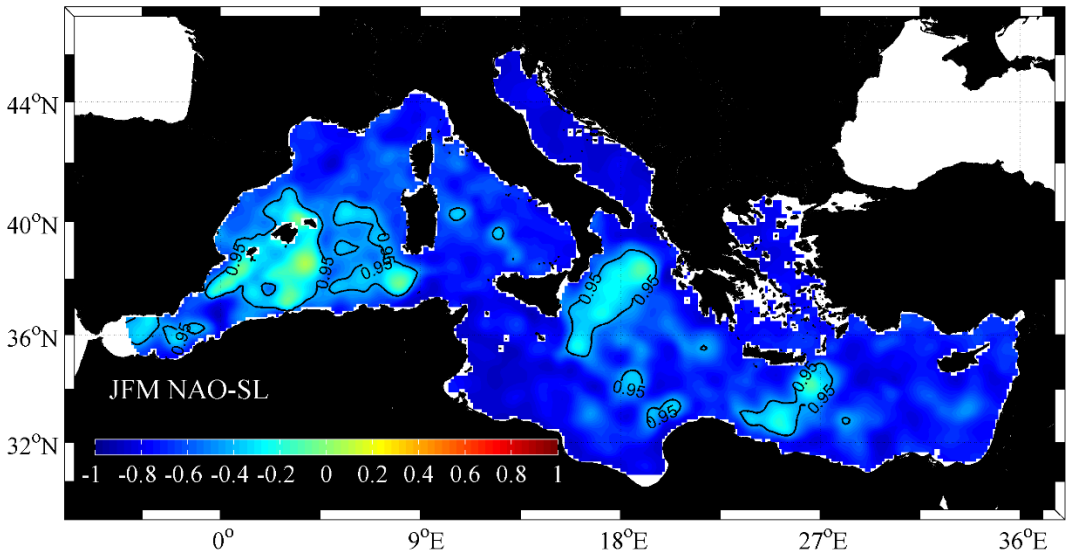

Figure 3- 12 Spatial distribution of the correlation coefficient between JFM NAOI and seal level height. The bold black line indicates the isoline of the 95% significance.

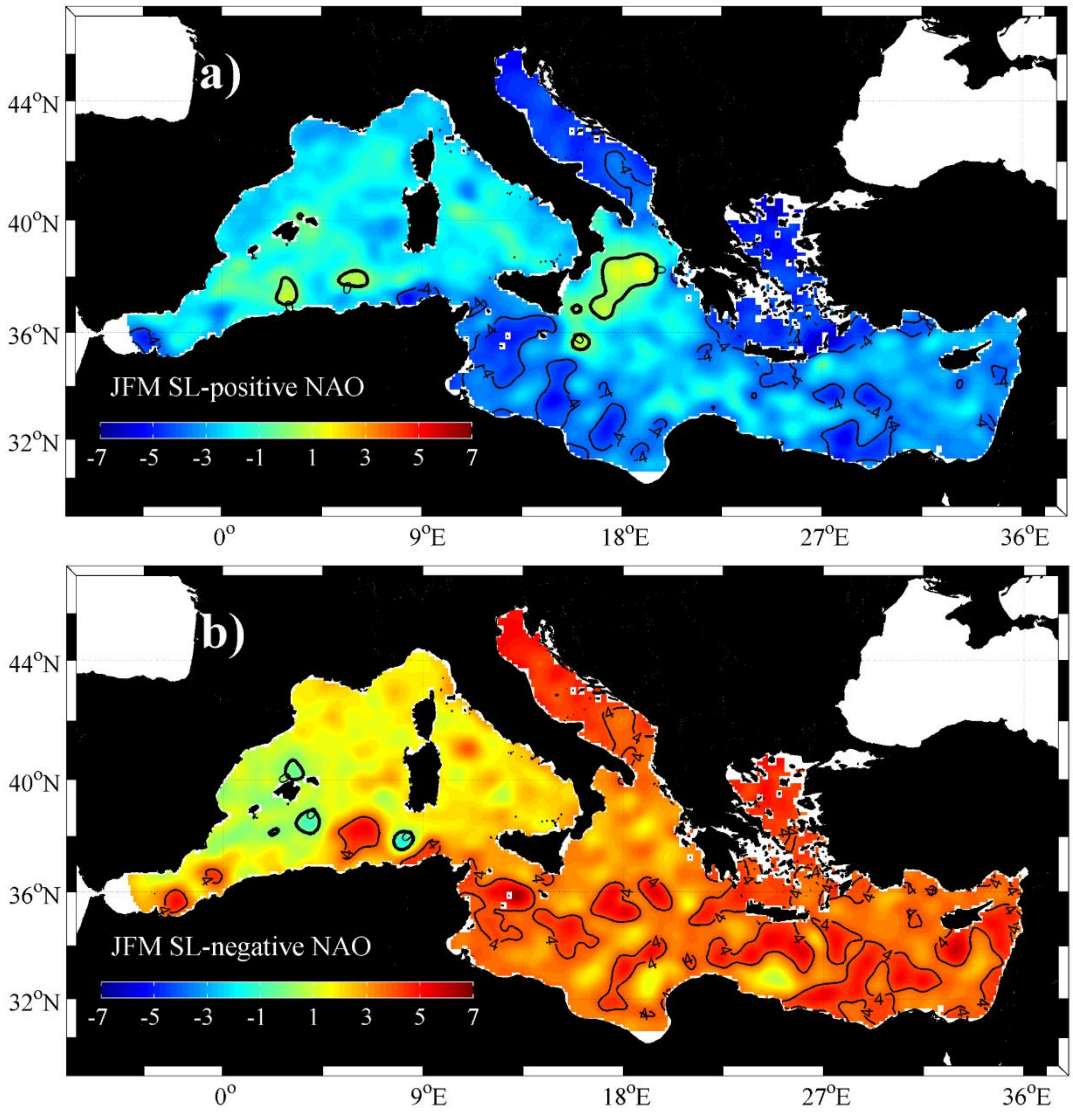

Figure 3- 13 Spatial distribution of the JFM mean of the sea level height anomaly during a) NAOI+ and b) NAOI-. The black contours indicate the isolines of the sea level with the interval of 2cm and the bold black line shows the isoline of 0.

3-2- Impacts of NAO on the Mediterranean sub-regions

Since some differences in the effects of NAO on the thermohaline properties are evident in parts of the basin, the response of some sub-basins to the climate pattern will be discussed here separately in terms of the changes in the wind pattern, heat and water exchanges and the buoyancy fluxes.

– **Gulf of Lion**

Gulf of Lion, located in the northwestern Mediterranean, is the main source of deep water formation and winter mixing in the western basin. The cyclonic circulation due to the westward flow of the northern current along the French coast and its eastward recirculation at the south of the convection area represents the preconditioning for the deep convection in this region (Millot 1987; Schott et al. 1996).

The AW occupies the surface layer from the top to the depth of 150 m which overlies the warmer and saltier LIW from 150 to 500 m and the deeper layer is filled by the WMDW. The deep convection takes place under the influence of the cold and dry mistral wind from the Rhone Valley and the tramontana wind from the north side of the Pyrenees leading to strong latent and sensible heat loss during the winter (Leaman and Schott 1991). The strong wind forcing erodes the near-surface and intermediate-layer buoyancy and forms the deep convection (Mertens and Schott 1998).

The average of the wind vorticity during the positive and the negative modes of NAO (Fig. 3-6) show that in the Gulf of Lion, mistral produces the positive vorticity (low atmospheric pressure) over the eastern side of the Gulf of Lion while the anticyclonic vorticity pattern (high pressure centre) is generated by the tramontane. The stronger zonal wind (*u)* during the negative NAOI, enhances the circulation in both pressure centres and therefore, the correlation between NAOI and wind stress vorticity reveals a dipole structure with the positive value on the west and negative correlation on the eastern side of the Gulf of Lion. However, the spatial average of the wind vorticity over the gulf of Lion is out of phase with the NAOI (Fig 3-8a).

The correlation between heat fluxes and NAOI during the winter (Fig. 3-2) shows that the heat flux components are in phase with NAOI in the Gulf of Lion. This can be explained by the stronger wind magnitude (see Fig. 3-4b) which increases the evaporation rate during the negative phase (Fig 3-10b). Therefore, the temperature decreases due to the cooling, while the salinity increases through the stronger evaporation which consequently reduces the buoyancy of the surface water. On the other hand, the negative mode is associated with the higher precipitation rate as a result of weakening of the Azores high and the lower atmospheric pressure over the Mediterranean particularly over the Gulf of Lion. Higher precipitation, in other words the fresher water flux from the atmosphere, increases the buoyancy during the NAOI- but the cooling effects are dominant.

Hence, the enhancement of the buoyancy loss during the negative phase provides the better conditions for the winter mixing and consequent deep water formation in this mode.

On the contrary, the positive NAO mode is associated with the lower magnitude of the wind which decreases the evaporation rate and the subsequent heat loss. Therefore, in comparison with the negative phase, NAOI+ is associated with the warmer and less salty surface water in the Gulf of Lion, which increases the stability and buoyancy of the water.

– **Alboran Sea**

The westernmost Mediterranean sub-basin is the Alboran Sea. The water exchange between the Mediterranean and the Atlantic Ocean through the Strait of Gibraltar takes place due to the excess of evaporation over precipitation and river runoff in the Mediterranean and produces the thermohaline circulation in the Alboran Sea which can be summarized by the inflow of the AW at the surface into the Alboran Sea and the outflow of the saltier and denser Mediterranean water at the deeper level toward the Atlantic. Moving eastward, AW changes its properties due to sea-air fluxes and the resulted mixing (Vargas-Yáñez et al, 2002). The rapid Atlantic current surrounds and feeds two anticyclonic gyres known by the Western Alboran Gyre (WAG) and the Eastern Alboran Gyre (EAG) which are subjected to the high temporal variability due to meteorological forcing (Cheney and Doblar, 1982). Atlantic inflow intensifies and moves southward by decreasing the atmospheric pressure over the WMED (Crepon 1965; Cheney and Doblar 1982; and Parrilla 1984).

The correlation between wintertime NAOI and temperature and salinity (figure 3-1) shows the different behavior of the WAG with respect to the rest of the western basin in response to NAO. More specifically, during the negative NAOI periods, WAG is characterized by the warmer and less salty water while in rest of WMED these conditions are evident in the positive mode and these characteristics are extended to the intermediate layer. This can be explained by the enhancement of the westerlies over the Alboran Sea (see figure 3-4) so-called ‘Poniente’ (Lionello et al, 2006; 2012) as a consequence of the lower atmospheric pressure over the Azores during the NAOI-. By decreasing the atmospheric pressure during the NAOI-, Atlantic inflow intensifies and moves southward. (Crepon 1965; Cheney and Doblar 1982; and Parrilla 1984). The westerly wind induces coastal upwelling mechanism near the Spanish coast, the water is transported offshore and sinks where it meets the less dense AW (Sarhan et al 2000). Figure 3-14 shows the vertical profile of

the average of the salinity along the 4.5 ° W for periods characterized by the NAOI+ (b) and NAOI- (c). The location of the cross-section is demonstrated in the Fig.3-14a. The doming of the isohaline close to the Spanish coasts (36.4 ° N) and the stronger vertical gradient of the salinity are clear during the negative mode (Fig. 3-14c). The figure also reveals the intensification of the AW inflow and sinking of the less salty surface water in the centre of the WAG in NAOI-. Furthermore, the more inflow of the AW causes the more outflow of the LIW to the Atlantic Ocean due to the mass conservation. This is evident in the location of the isoline of the 38.5 in the negative mode. On the other hand, during the positive phase the wind forcing diminished and the westerlies are not observed anymore (see figure 3-14b). Therefore, the upwelling mechanism and the subsequent southward transport of the less saline surface water don't take place and therefore, SAG is occupied by the relatively colder and saltier water.

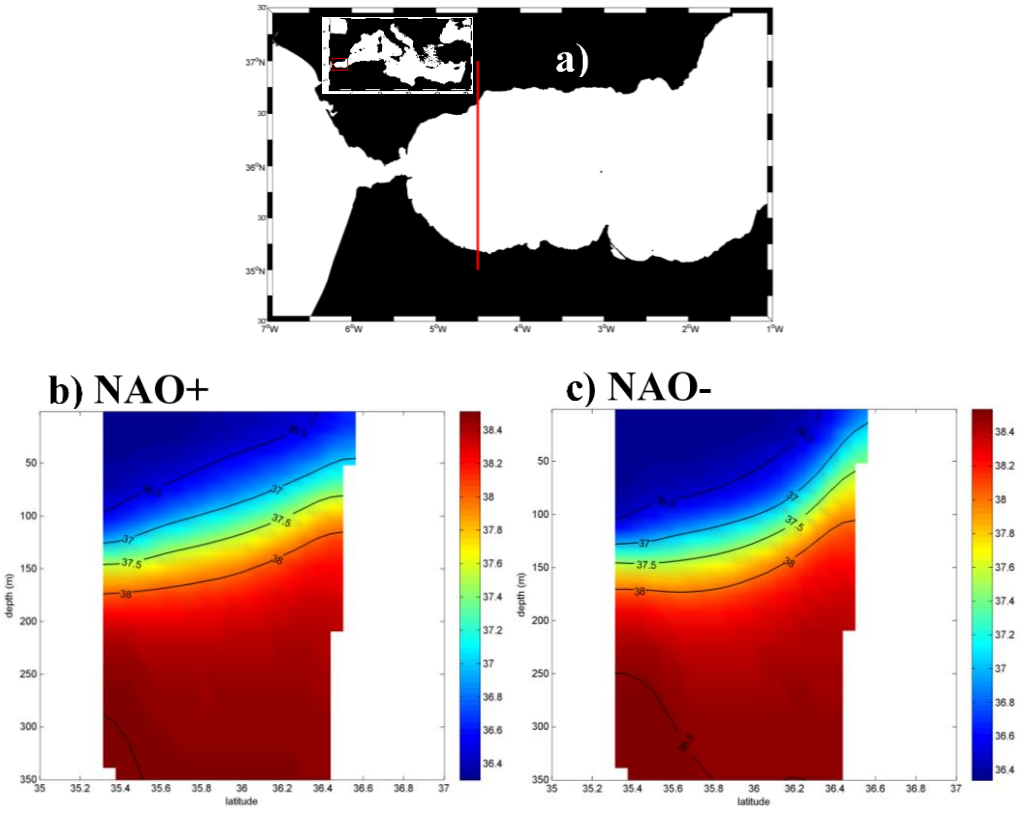

Figure 3- 14 The location of the Alboran Sea (red box) and the vertical profile (red line) a); the vertical profile of the average of the salinity along the 4.5 W for the periods associated with the b) NAOI+ and c) NAOI-. The black contours show the iso-halines with the spacing of the 0.5.

– **Adriatic Sea**

The Adriatic Sea is a semi-enclosed elongated basin located at the northernmost part of the central Mediterranean which connects to the Ionian Sea through the Strait of Otranto. It is divided into three sub-basins: The Northern Adriatic (NA) characterized by the shallow shelf area with the maximum depth of around 100 m. The Middle Adriatic (MA) (maximum depth∼250 m) located in the centre of the basin and the South Adriatic Sea includes the SAP where the bathymetry reaches 1200 m. The Adriatic Sea is the main site of the EMDWF. The major contribution of the Adriatic Deep Water (ADW) is formed in the SAP by the open convection mechanism within the cyclonic circulation in the SAG and the remaining portion is produced in the continental shelf of the NA and MA, moves southward and ultimately sinks to the bottom of the SAP (Ovchinnikov et al., 1985; Bignami et al., 1990; Malanotte-Rizzoli, 1991). The surface buoyancy loss resulted from the blowing the cold and dry Bora wind during the winter and presence of the LIW at the intermediate layers of the Adriatic Sea are the factors facilitating DWF in this area. The deep water formed in the Adriatic Sea then enters the bottom layer of the Ionian Sea through the Otranto Strait (Ovchinnikov et al., 1987; POEM Group, 1992, Mantziafou and Lascaratos, 2008).

Although the Adriatic Sea is highly affected by the meteorological conditions through the wind forcing and resulted heat exchanges, the temperature and salinity in the basin are not affected by the index. As the figures 3-1, 3-3 and 3-4 show, the negative NAO mode increases the water heat loss in the north of the basin due to the intensification of the north-easterlies (Bora wind). Therefore the NAOI- is associated with stronger evaporation rate in the North Adriatic Sea (please refer to Fig. 3-10b). However, there is no evidence of the relation between heat fluxes and temperature of the South Adriatic Sea. This suggests that the air-sea heat exchanges cannot be the only mechanism determining the thermohaline characteristics of the Adriatic Sea and the impacts of the internal processes should also be taken into consideration. In the South Adriatic Sea the wind configuration reveals the different pattern. Positive NAO phase is associated with the dry and cold north-easterlies and the low-pressure centre exists over the SA which generates the cyclonic atmospheric circulation in the Adriatic Sea with the maximum vorticity in over the southern parts. On the other hand, in the negative mode, the southerlies are observed over the Croatian coasts of the SA which intensifies the cyclonic circulation.

Therefore, in the Adriatic, particularly in the SAG, the wind vorticity is out of phase with NAO modes. The scatter plots of the average of the JFM wind stress curl and NAOI (see Fig 3-8a) shows

that wind vorticity is inversely proportional to the NAOI in this area. Moreover, the winter precipitation is out of phase with the index over the Adriatic Sea. This is due to the lower atmospheric pressure during the NAOI- which provides the better conditions for the rise in the precipitation. By increasing the precipitation in the negative mode, the net evaporation is reduced and so, it is in phase with the index over the most parts of the Adriatic. The long-term variability of the circulation in the South Adriatic Sea and its relation to the climate patterns will be discussed in the next chapter.

Long-term variability of the South Adriatic circulation in relation to NAO

Calculations of the spatially averaged current vorticity (see Fig. 3-15 for the averaging area and Fig. 3-16b for current vorticity variation) show that the South Adriatic was characterized, as expected, by a permanent positive vorticity since the SAG is a cyclonic circulation feature. Nevertheless, prominent interannual or decadal variability was present in the time-series (Fig. 3-16). The interannual variability prevailed also in the wind-stress curl (Fig. 3-16a), while decadal variability was prevalent in the vorticity field of the northern Ionian (Fig. 3-16c). In fact, the vorticity field in the northern Ionian is mainly subject to decadal variability due to BiOS (Gačić et al., 2010) as opposed to the Adriatic current vorticity and the wind-stress curl. The vorticity of the wind field was positive for the major part of the record with only short periods of negative values (Fig. 3-16a).

Considering the flow vorticity equation (2-10), interannual variability of the intensity of the geostrophic cyclonic circulation in the South Adriatic can be only partially explained in terms of the local wind vorticity input, this last one being prevalently positive. Thus in addition to the local wind curl effect, the vorticity advection from adjacent area should be taken into consideration (Shabrang et al., 2016).

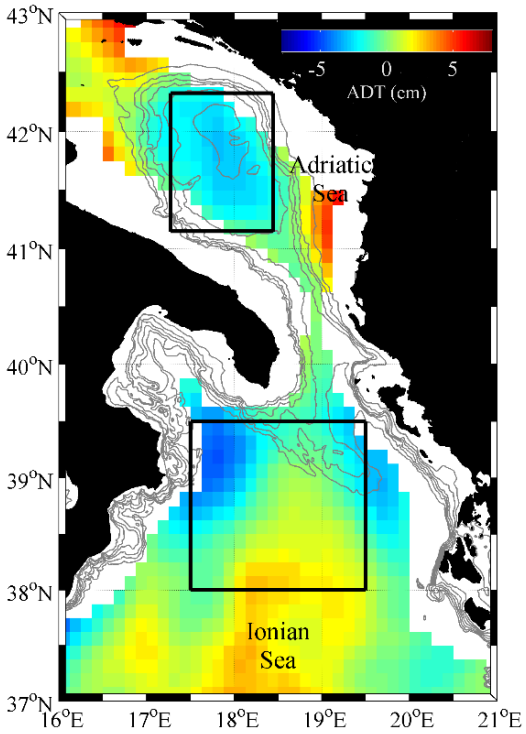

Figure 3- 15 Geography of the South Adriatic and North Ionian Seas. The black squares show the areas used to estimate the time-series in Figure 3-16. The grey contours indicate the isobaths between 200 m and 1200 m with the 200 m line space. Colours show the mean altimetry pattern in the period October 1992-December 2013; altimetry grid points located within 50 km from the coast have been deleted. The Adriatic square includes 81 altimetry measurement points; the Ionian square includes 232 altimetry measurement points.

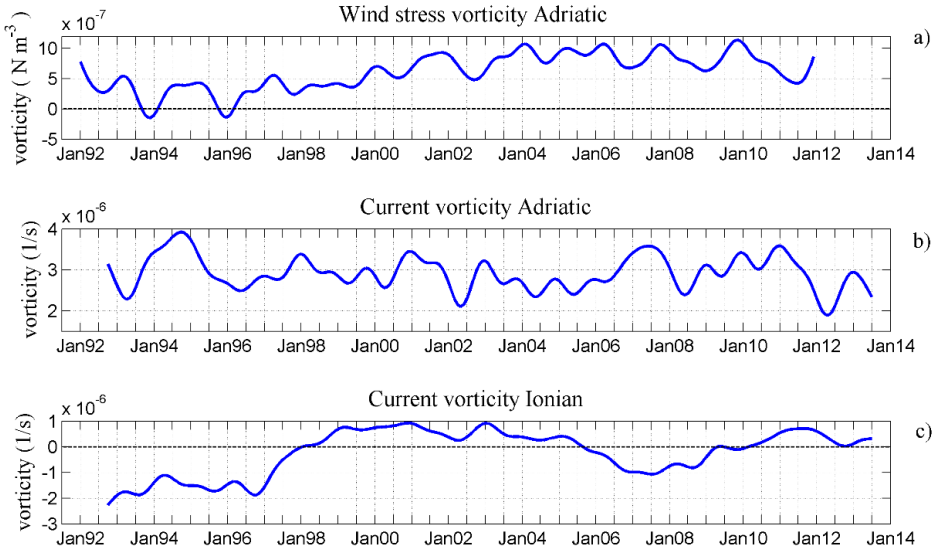

Figure 3- 16 Time-series of the spatially averaged, low-pass filtered (thirteen months), wind-stress vorticity (a) and current vorticity (b) in the Adriatic Sea, computed over the domain denoted in Figure 3-15. Time-series of the low-pass filtered current vorticity in the Ionian Sea (c) spatially averaged over the domain presented in Figure 3-15.

First, to estimate the importance of the local input in the vorticity equation, we compared the time-series of the current vorticity tendency with the curl of the wind-stress over the winter months, from January to March (hereafter we refer to this time period as JFM), calculating the linear correlation coefficient in each data point of the study domain. Wintertime values were chosen because strong air-sea interaction (wind forcing and possible relationship to NAO) occurs during the winter months when deep convection takes place. As it follows from the vorticity equation (Eq. 2-10) the vorticity tendency and the wind-stress curl should be positively correlated.

The spatial distribution of the correlation coefficients over the study area shows rather patchy pattern. The area of the significant positive correlation ($r \geq 0.6; s \geq 0.95$) northeast of the gyre (see Fig. 3-17a) coincides rather well with the maximum of the current vorticity average (Fig. 3-17b) and there probably the main wind vorticity input takes place. This suggests that in a limited area the Ekman suction controls the strength of the SAG determining the strength of the gyre. In the centre of the gyre, the correlation diminishes probably due to the generally small values of the current vorticity. In addition, some small-scale features characterized by the negative correlation are present west and south of the gyre, which can be explained in terms of the vortex stretching due to strong bathymetric features. The significant negative correlation ($r \leq -0.5; s \geq 0.95$) west of the gyre (around $17^{\circ}15'E$ and $41^{\circ}40'N$) is probably due to the topographic anomaly near the Bari Canyon (Cushman-Roisin et al., 2001) which may generate strong ageostrophic divergence. Therefore, in accordance with the quasi-geostrophic equation of the vorticity conservation, the mechanism partially responsible for the variations of the current vorticity is the wind-stress curl acting in a limited area of the SAG. The fact that direct forcing from the wind-stress curl could be an important mechanism determining the vorticity of the mean circulation pattern was also evidenced in some large lakes (Schwab and Beletsky, 2003).

Second term, which may contribute to the vorticity tendency in the SAP is the advection term. In order to study the extent to which the vorticity advection from the Ionian plays a role in controlling the curl of the flow in the South Adriatic, we first calculated the lagged correlation between the spatially averaged vorticity in the northern Ionian and South Adriatic (figure not shown).

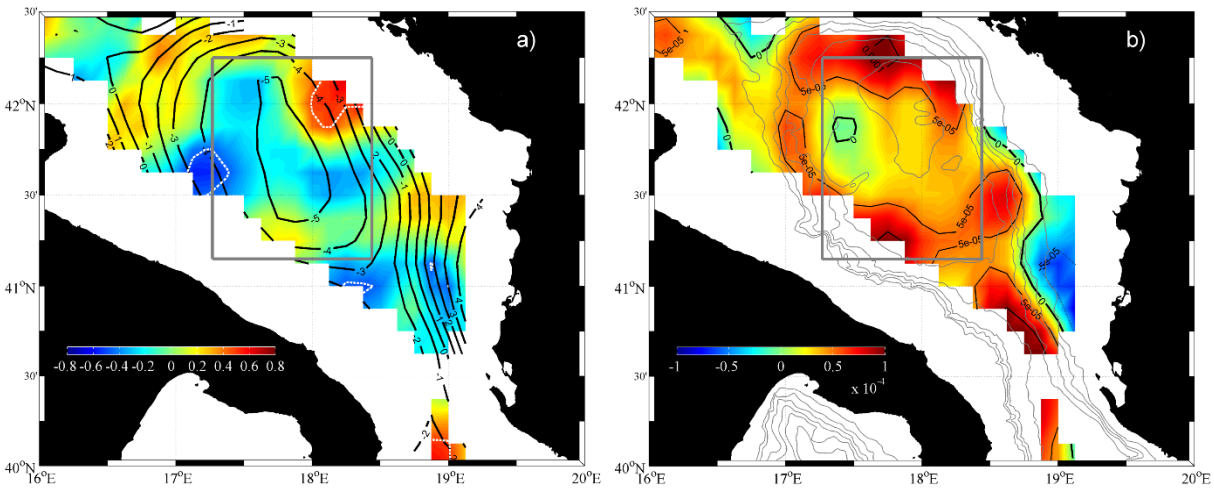

Figure 3- 17 Spatial distribution of the correlation coefficient between the JFM time derivative of the vorticity and the wind-stress curl for the period 1993-2011 (colours). Black bold contours outline the 20-years average of the JFM sea level height (cm) and the white dotted lines indicate the level of the 95% significance (a); Spatial distribution of the average of the JFM geostrophic current vorticity (colours and the black lines). The grey contours indicate the isobaths between 200 m and 1200 m with the 200 m line space (b). The grey squares show the areas used to estimate the time-series in Figure 3-16; altimetry grid points located within 50 km from the coast have been deleted.

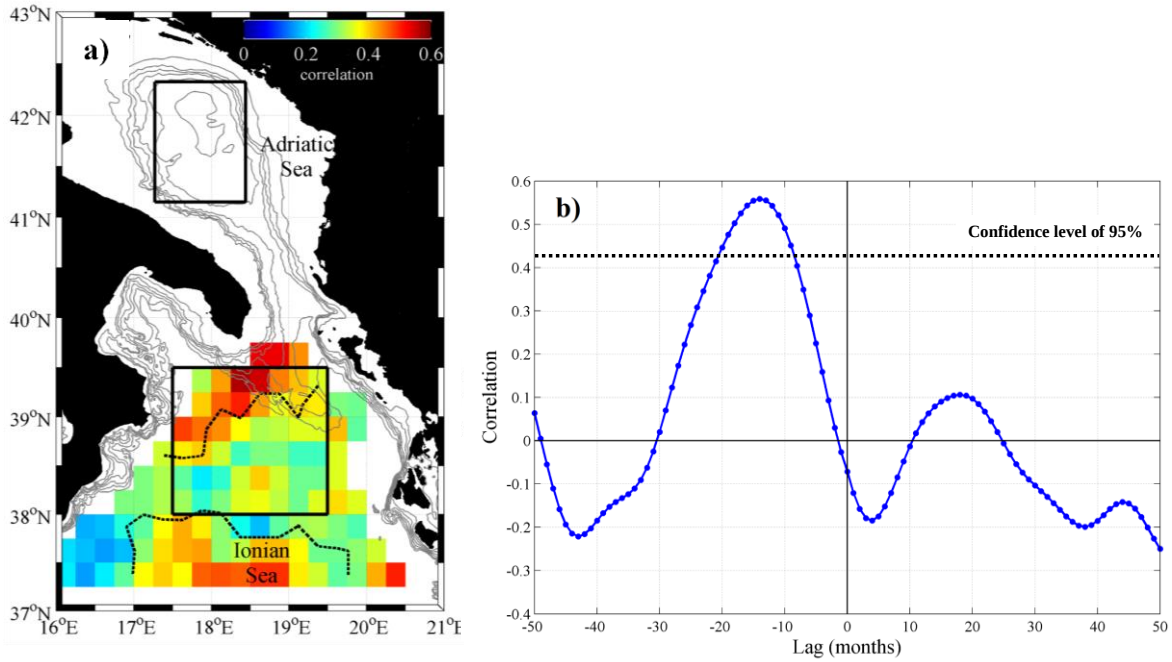

Figure 3- 18 Correlation between the time-series of the spatially averaged low-pass current vorticity in the Adriatic and $0.25^{\circ} \times 0.25^{\circ}$ domains in the Ionian for the 14-month time lag (a); lagged correlation between Adriatic and Ionian spatially averaged vorticities. For the Adriatic the averaging domain is the upper polygon while for the North Ionian the averaging domain corresponds to the area ($0.25^{\circ} \times 0.25^{\circ}$)with the maximum correlation (b); the black polygons show the areas used to estimate the time-series in Figure 3-16; the black dotted lines indicate the level of confidence of 95%.

The correlation between the low-pass Adriatic and Ionian flow vorticities reached maximum (r~ 0.4) for the Adriatic vorticity lagging the Ionian one by about 14 months. It should be mentioned that by decreasing the degrees of freedoms of the time-series from ~240 to ~20 due to the filtering procedure, the level of confidence of the correlation decreases. In other words, according to the standard t-table (e.g. Snedecor and Cochran, 1980) the correlation coefficients must exceed 0.423 to be significant at 95% confidence level. Furthermore, as far as the estimates of the time lag is concerned the same value (14 months) was obtained using either unfiltered data or data filtered with different window lengths (figure not shown). This time-lag corresponds approximately to the advection speed of 1 cm/s, rather reasonable value.

Then, in order to determine with more precision the vorticity source area in the North Ionian Sea, the 14-month lag correlations between the spatial average of the low-passed current vorticity in the SAG (the upper domain in the Fig. 3-18a) and average vorticity in smaller domains ($0.25^\circ \times 0.25^\circ$) in the North Ionian were calculated (see Fig. 3-18a). All over the area of the North Ionian the correlation coefficients are positive with a maximum located in the northern part of NIG (around $18^\circ 30' E; 39^\circ 30' N$) where the horizontal shear is the strongest during the anticyclonic mode of BiOS (Gačić et al., 2011). Afterwards, the lag correlation between the filtered time-series of the mean vorticities in the SAG and the area where maximum correlation between SAG and Ionian was evidenced (the small polygon located in $18^\circ 30' E; 39^\circ 30' N$ in the figure 3-18a) was calculated. The maximum correlation coefficient (r~ 0.56) with the higher level of confidence (99%) is evidenced again for the time lag = 14 months (see Fig. 3-18b) which confirms the impact of the vorticity in this area on the SAG circulation. Although the estimated correlation coefficient is relatively large, the relation between vorticities in these two areas is not visible inspecting the time-series (see Figures 3-16b; and 3-16c). This can be explained by the fact that according to the Eq.2-10, vorticity advection only partly determines the variation of the circulation in the SAP while the additional contribution comes from the wind input. Therefore, the influence of Ionian circulation to the current vorticity of the SAP cannot be clear in the visual examination of the vorticity time-series. More specifically, the advection term is not equally important in all situations; in 1997, the reversal of the north Ionian circulation took place from anticyclonic to cyclonic mode (Larnicol et al., 2002; Pujol and Larnicol, 2005). The continuous reduction of the current vorticity term between 1995 and 1999 (see figure 3-19a) is due to this circulation transition.

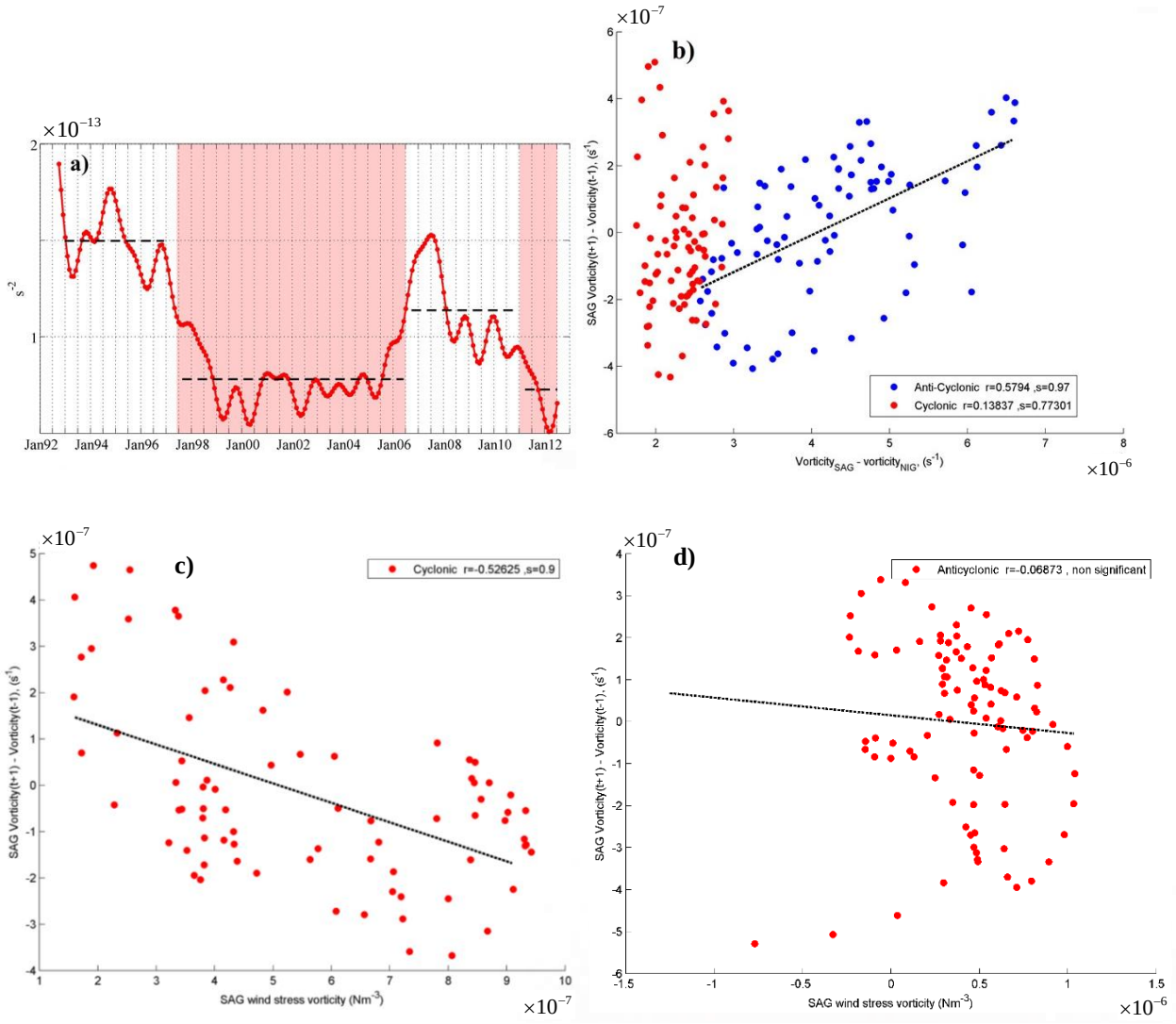

Figure 3- 19 Time series of the low-pass (13 months) current vorticity advection from the North Ionian Sea to the South Adriatic Sea. Areas shaded in red correspond to the time periods characterized by cyclonic circulation mode and the dashed lines show the average values of the advection over each cyclonic/anticyclonic period (a); The scatter plot of the vorticity tendency (in finite differences) in the SAP (Figure 3-16b) and the difference of vorticities in the Adriatic and the northern area of NIG during the cyclonic (red circles) and anticyclonic (bule circles) modes of BiOS (b); The scatter plot of the vorticity tendency (in finite differences) and wind stress vorticity in the SAP (Figure 3-16b) during the cyclonic (c) and anticyclonic (d) modes of BiOS.

The subsequent passage from cyclonic to anticyclonic circulation in the North Ionian Sea occurred in 2006 (Gačić et al. 2010) which has as a consequence an increase of the relative importance of the advection term. Therefore, when the Ionian circulation is in the anticyclonic phase the advection term is more important than in the cyclonic phase. In the former case, the advection term is proportional to the sum of the Ionian and Adriatic vorticities while in the latter case the advection term is proportional to the difference between the two vorticities (see Eq. 2-10). In order to examine the relative importance of the advection term in each mode of BiOS, we compare the vorticity tendency with the advection term in the Eq. 2-10:

$$\frac{\partial \xi_g}{\partial t} = -V_g.\nabla(\xi_g) + A \tag{3-1}$$

where A is the wind stress vorticity. The equation 3-1 expressed in terms of the finite differences becomes:

$$\frac{\Delta \xi_g}{\Delta t} = -V \times \frac{\Delta \xi_g}{\Delta x} + A \tag{3-2}$$

then considering only the advection term, we obtain:

$$\xi_{g-SAG}(t+1) - \xi_{g-SAG}(t-1) \propto C \times (\xi_{g-SAG}(t) - \xi_{g-NIG}(t)) \tag{3-3}$$

in which ξ_{g-SAG} and ξ_{g-NIG} are the spatial average of the curl of geostrophic current in SAG and in the small polygon in the NIG located around $18^{\circ}30'E;39^{\circ}30'N$, respectively. Furthermore, we assume that $C = \left| -V \frac{\Delta t}{\Delta x} \right|$ is a constant obtained from the time step, the distance between the Ionian vorticity source area and the SAP, and considering the constant advection speed.

Furthermore, the importance of wind stress vorticity in the variation of the current vorticity were evaluated for the periods associated with the cyclonic and anticyclonic modes of North Ionian circulation. For this purpose, we considered Eq. 2-10 in terms of finite differences as follows:

$$\frac{\partial \zeta_g}{\partial t} = B + \frac{1}{\rho D} curl(\tau_s) \tag{3-4}$$

$$\frac{\Delta \zeta_g}{\Delta t} = B + \frac{1}{\rho D} curl(\tau_s) \tag{3-5}$$

$$\Delta \zeta_g \propto C \times curl(\tau_s) \tag{3-6}$$

where B is vorticity advection and $C = \frac{\Delta t}{\rho D}$ is a constant value.

Using Eq. 3-3, vorticity tendency in the SAP was compared to the difference of the vorticities between the SAP and the northern portion of NIG plotting the scatter diagram for the periods associated with the cyclonic (red) and anticyclonic (blue) modes of BiOS (figure 3-19b). The figure reveals rather satisfactory linear relation between two terms during the anticyclonic phase, when the vorticity advection becomes more important. Conversely, in the cyclonic mode of the Ionian circulation, the difference of the vorticities in the SAP and NIG is smaller and the advection does not have the significant influence on the vorticity variations in the SAG. In addition, from the calculated linear regression between two terms of Eq. 3-3, we obtained the advection speed of about 0.8 cm/s which is rather consistent with the estimate obtained from the lagged correlation between the NIG and SAP vorticities.

Moreover, according to Eq. 3-6, relation between vorticity tendency and wind stress vorticity in SAP during the cyclonic and anticylonic phases of BiOS were analyzed and the scatter plots were compared (see figures 3-19 c and d). The figures indicate the relatively significant correlation between current vorticity tendency and wind stress curl during the cyclonic mode of Ionian circulation, when the vorticity advection from NIG becomes smaller, while there is no evidence of current vorticity variation influenced by the external forcing during the anicyclonic BiOS.

Therefore, the local current vorticity input prevailed in the period 1997-2006 when the Ionian was in the cyclonic phase and the advection term was less important. Before 1997 and after 2006 the Ionian was characterized by the anticyclonic circulation mode and the vorticity advection term was more important.

In order to relate the interannual variability of the wind-stress curl (one of the important factors affecting the variation of the strength of the gyre according to Eq. 2-10) to NAO as a large climatic system, we compared time-series of the wintertime NAOI with the wind-stress curl. More specifically, we calculated the correlation coefficient between the two time-series in each point of the study area for the period 1988-2011 (Fig. 3-20). Previous research showed that the correlation between the wind speed and NAOI in the Adriatic was statistically insignificant (Pirazzoli and Tomasin, 2003). Considering however the wind-stress curl, the results revealed the significant (95%) negative correlation between the wind-stress curl and NAOI for the major portion of the

open Adriatic Sea: NAOI negative values were concomitant with maximum wind-stress curl, and conversely minima of the wind-stress curl were associated with NAOI maximum values.

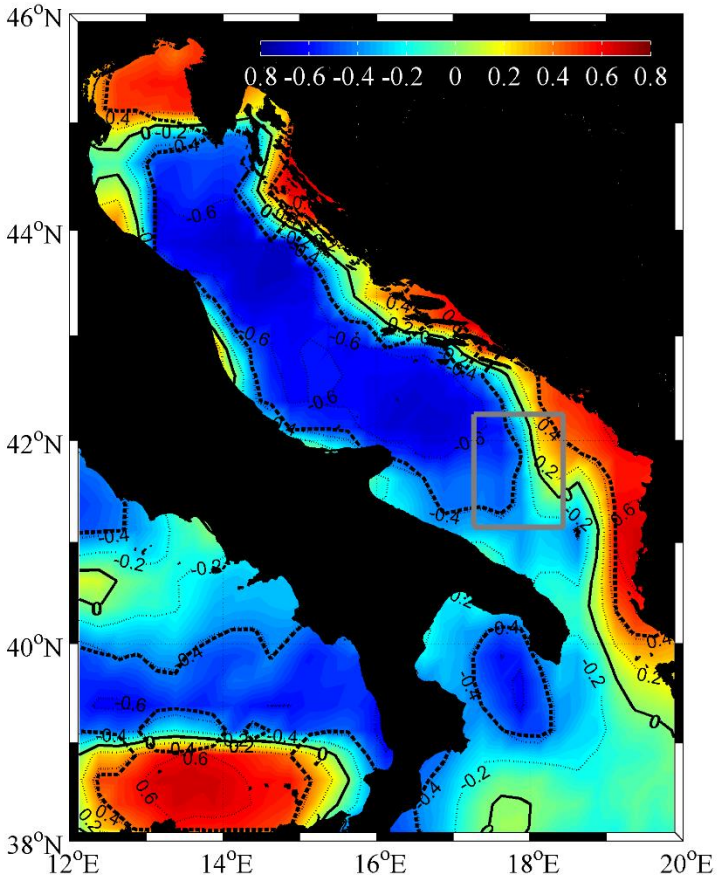

Figure 3- 20 Spatial distribution of the correlation coefficient of the JFM NAOI and wind-stress vorticity, 1988 - 2011 (coloured area and dotted lines). The bold solid and dashed lines indicate the 0 correlation and the 95% significance isoline, respectively. The square shows the area used to estimate the time-series in Figure 3-16.

During the positive NAO phase, north-westerlies are dominant in southern Europe and Mediterranean Sea as the result of the enhancement of the Icelandic Low as well as of the Azores High. Conversely, in the negative phase, the intensification of the westerlies is observed in these regions (Jerez et al., 2013). More specifically, depending on the phase of NAO, the pressure gradient over the North Atlantic changes the magnitude and orientation, which causes the differences in the speed and direction of winds in mid-latitudes (Lamb and Peppler, 1987). In agreement with Trigo et al. (2002), the local maximum of the wind vorticity were present in the southern Adriatic Sea during both positive and negative NAO phases. The positive winter NAOI

were followed by strong northwesterly winds over the Mediterranean, which is the consequence of the intensification of the high pressure over the Mediterranean region (Fig. 3-21a). This configuration resulted in a rather weak low pressure centre over the southern Adriatic and a weakening of the cyclonic vorticity. On the contrary, during the negative NAOI periods rather strong northward atmospheric flow along the eastern coast of the southern Adriatic was observed, reinforcing the wind-stress curl (Fig. 3-21b).

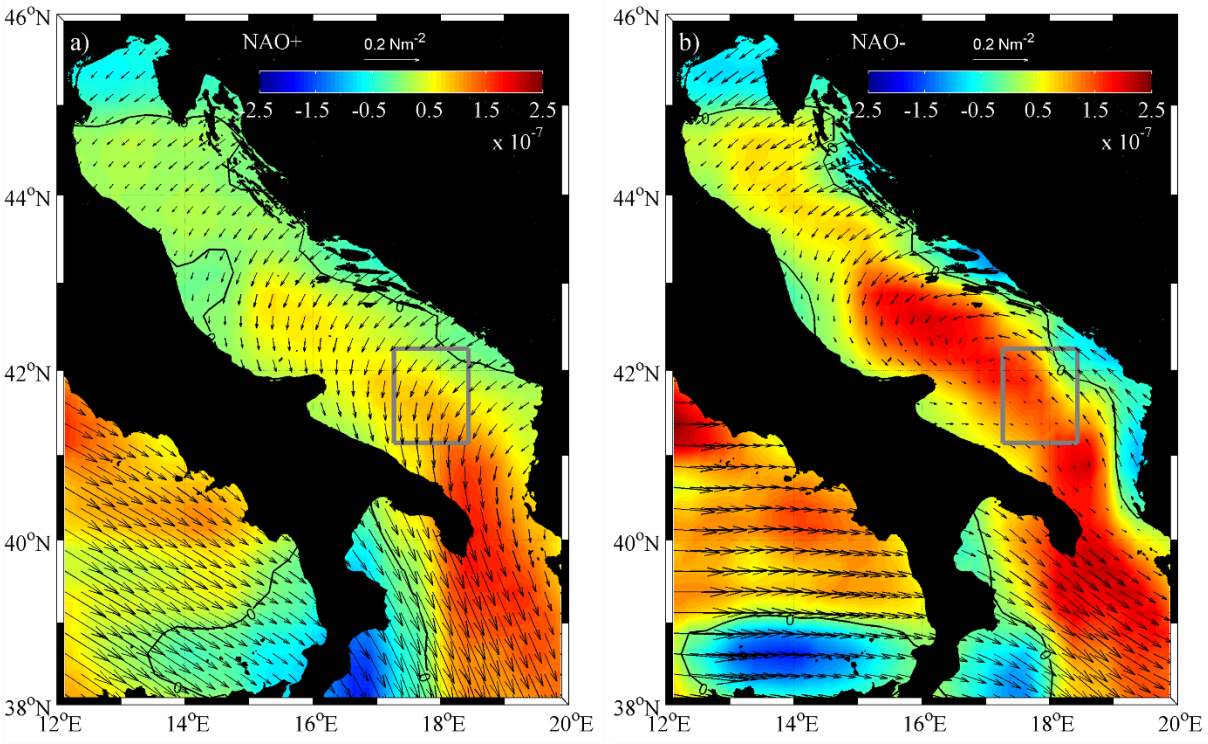

Figure 3- 21 Spatial distribution of the mean JFM wind-stress vorticity (colours; Nm-3) and wind-stress vectors (arrows; Nm-2) in the positive NAO phase (a) and negative NAO phase (b), 1988-2011. The squares show the areas used to estimate the time-series in Figure 3-16.

Therefore, we can say that the large-scale climatic conditions associated with a positive NAO phase weaken the positive wind-stress curl, while the stronger positive wind-stress curl is related to the negative NAOI. The wind-stress curl, on its turn, affects the current vorticity tendency in the central part of the southern Adriatic however depending on the circulation mode of BiOS. In the cyclonic phase, the wind stress curl is presumably prevailing in determining the vorticity tendency, while in the anticyclonic phase the vorticity advection term becomes important. In conclusion, due to the varying importance of the vorticity advection term, which depends on the

Ionian circulation mode, it is not possible to establish unequivocal relationship between NAO and the strength of the SAG (Shabrang et al., 2016).

– **Ionian Sea**

The Ionian Sea is a sub-basin of the central Mediterranean between Greece and Sicily. The water exchanges between EMED and WMED and between Adriatic and Aegean Sea take place through the Ionian Sea. The circulation in the upper layer of the North Ionian Sea is subject to the reversal in the decadal time-scales through the BiOS feedback mechanism. This phenomenon is interconnected to the thermohaline properties of the EMDW and the salt distribution over the EM (Borzelli et al. 2009; Gacic et al. 2010; and Gacic et al. 2011). The correlation between wintertime sea surface height and NAOI (Fig. 3-12) shows that sea level in the NIG is not affected by NAO pattern despite the strong anti-correlation of the time-series in the most areas of the basin, particularly in the EMED. Moreover, no considerable differences between temperature and salinity fields in the location of NIG are evidenced between two modes of NAO. This implies that internal mechanisms and meso-scale processes are responsible for the circulation of the gyres and variation of the sea level of these areas. In addition, the heat fluxes and temperature, as well as wind velocity and vorticity in the Ionian Sea, don't reveal any variations with the index. However, the higher precipitation rate is evidenced during the negative mode due to the lower atmospheric pressure. Furthermore, the lower salinity in the North Ionian Sea during the positive phase and the negative correlation between NAOI and salinity in the intermediate layer cannot be explained in terms of the heat exchanges. This suggests that in addition to the atmospheric forcing, there should be the other factor affecting the salt distribution in this area. Here, it should be stressed that water salinity is mainly controlled by the inflow of the water masses with different origins driven by BiOS mechanism. In other words, the variation in the salt content of the NI highly depends on the circulation changes in the upper thermocline layer of the basin. The anticyclonic mode of BiOS is associated with the inflow of the low salinity AW into the NI while during the cyclonic Ionian circulation, the basin is occupied by the warmer and more saline Levantine waters, LIW and CIW (Gačić et al., 2011; Malanotte-Rizzoli et al., 1999). Therefore, the difference in salinity between the waters entering NI is the important factor determining the salinity of the basin. This highlights the role of water exchanges in the thermohaline characteristics of the North Ionian Sea.

– **Eastern coasts of Sicily**

AW has been described to have a predominantly two-jet structure characterized by the minimum salinity in the upper layer after inflowing the EMED through the Strait of Sicily. More specifically, AW bifurcates and partly flows into the upper, Western Ionian Sea meandering northward and the other one follows the eastward direction and enters the Levantine basin (Grancini and Michelato, 1987; Moretti et al., 1993; Manzella et al., 1990). The intensities of these branches are out of phase and strongly depend on the phase of BiOS. The correlation coefficients between the NAOI and temperature and salinity (Fig. 3-1 and 3-3) show the existence of the warmer and less salty water in the eastern coasts of the Central Ionian Sea which is the pathway of the AW while there is no evidence of the different heat flux pattern between two modes of NAO (Fig. 3-3e and f). This suggests that a more stable water in this area during NAOI+ cannot be related to the heat gain in this mode. According to the figures 3-2 and 3-3, the variation of the water characteristics in this area is in phase with the thermohaline properties of the AW. In other words, by increasing the temperature and decreasing the salinity of the AW during the NAOI+, the warmer and more fresh water enters the eastern coasts of Sicily in this phase. Conversely, NAOI- is associated with the inflow of the colder and the less saline AW into this region. Therefore, the horizontal advection and the inflow of the AW is responsible for the changes in the temperature and salinity of the surface layer of the western Ionian Sea which follows the AW characteristics.

– **Levantine Sea**

The second largest basin of the EMED is the Levantine Sea. Due to the meteorological and hydrological conditions, the Levantine basin is a suitable place for the convergence and convective sinking of the salty water. In other words, the strong air-sea interaction processes and favorable oceanic conditions are responsible for the vertical mixing and the transformations of surface water into intermediate and deep layers and formation of LIW which is characterized by the layer of maximum salinity at intermediate layer (~200–800 m) which is mostly generated in the Rhodes gyre. It is present in the entire Mediterranean Sea, circulates in the both Eastern and Western basins and has an important contribution in the water exchanges from Mediterranean to the Atlantic Ocean within the strait of Gibraltar (Marullo et al., 2003; Malanotte-Rizzoli and Eremeev, 2012).

In the positive phase of NAO, the upper and intermediate layers of the Levantine Sea are characterized by lower temperature and salinity (Fig 3-1). The stronger heat loss during NAOI+ is

responsible for the decrease of the temperature in this mode. It can be related to the intensification of the northerlies and outbreak of the cold and dry continental air into the basin in the positive NAO phase. Moreover, during NAOI+, lower salinity in the Levantine Sea is evidenced which may be explained by the decrease of the AW salinity during NAOI+ due to the weakening of heat loss and consequent present of the more stable water column in the entire WMED. By inflowing the less saline AW into the Levantine basin, more fresh water occupies the upper layer which subsequently leads to the formation of the LIW with the lower salinity in the positive NAO mode. In addition, it should be emphasized that the characteristics of the LIW are strongly influenced by the BiOS mode. During the anticyclonic phase of the NIG circulation, higher salinity is evidenced in the Levantine basin due to the northward deviation of the AW and its longer pathway toward Levantine and longer residence time for mixing. Conversely, in the cyclonic BiOS mode, AW travels directly and reaches the Levantine Sea by the shorter route. Therefore, the Levantine upper thermocline layer is characterized by the lower salinity. Therefore, it can be hypothesized that the coincidence of the consistent positive NAO mode with the cyclonic mode of Ionian circulation (1997- 2006) may be responsible for the reduction of salinity in the Levantine Basin.

In addition, the wind vorticity in the large area of the Levantine Sea especially over the Rhodes Gyre is in phase with the index. The wind stress curl intensifies during the NAOI+ and the negative NAOI is associated with the weaker wind stress curl (fig 3-6). However, the correlation is rather low but significant in this area. It is in agreement with the results obtained from Tsimplis and Josey (2001).

Affecting both salinity and temperature (through the latent heat loss), evaporation plays an important role in preconditioning water prior to deep convection. In the eastern basin, particularly the Levantine Sea, the stronger evaporation rate is evident during the NAOI+ which can reinforce the net evaporation (see Fig. 3-10). The stronger influence of NAO on evaporation rate is evident in the Levantine and the Aegean Sea than in the Gulf of Lion. This is consistent with the results obtained by Tsimplis and Josey (2001). Higher evaporation and heat loss associated with the NAOI+ in the Levantine basin increase the buoyancy loss in this mode.

3-3- Relationship between EA pattern and oceanography of the Mediterranean Sea

The spatial distribution of the correlation coefficients between wintertime EAI and temperature and salinity in the upper and intermediate layers of the basin are shown in the figure 3-22. Upper layer temperature is in phase with EAI in the major parts of the western basin. However, the weaker influence of the EA is evidenced in the Alboran and Balearic seas. Furthermore, the temperature in the Strait of Sicily and South Ionian Sea is positively correlated with EAI. The warming of the WMED during the winters associated with the positive mode of EA has been documented in the other studies (e.g. Saenz et al., 2001). The temperature in the rest of the Mediterranean is not much influenced by this index. In addition, the correlation coefficient between wintertime EAI and salinity in the upper layer reveals the significant negative values in the middle of western basin including the Gulf of Lion, Ligurian Sea and the west and south of Sardinia. To put it another way, positive EAI is associated with the warming of the western basin and provides more stability to the water column. Therefore, the upper layer is characterized by the warmer and the less saline conditions. In contrast, negative EAI corresponds to the colder and more saline surface layer due to the stronger vertical mixing. These effects are extended to the intermediate layer with 1-year time-lag due to the retarded response of the deeper layers of water to the meteorological conditions (see Fig. 3-22c and d). Comparing with the NAO, the influence of the EA is stronger on the temperature of the WMED and the Strait of Sicily while the impact of EA on the most parts of the central and eastern Mediterranean is not important.

Variation of the sea water temperature is strongly dependent on the air-sea heat exchanges. Therefore, in order to explain the impacts of the EA on the thermal and saline properties of the Mediterranean water, first, the variability of the heat flux components with this climate index is analyzed. Using ERA-Interim dataset and Eq. 2-1, the net heat flux during the winter periods is calculated and then the spatial distribution of the correlation coefficients between JFM EAI and net heat flux, as well as the sensible and latent heat flux components, are obtained. The positive correlation between wintertime heat flux components and EAI is evidenced in the major parts of the basin (see Fig. 3-23). In other words, positive EAI is associated with the stronger transfer of the heat from the atmosphere to the sea in a large part of Mediterranean. Contrarily, during the negative EA mode, heat loss intensification is evidenced over the basin. Previous studies also

showed the stronger heat loss during the EAI- (e.g. Josey et al., 2011).This suggests that the negative mode of EA represents favorable conditions of the formation of the dense water in the Mediterranean.

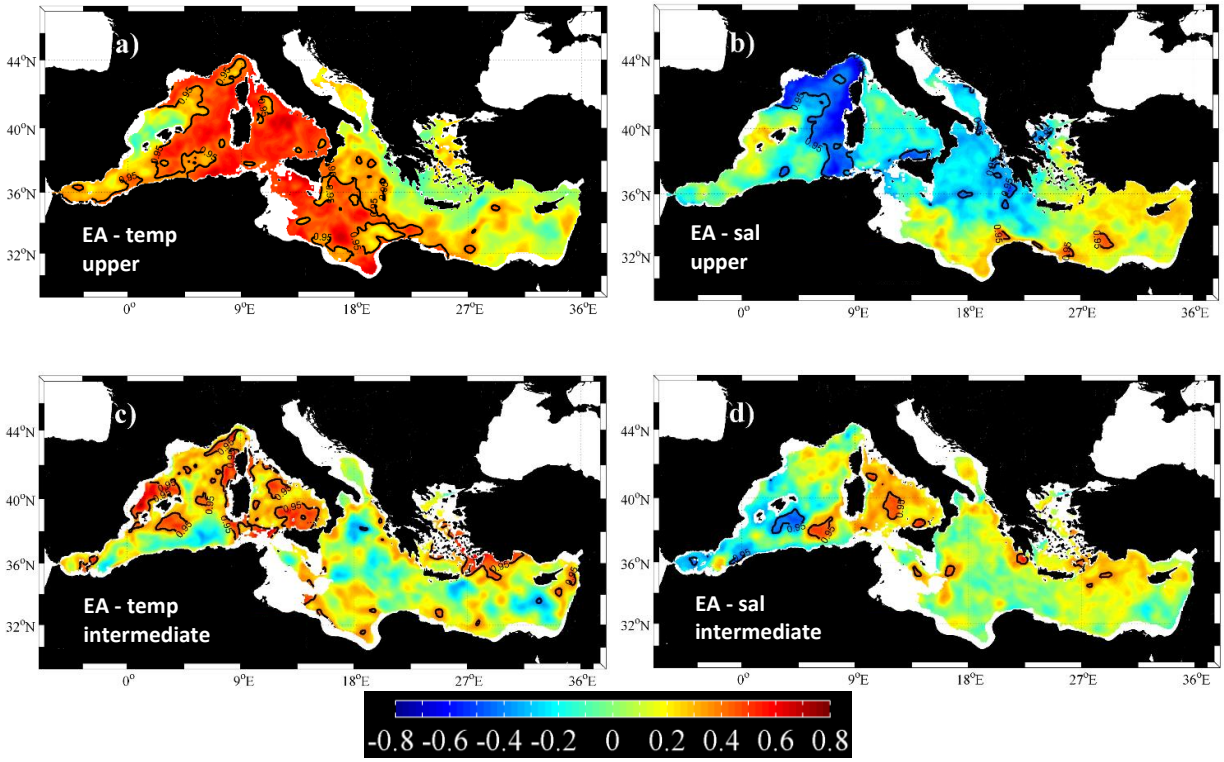

Figure 3- 22 Spatial distribution of the correlation coefficient between JFM EAI with a) JFM upper layer temperature, b) JFM upper layer salinity, c) JFM intermediate temperature (lag =1 year), and d) JFM intermediate salinity (lag =1 year). The bold black line indicates the isoline of the 95% significance.

Unlike NAO, which shows the local effects on the heat exchanges of the Mediterranean, EA pattern reveals the strong impact on the heat flux over the major parts of the basin (see figure 3-23). However, this effect is more pronounced in the northern areas including Ligurian and Tyrrhenian Seas, the Gulf of Lion, Adriatic, Aegean, North Ionian and North Levantine Seas but the maximum effects of the EA on the heat fluxes are observed over the South Adriatic Sea.

The winter averages of the anomaly of Q_{net}, as well as the upper layer temperature and salinity, for the periods characterized by the positive and negative EA are demonstrated in the figure 3-24. The averages were calculated with the same method which is described for NAOI (see section 3-1) and the corresponding years as well as related index value are demonstrated in Table 3-2.

Table 3- 2 list of years characterized by positive and negative EA modes used for calculating the averages and corresponded EAI.

EAI +										
Year	1990	1991	1997	1998	2001	2002	2003	2004	2007	2010
Index value	1.02	0.59	0.4	0.65	0.79	1.25	0.66	0.36	1.13	0.95
EAI -										
Year	1992	1993	1995	1996	1999	2000	2005	2006	2009	2011
Index value	-0.27	-0.41	-.45	-0.77	-1.31	-0.75	-0.93	-0.77	-0.31	-0.56

During the positive EAI, the positive anomaly of temperature is observed over the WMED and South Ionian Sea (Fig. 3-24a). In addition, the lower salinity water occupies these areas during EAI+ (see Fig. 3-24c). Conversely, EAI- is characterized by the lower than normal temperature in the upper layer of these regions as well as higher salinity over WMED and North Ionian Sea (Fig. 3-24b and d).

Figures 3-24 e and f show the positive anomaly of the net heat flux during EAI+ and lower than normal Q_{net} over the periods of the negative EAI in the entire Mediterranean. Therefore, the warmer temperature associated with the EAI+ is due to the increase of the sea water heat gain from the atmosphere. On the other hand, stronger heat loss during EAI- reduces the temperature of the sea water. The occurrence of the cold and dry northerly winds, which produce the stronger gradients of the temperature and humidity over this area, is responsible for the heat loss reinforcement during the negative mode of EA (Josey et al., 2011). Therefore, the more stable condition is observed at the upper layer of WMED due to the presence of the water characterized by the higher temperature and lower salinity. Despite the strong influence of the EA pattern on the heat fluxes over the Adriatic Sea and EMED, the temperature in these parts of the basin is not noticeably affected by EA. This suggests the importance of the internal processes which compensate for the impacts of the heat exchanges.

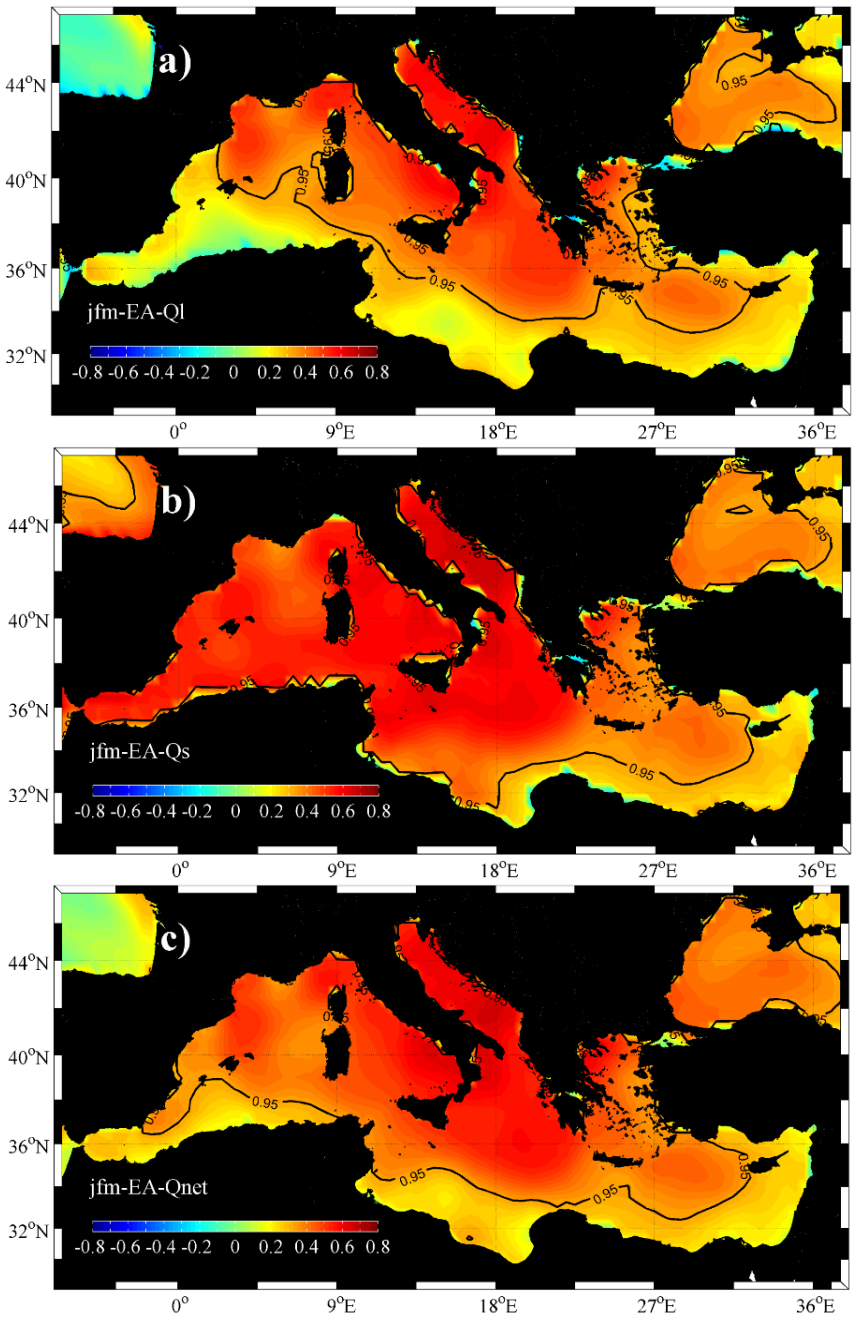

Figure 3- 23 Spatial distribution of the correlation coefficient between JFM EAI and a) latent heat flux, b) sensible heat flux, c) net heat flux. The bold black line indicates the isoline of the 95% significance.

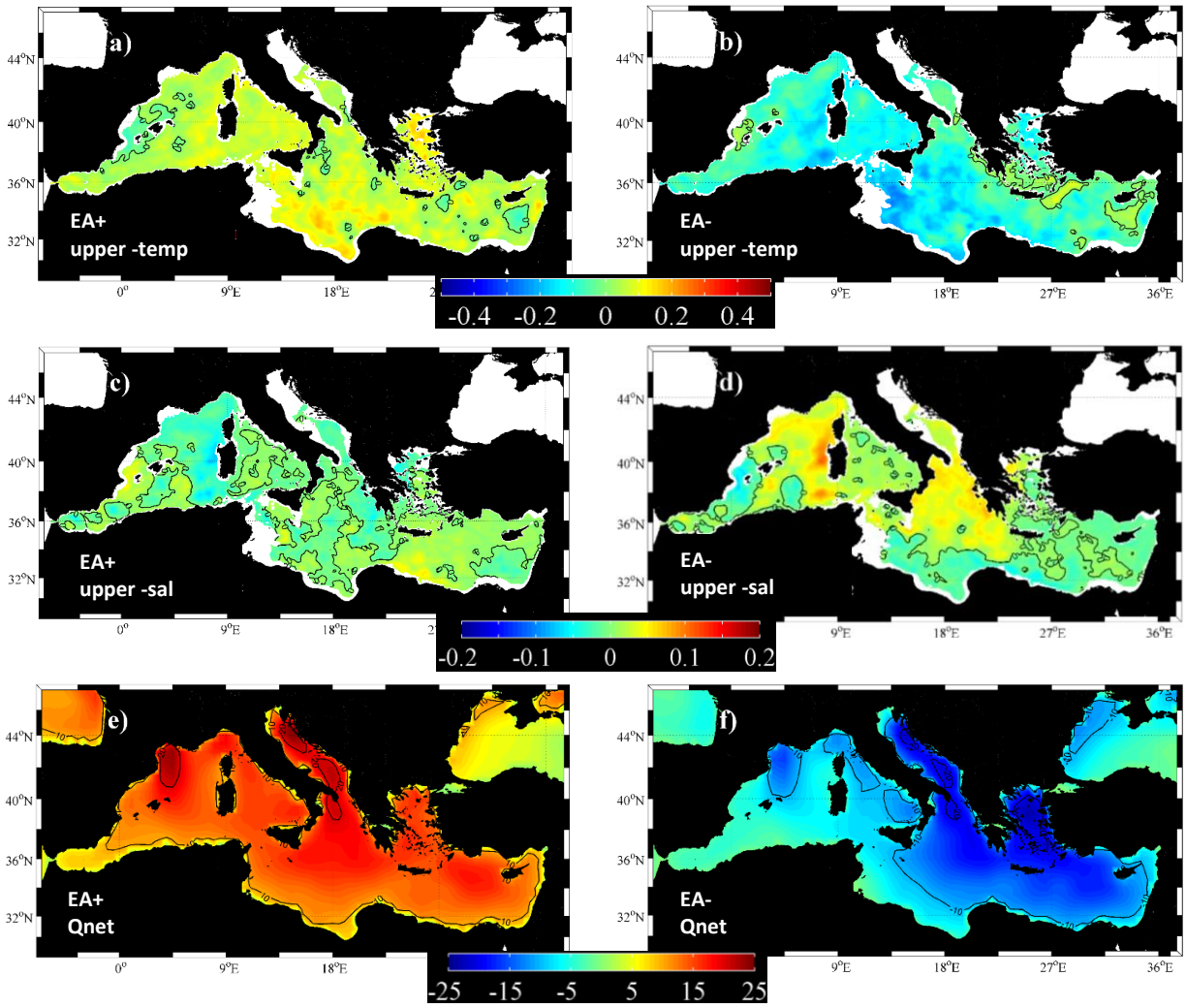

Figure 3- 24 Spatial distribution of the mean JFM a) temperature anomaly (°C) during EAI+, b) temperature anomaly (°C) during EAI-, c) salinity anomaly during EAI+, d) salinity anomaly during EAI-, e) net heat flux (Wm^{-2}) anomaly during EAI+, f) net heat flux (Wm^{-2}) anomaly during EAI-. The black contours show the isoline of 0.

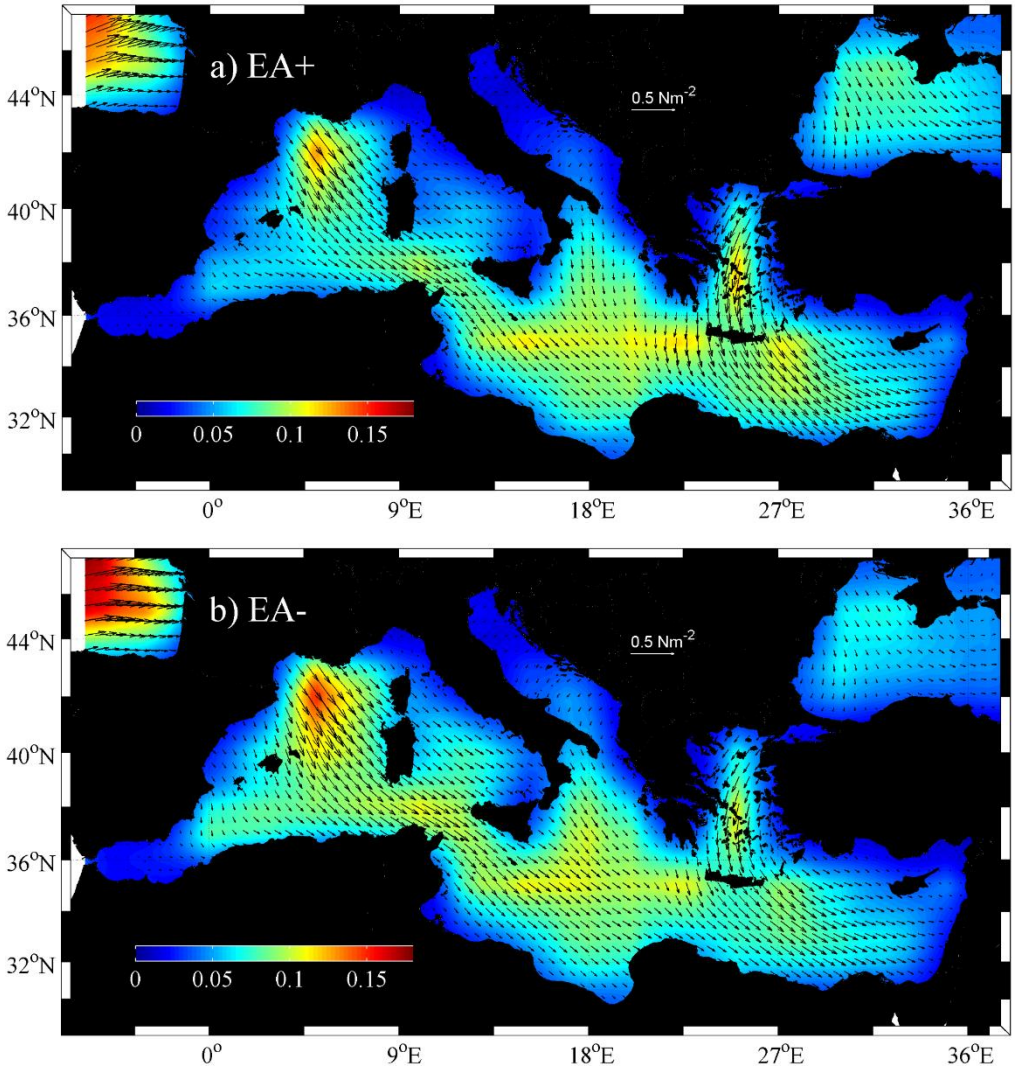

Figure 3- 25 Spatial distribution of the mean JFM wind-stress magnitude (colours; Nm^{-2}) and wind-stress vectors (arrows; Nm^{-2}) in the positive MOI phase (a) and negative MOI phase (b), 1988-2011.

In order to explain the variation of heat loss associated with the EA modes, the patterns of the average wintertime wind stress magnitude super-imposed with the wind vectors for the periods of the positive and negative modes of EA are calculated separately and shown in the Fig. 3-25. The patterns are consistent with the atmosphere pressure fields during EA modes. During the EAI+, the magnitude of the north-westerlies over the Western Mediterranean, Strait of Sicily and to the less extent North Ionian is reduced. This is due to intensification of the low-pressure centre and resulted south-westerlies over Atlantic Ocean during EAI+ which weaken the intensity of the north-westerlies in the northern and western Mediterranean.

Contrarily, EAI- is characterized by higher atmospheric pressure in the Atlantic Ocean and intensification of the north-westerlies over the western and northern parts of the basin. The increase of the wind magnitude intensifies the heat loss through the stronger evaporation in these regions and reduces the surface temperature. The resulted vertical convection, subsequently gives the rise to the surface salinity.

Since according to Eq. 2-10, wind stress vorticity is considered as one of the important factors determining the variability of the ocean current circulation, the role of EA pattern in the variation of the wind stress curl is evaluated in this part. Using CCMP wind products and Equations 2-3 and 2-4, the time-series of wind vorticity over the Mediterranean basin are calculated and the correlation coefficients between these time-series and EAI in each grid point of the study domain during JFM periods are obtained. The spatial distribution of the correlation coefficients is demonstrated in Fig. 3-26. In comparison with NAO, EA pattern has less influence on the wind stress vorticity over the Mediterranean basin. The wind vorticity is uncorrelated with the index in the basin, except in the centre of the WMED, with a dipole of the positive correlation around the Balearic Islands and the negative correlation in the west of Sardinia, and one small area at the most eastern part of the basin.

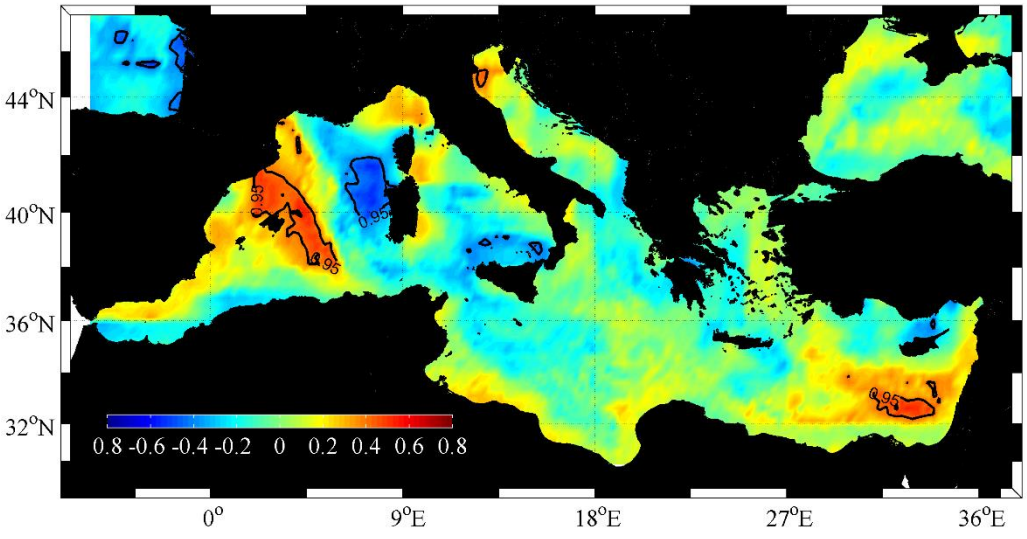

Figure 3- 26 Spatial distribution of the correlation coefficient between JFM EAI and the wind stress curl. The bold black line indicates the isoline of the 95% significance.

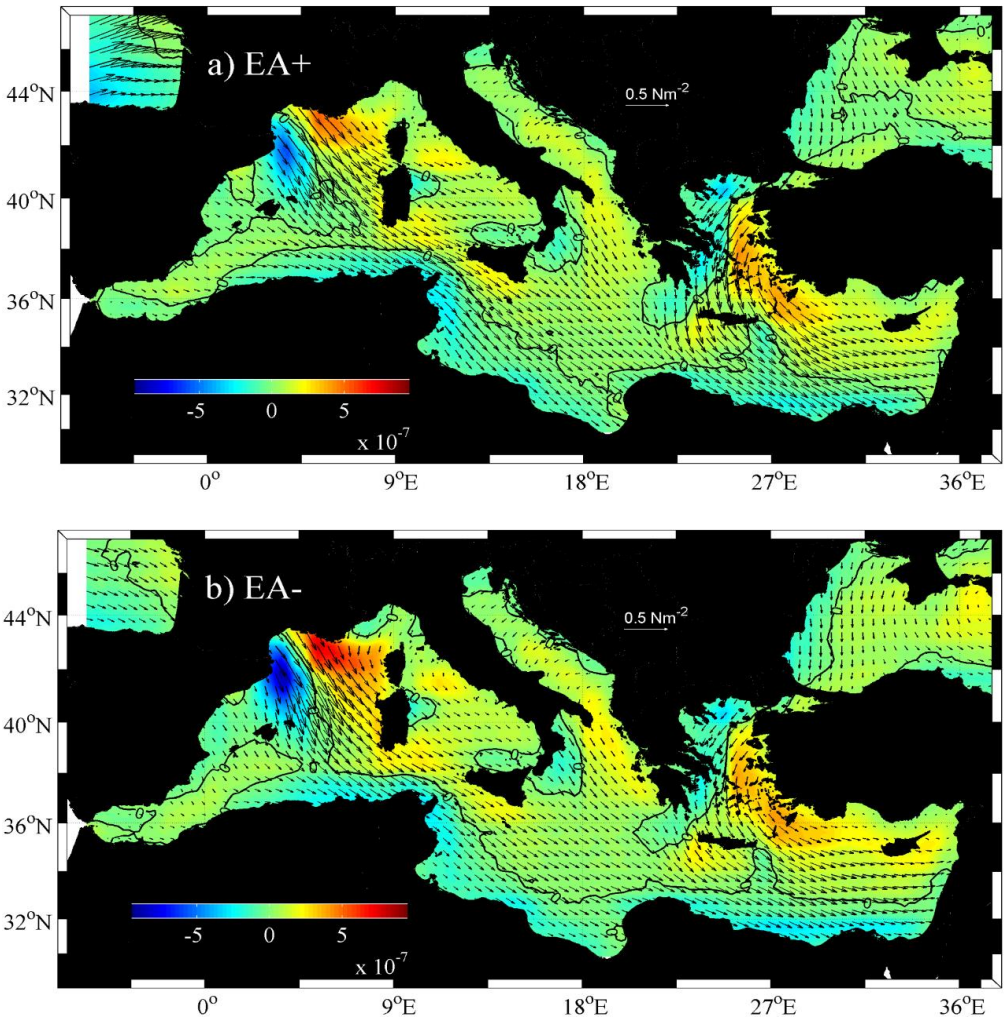

Figure 3- 27 Spatial distribution of the mean JFM wind-stress vorticity (colours; Nm-3) and wind-stress vectors (arrows; Nm-2) in the positive EA phase (a) and negative EA phase (b), 1988-2011.

The spatial patterns of the average of the JFM wind stress vorticity and velocities for the positive and negative EA modes (Fig. 3-27) shows the intensification of the both pressure centres over the Gulf of Lion and consequent stronger north-westerlies during EAI-. The difference of the wind configuration between positive and negative EA phases can explain the significant and relatively high correlations of the vorticity and EA pattern over the north-western Mediterranean. In the rest of the basin, no considerable difference between the wind fields during EAI+ and EAI- is evidenced. Therefore, it can be concluded that the Northwestern Mediterranean is the only source of the deep water formation in the basin affected by the EA pattern through the wind forcing. This is consistent with what was suggested by Schroeder et al. (2010) which found the link between

deep convection observed in the Gulf of Lion during the winters of 2004–05 and 2005–06 and the negative phase of the EAI.

Thermohaline properties of the ocean are strongly influenced by air-sea water exchanges. Higher evaporation plays an important role in the variation of the water characteristics through the increase of the latent heat loss and higher precipitation reduces the water salinity. The subsequent change in the surface buoyancy controls the ocean circulation. In order to understand the role of EA pattern on the variation of the water exchanges, correlation coefficients between the wintertime EAI and evaporation and precipitation rates over the Mediterranean basin are computed and studied. The results show that the evaporation rate over the vast area of the Mediterranean Sea (the northern half of the basin including the Gulf of Lion, Ligurian and Tyrrhenian Seas as well as Adriatic and North Ionian and Northwest of Aegean Seas and to a less extent Strait of Sicily, Levantine and South Aegean Seas) is highly affected by EA pattern. Figure 3-28a shows the significant negative correlation between wintertime evaporation rate and the index. Spatial patterns of the average JFM evaporation rate over the positive and negative periods of EAI (Figure 3-29a, b) show the higher evaporation rate in the entire basin except the Alboran and the Balearic Seas during the negative mode. This is due to the higher atmospheric pressure during the negative mode which generates the stronger northerlies and results the enhancement of heat loss (see Fig. 3-24 e, f; and Fig. 3-25).

In contrast, precipitation in the basin is not much affected by EA. As it is demonstrated in the Fig. 3-28b, there is no correlation between P and index in the western basin. However, low correlation ($r\sim0.4$; $s>0.95$) is evidenced in southern parts of the eastern basin but the average patterns of precipitation rate during the positive and negative EAI, don't reveal any considerable differences between two modes of this index (see Fig. 3-29c, and 3-29d).

Since during the negative EAI, evaporation exceeds precipitation in the Northern parts of the basin, particularly in the Gulf of Lion and to a larger extent in the North and Middle Adriatic Sea, the negative correlation appears between the wintertime net evaporation and EAI. In the east and south of the basin effect of the evaporation is reduced by the higher precipitation and therefore, the net evaporation patterns for the positive and negative modes are similar.

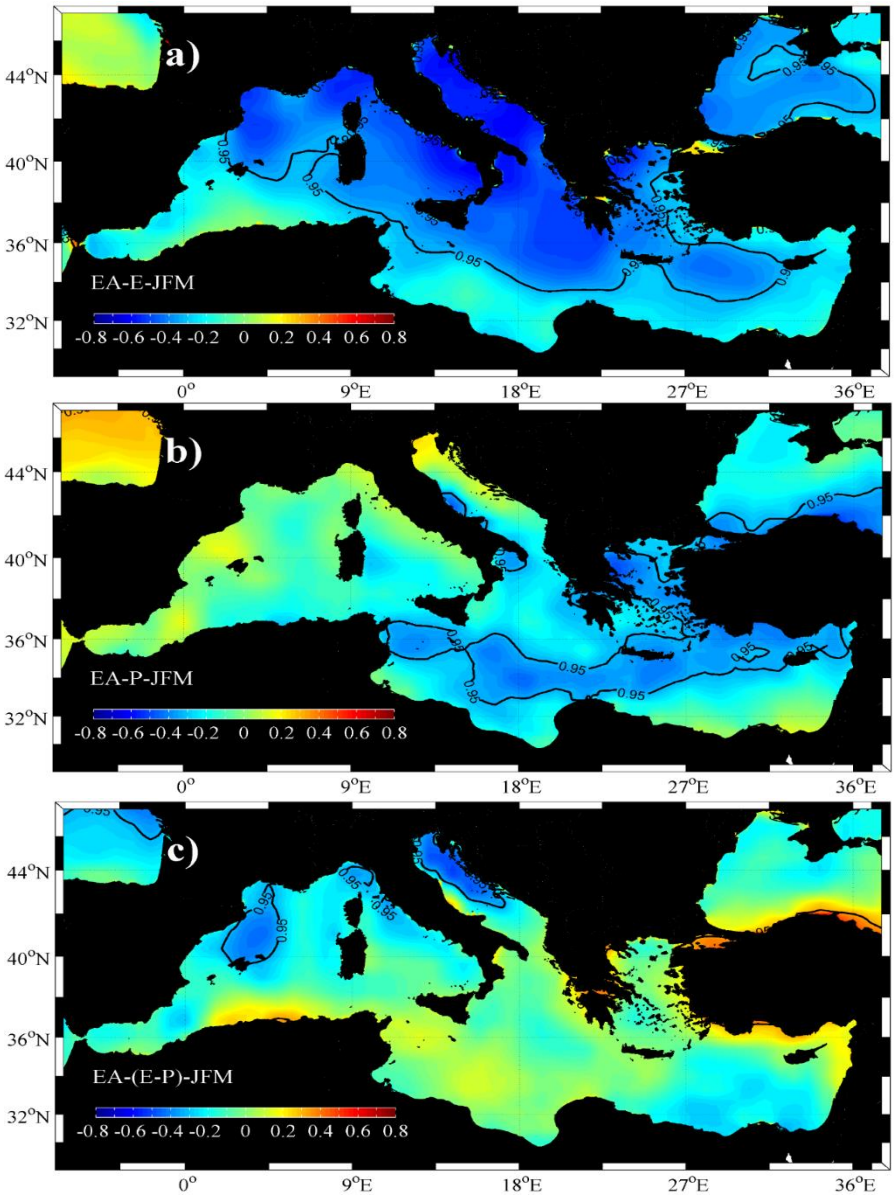

Figure 3- 28 Spatial distribution of the correlation coefficient between JFM EAI and a) evaporation, b) precipitation and c) evaporation-precipitation. The bold black line indicates the isoline of the 95% significance.

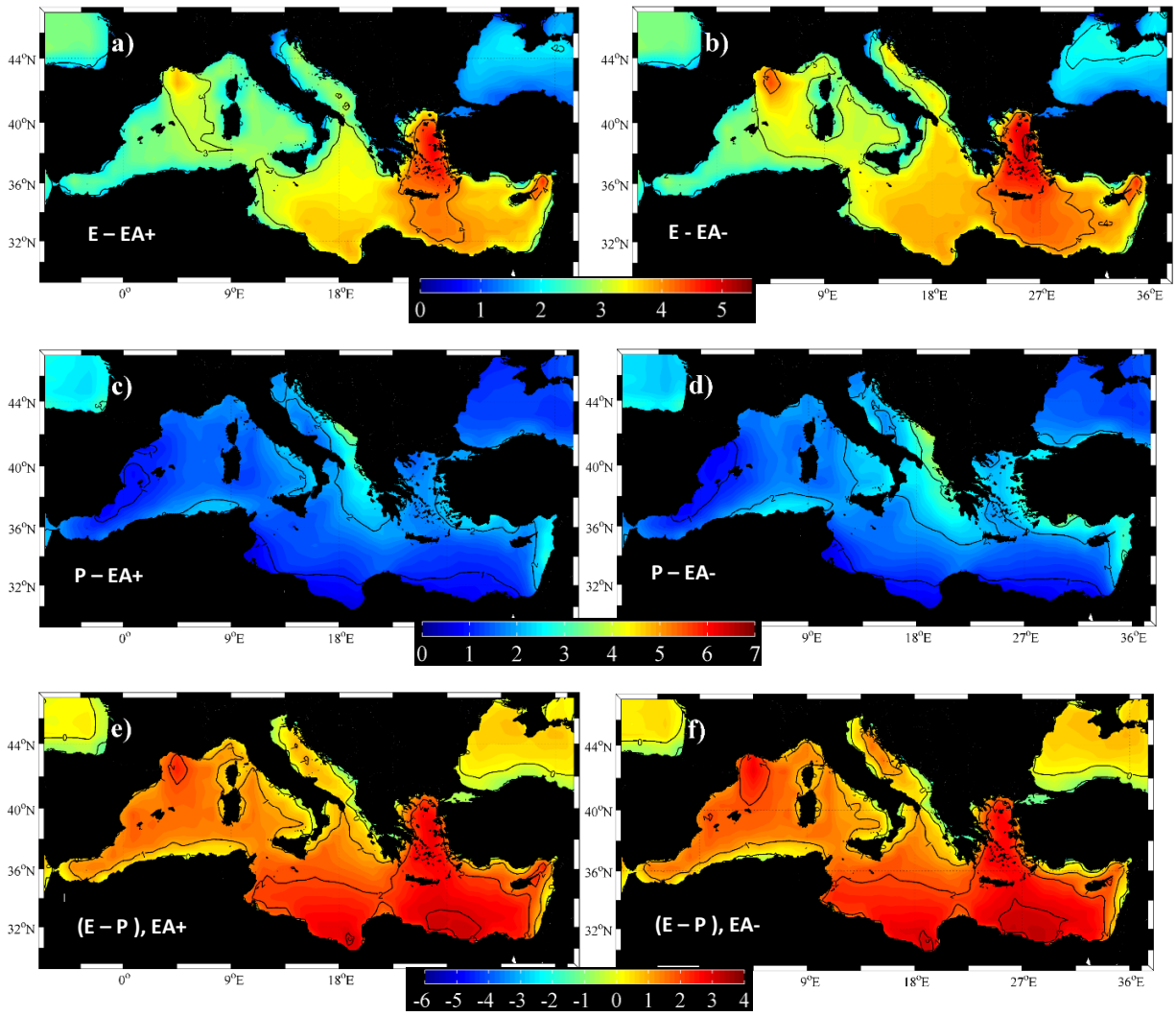

Figure 3- 29 Spatial distribution of the mean JFM a) evaporation during EAI+, b) evaporation during EAI-, c) precipitation during EAI+, d) precipitation during EAI-, e) net evaporation during EAI +, f) net evaporation during EAI- (mm/day). The black contours show the isolines with the interval of 2 mm/day.

Affecting the air-sea heat and water exchanges, EA pattern has a significant impact on the buoyancy fluxes in the western basin as well as in the Adriatic, Aegean and some parts of the Ionian Sea. The strong influence of EA pattern on the buoyancy is evidenced over most parts of the basin except the southern and eastern most coasts (see Fig. 3-30). Due to weakening of the wind speed during the EAI+, evaporation rate, and the consequent latent heat loss is reduced. Therefore, the Mediterranean Sea is characterized by the buoyancy rise and more stable condition in this phase. Conversely, during the negative EAI buoyancy loss is intensified as a result of

reinforcement of wind speed and associated increase of the evaporation rate. More briefly, higher evaporation due to the stronger wind fields gives rise to buoyancy loss in the major parts of the basin during the EAI-.

In addition, the net buoyancy flux reveals the pattern similar to the thermal component. This can be explained by the prevailing effect of the heat flux in buoyancy variations.

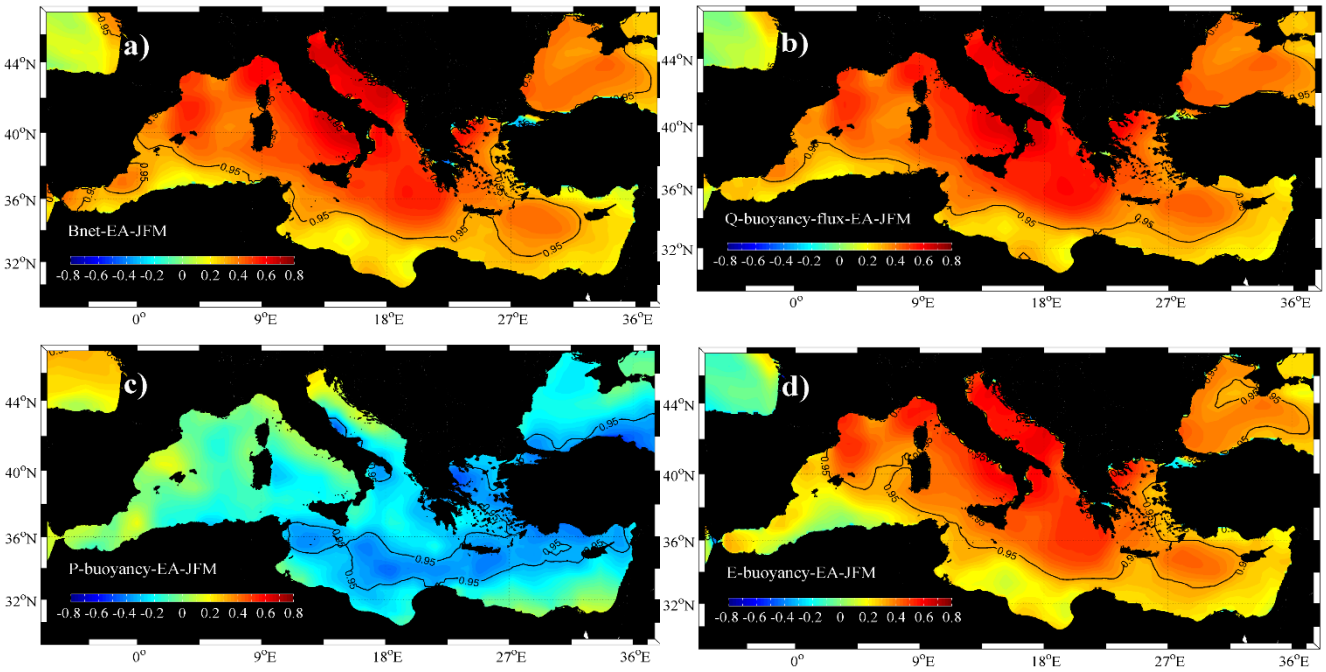

Figure 3- 30 Spatial distribution of the correlation coefficient between JFM EAI and a) net buoyancy flux, b) thermal buoyancy flux, c) precipitation buoyancy flux and d) evaporation buoyancy flux. The bold black line indicates the isoline of the 95% significance.

Unlike NAOI, which is negatively correlated with sea level of major portions of the basin, EAI is in phase with sea level height and this impact is limited to smaller parts of the basin including the eastern half of the WMED, and to a lesser extent to some areas of the South Ionian Sea (see Fig. 3-31 and 3-32). Intensification of the low-pressure centre during the positive mode of EA is responsible for the higher sea level in this phase. Conversely, negative EAI is characterized by the positive anomaly of the atmospheric pressure which reduces the sea surface height in the WMED.

In addition, change of winter thermosteric sea level in the WMED is strongly related to the EA pattern. More specifically, sea surface height increases by warming of the water during the positive

mode. On the other hand, cooling effects of the EAI- on the WMED is associated with the lower sea level. The same result has been obtained by Martínez-Asensio et al. in 2014.

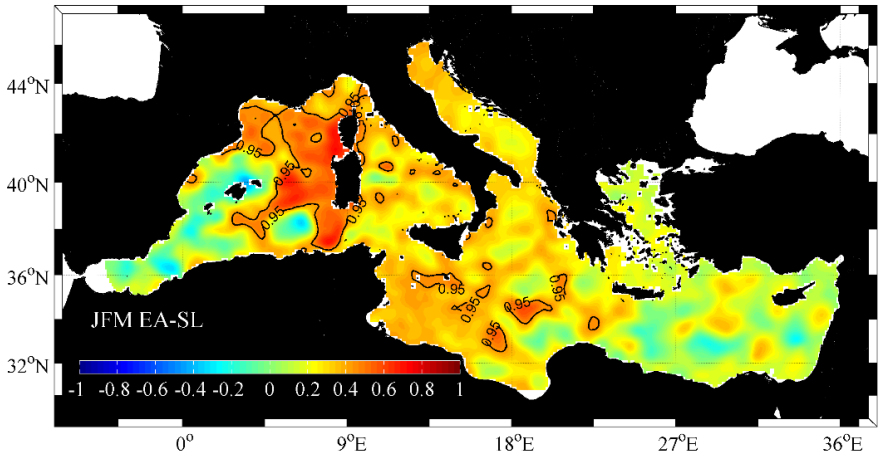

Figure 3- 31 Spatial distribution of the correlation coefficient between JFM EAI and seal level height. The bold black line indicates the isoline of the 95% significance.

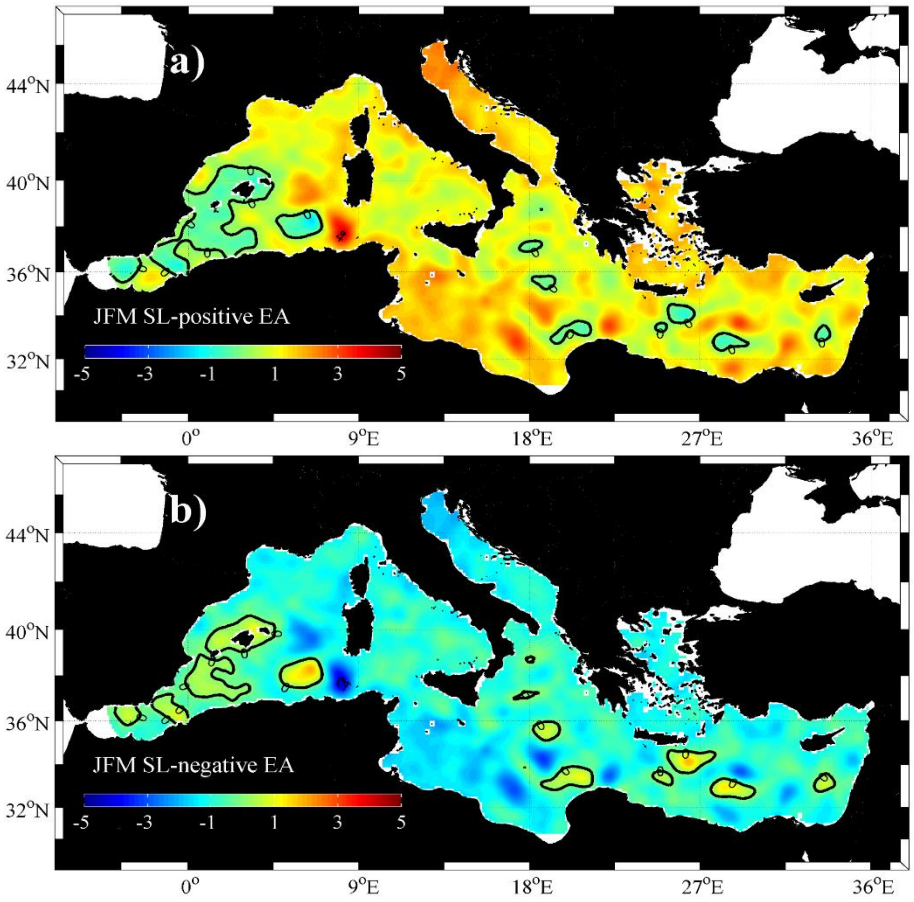

Figure 3- 32 Spatial distribution of the JFM mean of the sea level height anomaly during a) EAI+ and b) EAI-. The black contours indicate the isolines of the sea level with the interval of 2cm and the bolk black line shows the isoline of 0.

3-4- Relationship between MO and oceanography of the Mediterranean Sea

MOI, defined as the anomaly of the sea level pressure between south France and the Levantine Sea, has been found to be the best illustrative of the heat loss in the eastern basin especially Cretan Sea with the strong area-dependent influence on the air–sea heat exchanges in the Basin. MO is not considered as an independent mode of the atmospheric variability and reflects some combination of the other independent ones and it is developed to capture SLP variability within the Mediterranean (Papadopoulos et al., 2012b).

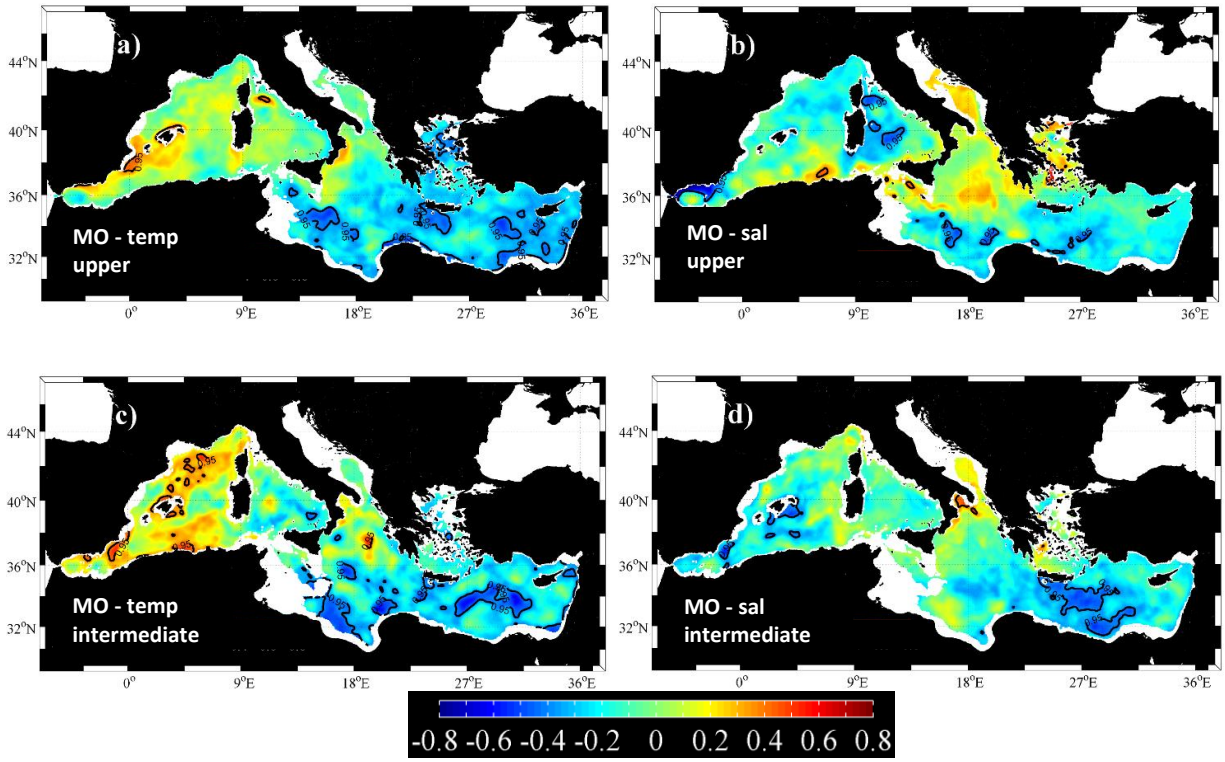

Figure 3- 33 Spatial distribution of the correlation coefficient between JFM MOI with a) JFM upper layer temperature, b) JFM upper layer salinity, c) JFM intermediate temperature (lag =1 year), and d) JFM intermediate salinity (lag =1 year). The bold black line indicates the isoline of the 95% significance.

In order to understand the extent to which the Mediterranean thermohaline characteristics are influenced by MO, the spatial pattern of the correlation coefficients between the winter-time index and temperature and salinity at the upper and intermediate layers of the basin were calculated (Fig 3-33). The impacts of the index on the temperature is more prevalent in the EMED (Fig. 3-33a and c) with the negative correlation while the correlations are not significant in the western basin. In

addition, salinity is out of phase with MOI in some small areas in EMED, as well as in the northwest of the Alboran Sea. In the Levantine Basin, this effect is more pronounced in the intermediate layer.

In order to explain the temperature variability in relation to MO, the correlation coefficients between the index and heat flux components were evaluated. The patterns reveal a dipole structure with the positive values in the west and negative correlations in the eastern basin (Fig. 3-34). In the western Mediterranean, the correlation is low and it cannot be explained in terms of the neither sensible nor latent heat exchanges while in the EMED the heat flux components are strongly out of phase with the index. This is in agreement with Papadopoulos et al. (2012c) which connected the strong heat loss over the Cretan and the Levantine Seas to the MO.

Using the method explained in the previous sections, the JFM average patterns of anomaly of the upper layer temperature and salinity as well as net heat flux anomaly were calculated for the periods characterized by the low and high phases of MO (Fig. 3-35; Table 3-3). It should be stressed here that the period of study is mostly corresponded to the positive phase of MOI (see Fig. 1-6). Positive MOI influences on the EMED by decreasing the temperature. The opposite condition is present during the MOI- (Fig 3-35 a, b). The cooling effect associated with the positive mode can be explained by the enhancement of the heat loss (see Fig 3-35 e, f) due to the stronger northerlies generated by the intensification of the pressure gradient between WMED and EMED. Figure 3-35 e indicates the strong heat loss over the EMED during the positive MOI. On contrary, negative mode of the index provides the warming conditions due to the downward heat flux toward the sea.

Table 3- 3 list of years characterized by positive and negative MO modes used for calculating the averages and corresponded MOI.

High MOI +				
Year	1990	1993	1998	2012
Index value	6.09	7.09	6.20	8.48
Low MOI -				
Year	1996	2009	2001	2010
Index value	0.24	0.35	-2.18	-1.60

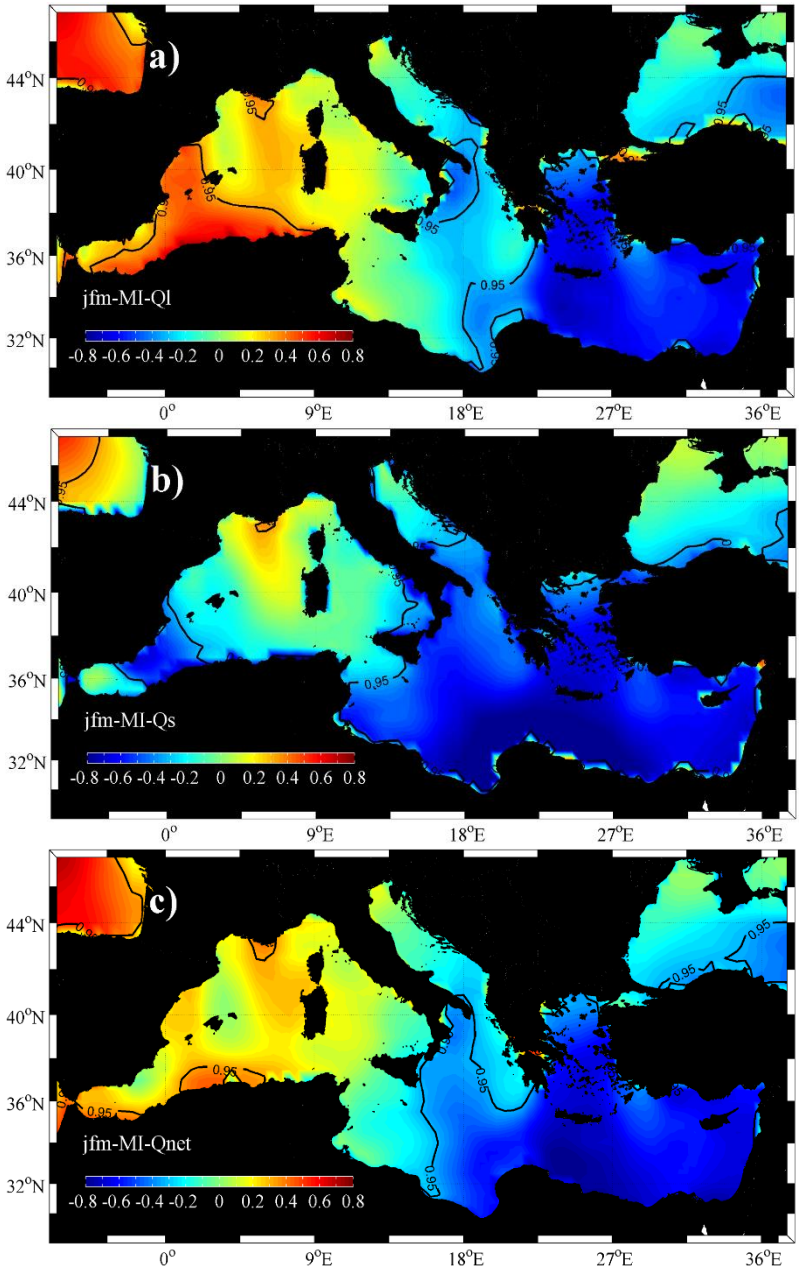

Figure 3- 34 Spatial distribution of the correlation coefficient between JFM MOI and a) latent heat flux, b) sensible heat flux, c) net heat flux. The bold black line indicates the isoline of the 95% significance.

Furthermore, spatial distributions of the average of salinity anomalies for the periods characterized by the positive and negative MOI show a rather weak increase of salinity during the negative MOI, when the stronger heat gain takes place over the EMED. In other words, although the strong winter convection is evidenced during the positive mode, salinity doesn't reveal the noticeable change in this phase. To explain that, we can refer to the fact that the BiOS mechanism is responsible for the salinity variations in the EMED. More specifically, during the anticyclonic BiOS, Levantine water is characterized by the higher salinity while the cyclonic mode of the Ionian circulation is associated with the reduction of the Levantine salt content. Therefore salinity variability can be controlled by both atmospheric forcing as well as the inflow of the water with different characteristics due to the influence of the reversal in the Ionian circulations.

Variability of air-sea heat flux is mainly related to the wind configuration resulting from the change in intensity and direction of pressure gradient axis. Therefore, in order to explain the variation of the heat exchanges in relation to MO, wind patterns associated with the MO modes are evaluated.

Strength and orientation of pressure gradient axis determine the magnitude and direction of the wind. Therefore, change of MO mode is followed by variation of wind pattern. Fig. 3-36 indicates the average of the wind stress magnitude over the Mediterranean area during the positive and negative MOI. In general, MOI+ is associated with the stronger northerly winds over the basin while the westerlies are evidenced during the negative mode. In the WMED maximum wind speed is revealed in the Gulf of Lion which is slightly stronger during the positive phase. In the eastern basin, the enhancement of the northerlies over the Aegean and Levantine Seas is considerable during MOI+.

According to vorticity equation (Eq.2-10), wind stress curl is an important factor responsible for the variation of the sea circulation. In order to understand to what extent current vorticity is affected by the MO, the time-series of the wintertime index is compared with the wind stress curl using correlation coefficients. The spatial distribution of these correlations (Fig 3-37) is similar to the one for NAO (see Fig. 3-5). In the other words, in the major parts of the WMED as well as the Adriatic and Aegean Seas wind stress vorticity is out of phase with MOI. The strong correlation between NAOI and MOI has been documented in some other studies (e.g. Papadopoulos et al., 2012c). However, wind vorticity in the Levantine basin reveals positive correlation with this index.

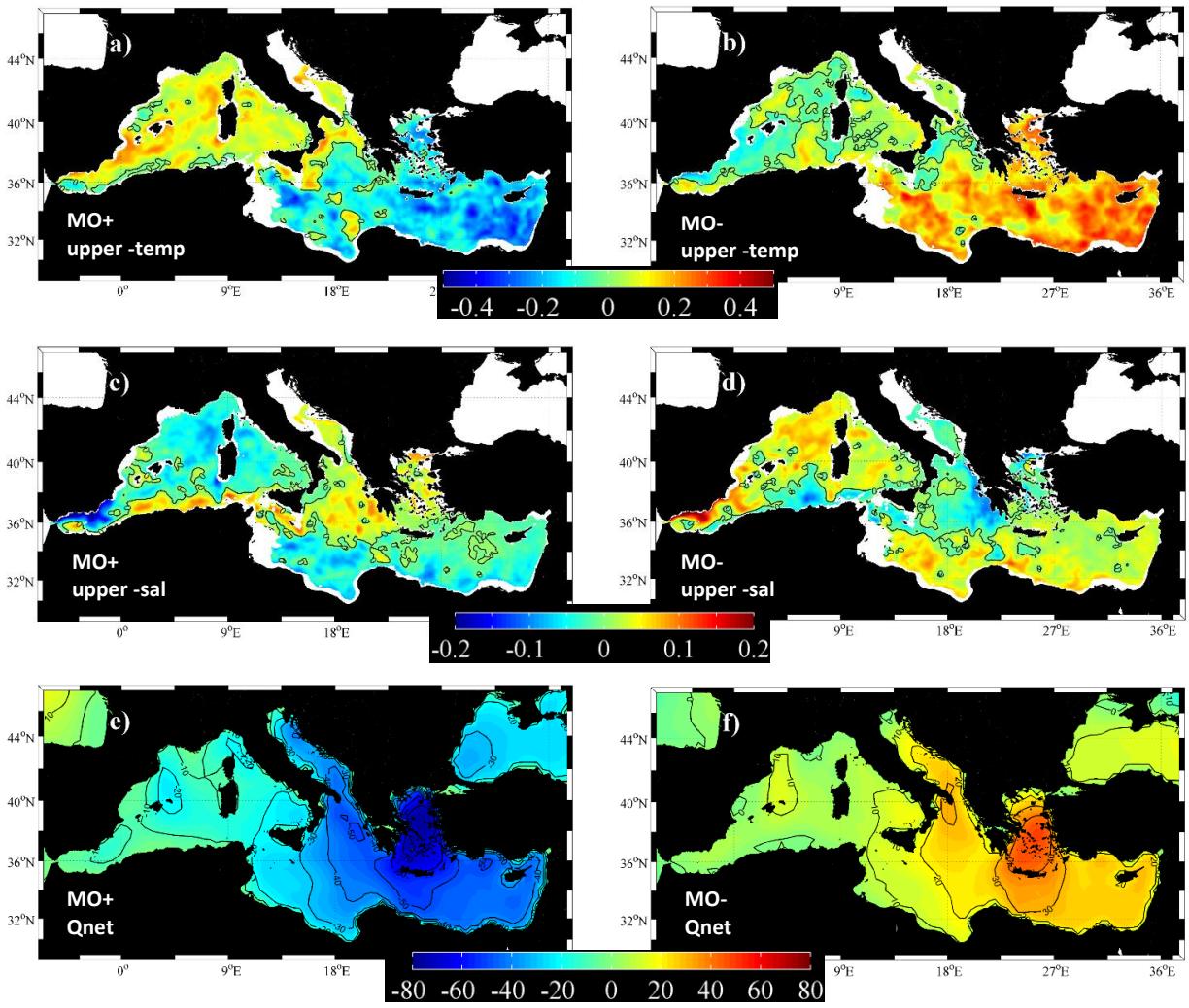

Figure 3- 35 Spatial distribution of the mean JFM a) temperature anomaly ($^{\circ}C$) during MOI+, b) temperature anomaly ($^{\circ}C$) during MOI-, c) salinity anomaly during MOI+, d) salinity anomaly during MOI-, e) net heat flux (Wm^{-2}) anomaly during MOI+, f) net heat flux (Wm^{-2}) anomaly during MOI-. The black contours show the isoline of 0.

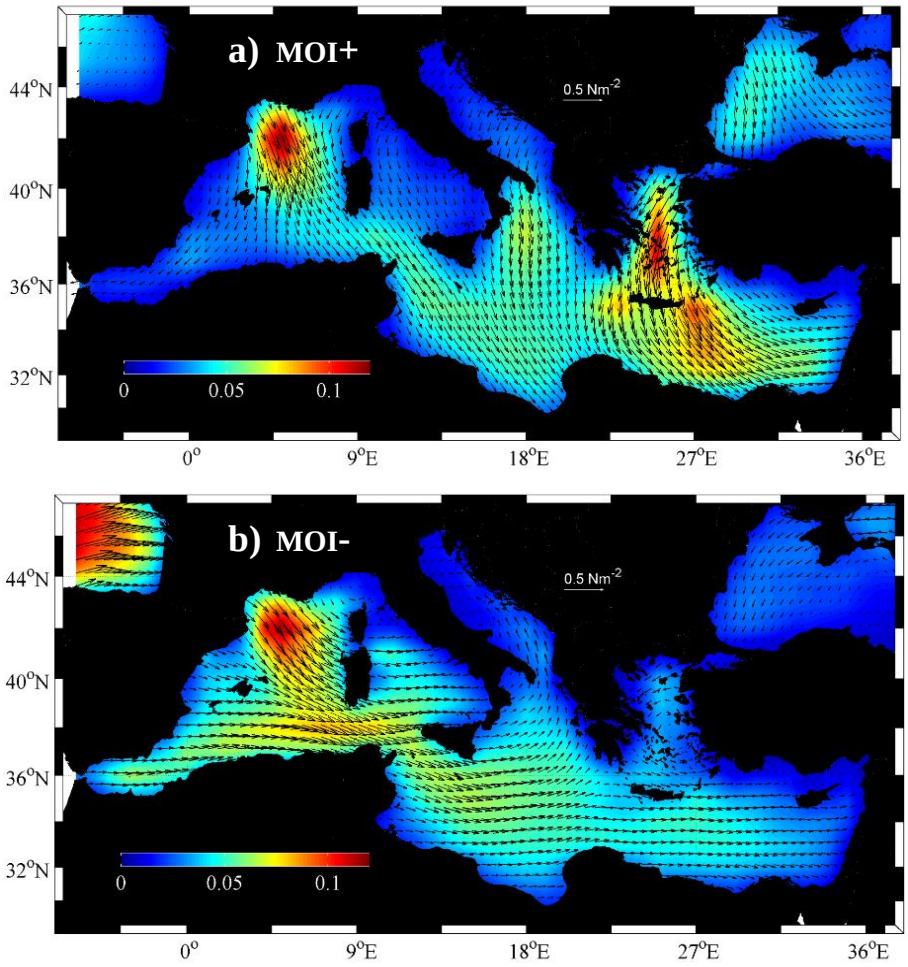

Figure 3- 36 Spatial distribution of the mean JFM wind-stress magnitude (colours; Nm^{-2}) and wind-stress vectors (arrows; Nm-2) in the positive MO phase (a) and negative MO phase (b), 1988-2011.

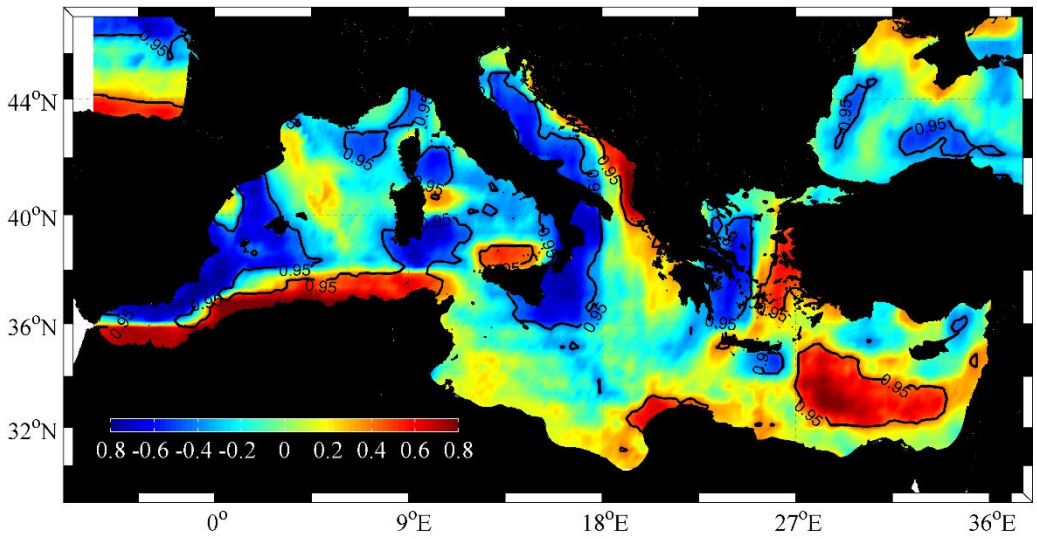

Figure 3- 37 Spatial distribution of the correlation coefficient between JFM MOI and the wind stress curl. The bold black line indicates the isoline of the 95% significance.

The positive MO mode is characterized by enhancement of pressure gradient between the west and east Mediterranean and subsequent reinforcement of the northerly winds. The higher atmospheric pressure in southern France intensifies the anti-cyclonic vorticity in the western most part of the basin during the positive phase. In the same way, the cyclonic wind circulation increases due to the lower atmospheric pressure in Levantine (see Fig. 3-38a). Conversely, by weakening the pressure gradient between the WMED and the EMED in the negative phase of MO, anticyclonic activity in the west and cyclonic circulation in the east of the basin is reduced. These results are also evidenced in the scatter diagrams between the spatially averaged vorticity in the Gulf of Lion, Aegean Sea, South Adriatic Sea as well as Levantine basin (Fig 3-39).

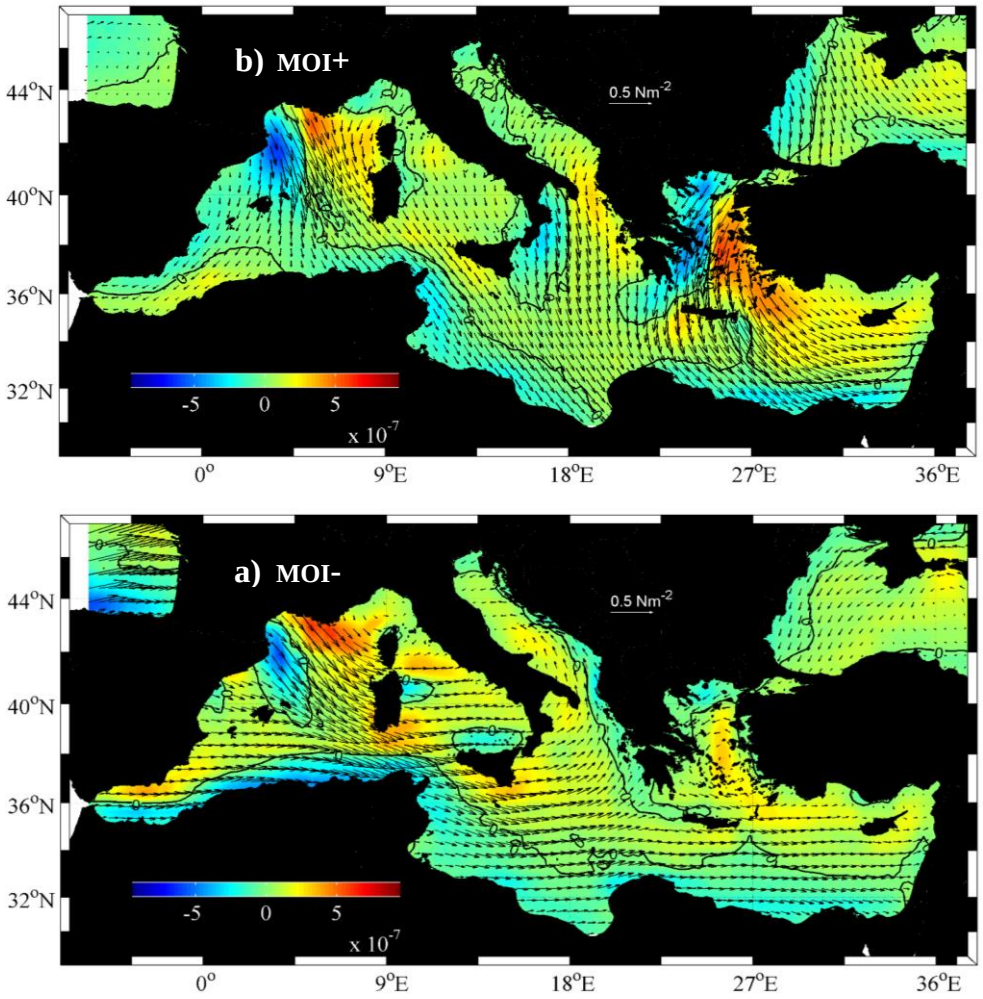

Figure 3- 38 Spatial distribution of the mean JFM wind-stress vorticity (colours; Nm-3) and wind-stress vectors (arrows; Nm-2) in the positive MO phase (a) and negative MO phase (b), 1988-2011.

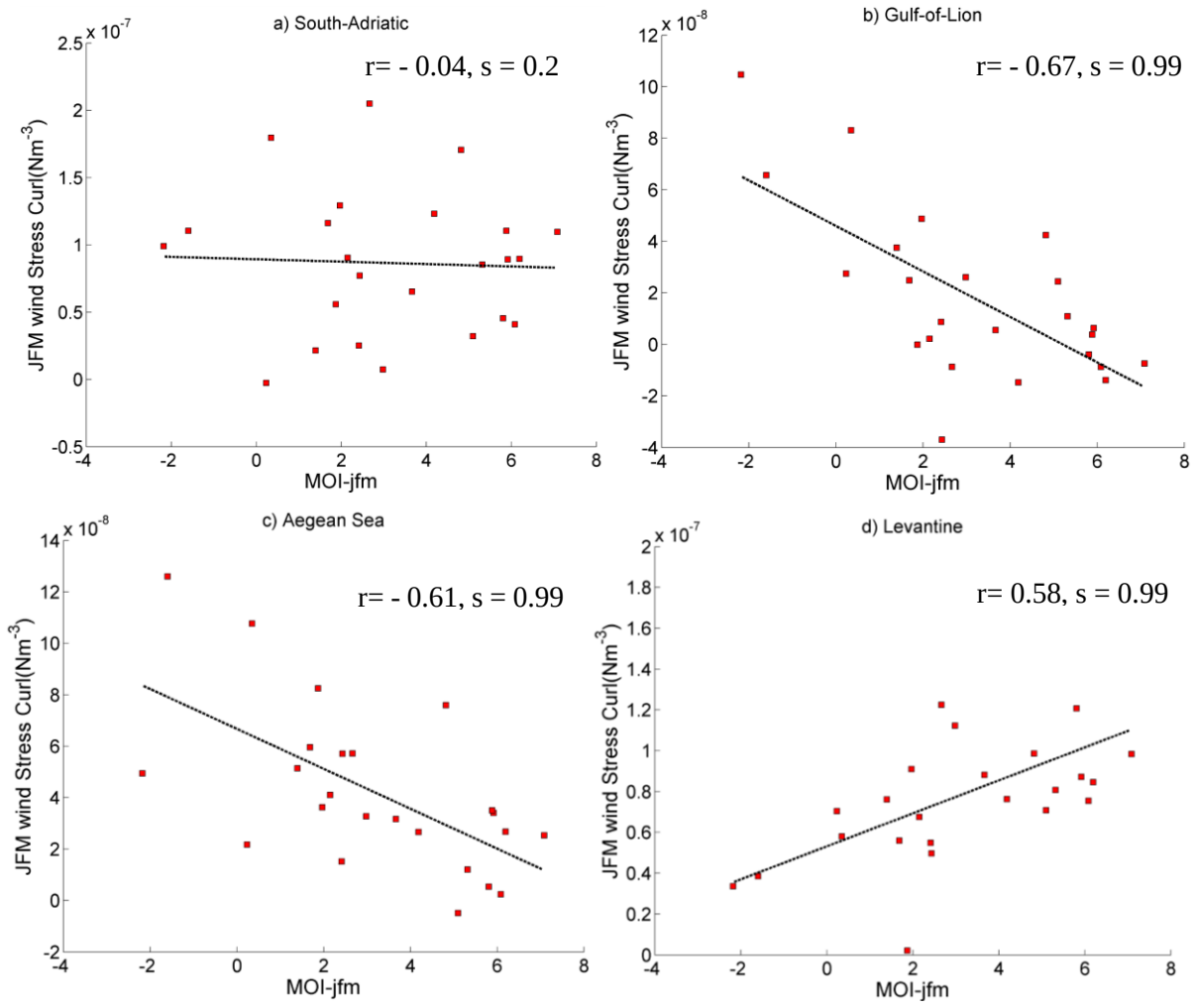

Figure 3- 39 Scatter plots of the wintertime MOI and the average of the wind stress curl in a) South Adriatic Sea, b) Gulf of Lion, c) Aegean Sea and d) Levantine Sea (see fig. 3-7 for the averaging areas).

The intense cold-air outbreak over the sea is associated with the increase of evaporation rate and consequent heat loss. The spatial distribution of the correlation coefficients between JFM evaporation rate and the MOI (Fig. 3-40a) shows the dipole structure of the negative correlation in the western most parts and the high positive correlation in the eastern basin with the maximum correlation over the Levantine Sea. The significant correlation is also evidenced in the northwest of the Ionian Sea. During the positive MOI, the strong evaporation events occur over the eastern basin with maximum located in the Aegean Sea. Intensification of the northerlies (Fig. 3-36) over the EMED during MOI+ is responsible for the evaporation increase (Fig. 3-41a, b) and consequently stronger heat loss during the positive phase (see Fig. 3-35). Evaporation during the negative MOI is not much considerable.

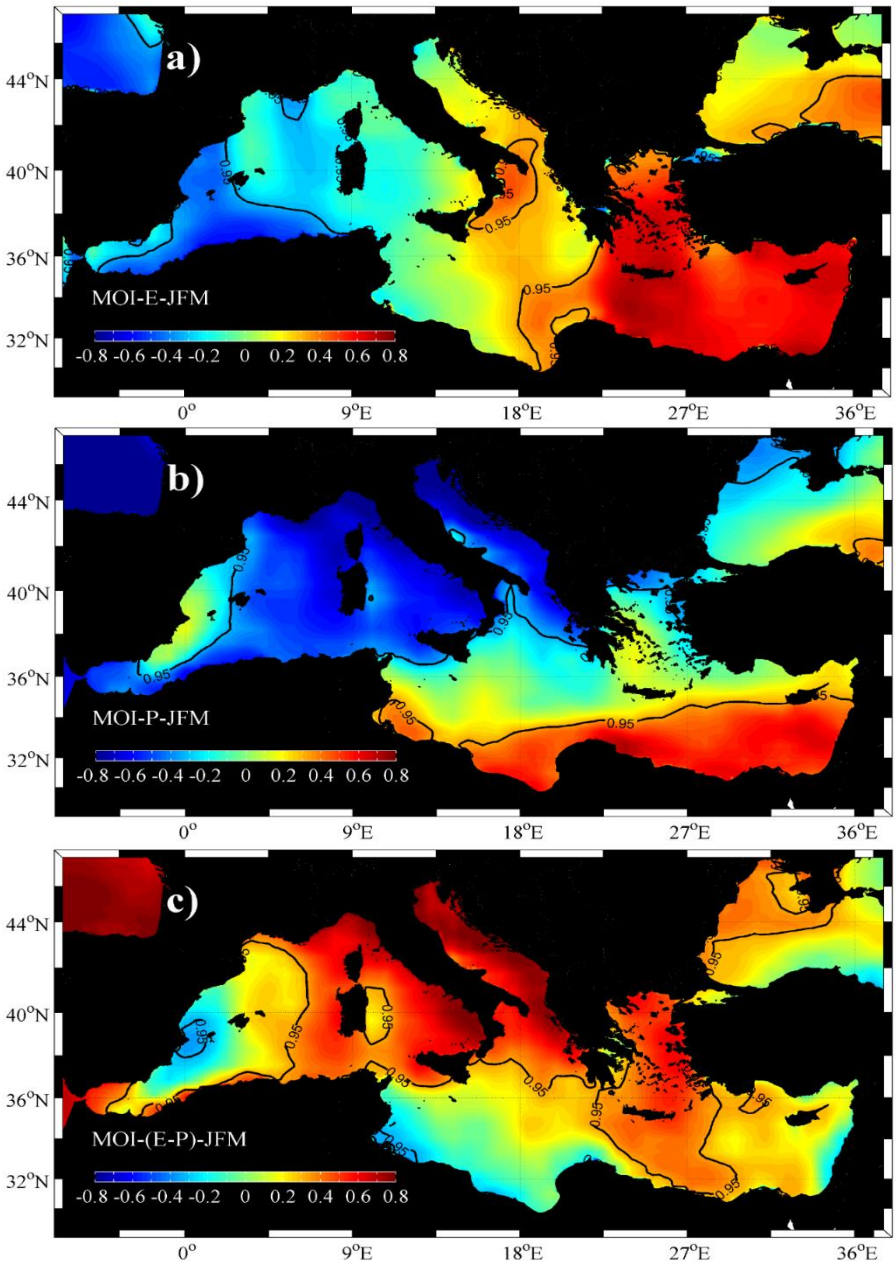

Figure 3- 40 Spatial distribution of the correlation coefficient between JFM MOI and a) evaporation, b) precipitation and c) evaporation-precipitation. The bold black line indicates the isoline of the 95% significance.

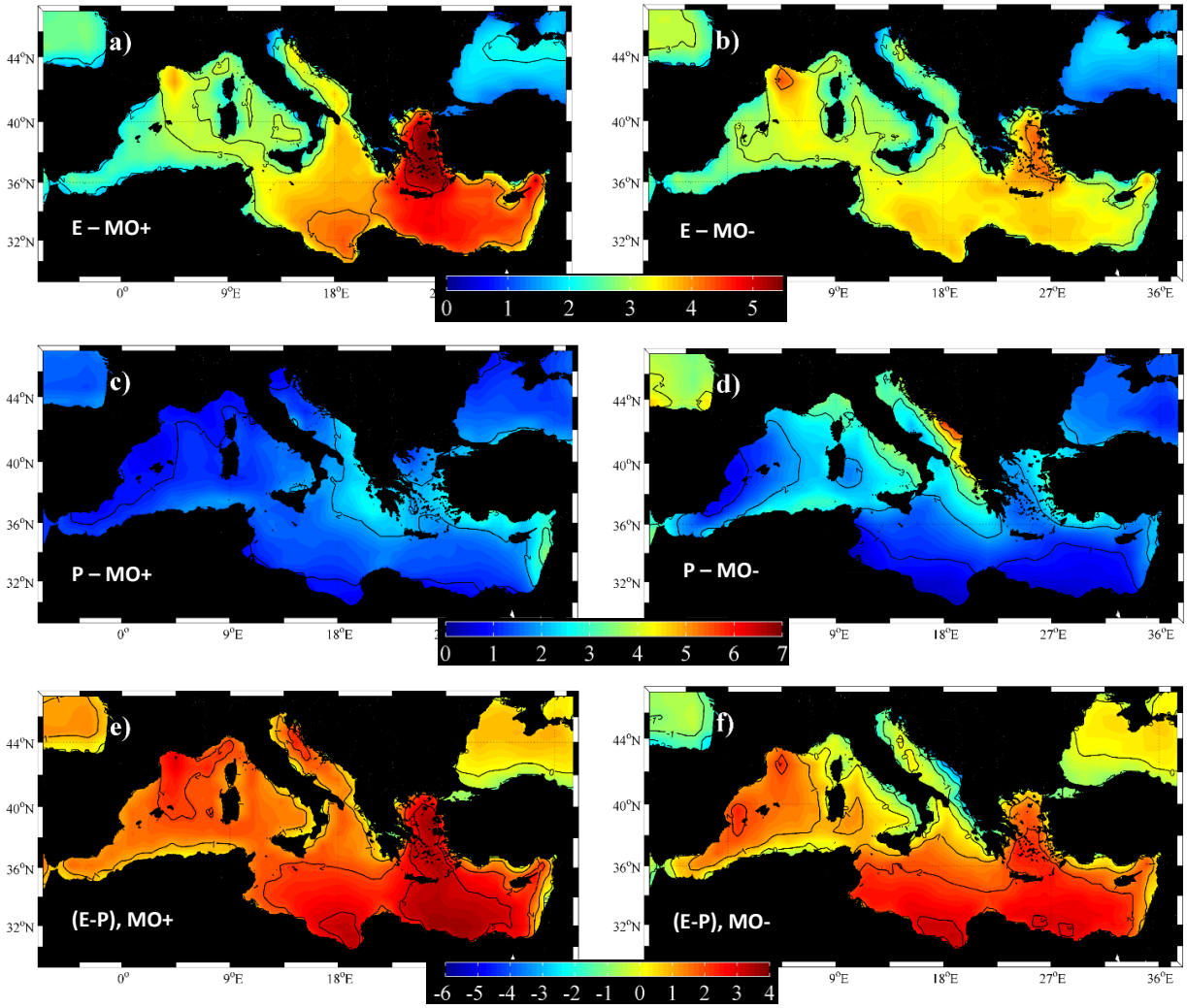

Figure 3- 41 Spatial distribution of the mean JFM a) evaporation during MOI+, b) evaporation during MOI-, c) precipitation during MOI+, d) precipitation during MOI-, e) net evaporation during MOI+, f) net evaporation during MOI- (mm/day). The black contours show the isolines with the interval of 2 mm/day.

Precipitation rate is out of phase with MOI over the WMED while it is in phase in the EMED (Fig. 3-40b). Obviously the higher atmospheric pressure in the western basin and the lower pressure in the eastern part during the MOI+ is responsible for this structure. Therefore MOI+ provides drier conditions in the west and more precipitation in the east of the basin. The opposite pattern is revealed for the periods of the negative MOI (Fig 3-41b and c). Similar to NAO, MO has a weak impact on the precipitation rate in the Balearic Sea. The mean atmospheric pressure configuration in this area characterized by the anticyclonic or low cyclonic wind circulation might be responsible for the low average precipitation in this sub-basin during the both MO phases.

The net evaporation is strongly correlated with MOI in the Adriatic Sea as well as in the eastern regions of the WMED and, to a lesser extent, in the Aegean and Levantine Seas (Fig. 3-40c). The average of the JFM net evaporation for the periods characterized by the positive and negative MOI are separately shown in the Fig. 3-41e and f. Comparison between these patterns shows that the net evaporation in the Adriatic and eastern side of WMED is more influenced by precipitation while in the eastern basin effect of evaporation is dominant.

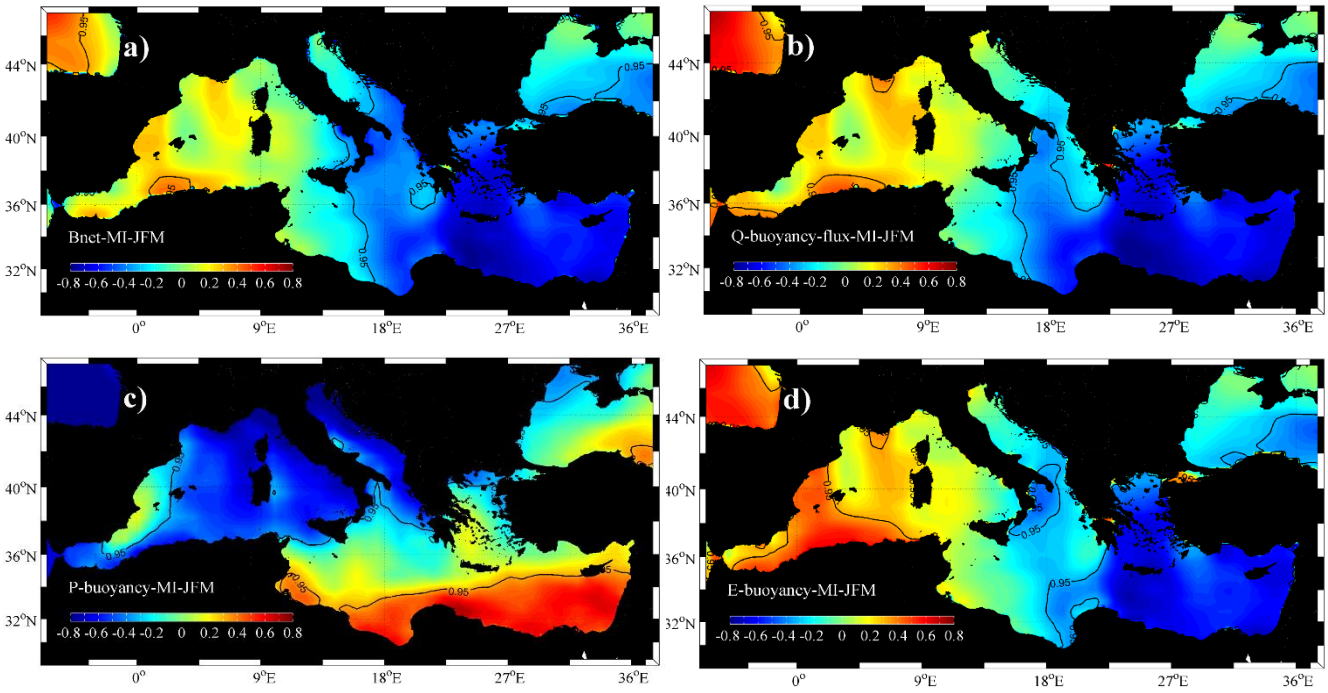

Figure 3- 42 Spatial distribution of the correlation coefficient between JFM MOI and a) net buoyancy flux, b) thermal buoyancy flux, c) precipitation buoyancy flux and d) evaporation buoyancy flux. The bold black line indicates the isoline of the 95% significance.

The buoyancy fluxes induced by the fresh water and heat exchanges are the important forcing for Mediterranean circulation (Robinson et al. 2001). The regions characterized by the high buoyancy loss are the potential areas for deep convection and dense water formation by forming the weakly stratified water and intense mixing (Grignon et al., 2010).

Response of the Mediterranean Sea to the climate patterns in terms of buoyancy variations is investigated in this part.

Net buoyancy flux is strongly out of phase with the MOI in the eastern basin (Fig. 3-42a). In other words, positive MOI is associated with the buoyancy loss in this area while the negative phase of MO exhibits the increase of surface buoyancy.

During the MOI+, the effect of thermal buoyancy gain in the western basin can be reduced by lower precipitation while buoyancy loss will be intensified in the EMED by stronger heat loss due to the higher evaporation. Therefore, the buoyancy loss is significant in the eastern basin during the MOI+.

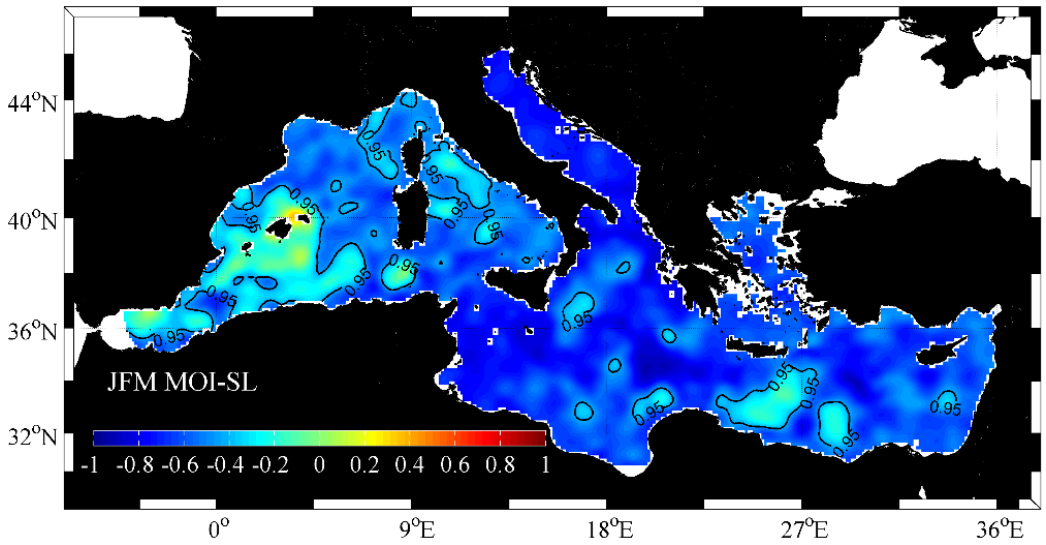

Figure 3- 43 Spatial distribution of the correlation coefficient between JFM MOI and seal level height. The bold black line indicates the isoline of the 95% significance.

The impact of the MO on the sea level height is similar to the NAOI and wintertime sea level height is anti-correlated with this index (Fig. 3-43). In other words, during the positive MOI lower sea level is evidenced due to the higher atmospheric pressure in the western basin. Conversely, in MOI- the sea level in the basin is higher than average (see Fig. 3-44). This is consistent with the results obtained by Sušelj et al. (2008) showing that MO is responsible for the 46% of the variance of the sea surface height in winter. The effects of MO on the sea level height of the western-most part of the basin is not much considerable. It should be mentioned that positive mode of MO does not necessarily correspond with the higher atmospheric pressure in the western and lower pressure in the eastern basin but it is defined by the high gradient of SLP between WMED and EMED. For

this reason, there is no evidence of Mediterranean Sea level being high neither in the east during MOI+ nor in the west during MOI-.

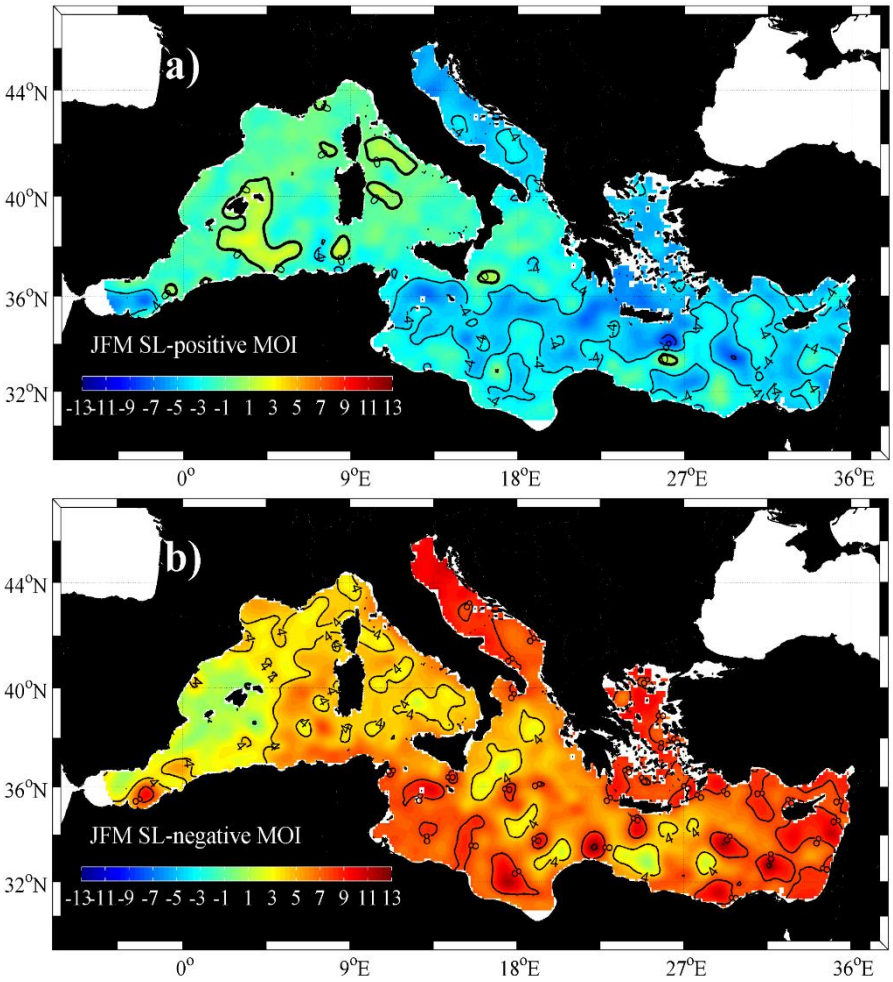

Figure 3- 44 Spatial distribution of the JFM mean of the sea level height anomaly during a) MOI+ and b) MOI-. The black contours indicate the isolines of the sea level with the interval of 2cm and the bold black line shows the isoline of 0.

3-5- Impacts of MO on the Mediterranean sub-regions

MO does not influence equally on the characteristics of the different sub-basins of the Mediterranean. Therefore, the different behaviors of the sub-basins in response to the Mediterranean Oscillation are described as follows:

– **Gulf of Lion**

The north-westerly wind over the Gulf of Lion is present during both modes of MO but is deflected into more northerly direction during the positive MOI which, to some extent, intensifies the winter heat loss. However, the difference is not much considerable and therefore, it doesn't reveal the strong influence of the index on the heat exchanges, temperature, salinity and evaporation in this area.

On the other hand, higher atmospheric pressure over the region reduces the cyclonic vorticity which subsequently decreases the precipitation rate in the positive mode. Therefore, vorticity and precipitation in the Gulf of Lion are out of phase with the index (see Fig. 3-37b and 3-40b). More precipitation during the negative phase gives the rise to buoyancy but since the thermal effect is dominant, the net buoyancy flux is not much influenced by the index in Gulf of Lion.

– **Alboran Sea**

The higher salinity is observed in the north-western coasts of the Alboran Sea during the negative MOI. This can be related to the westerly winds generated by the weakening of the atmospheric pressure during the MOI- which induce the coastal upwelling and increase salinity in this area. This pattern is not evidenced in the MOI+ therefore, the upper layer is occupied by the low-salinity AW.

In addition, the higher atmospheric pressure during MOI+ is responsible for relatively low north-easterly winds, anticyclonic vorticity, and decrease of precipitation in this area. However, heat and buoyancy fluxes are not influenced by the index in this region.

– **Adriatic Sea**

In the Adriatic Sea positive MOI is associated with the cold and dry north-easterly wind and consequent enhancement of the heat loss due to the higher evaporation rate. Therefore, the buoyancy loss is relatively stronger in this mode. Moreover, the weak cyclonic vorticity is present in the south of the basin. Conversely, during the negative mode southerlies are evidenced over the south Adriatic while the easterlies are present in the north and middle of the basin. This wind configuration generates the relatively stronger atmospheric cyclonic circulation with the centre located in the middle of the basin. In other words, cyclonic circulation intensifies during the negative mode everywhere in the Adriatic except in the eastern coasts. Therefore, the negative

correlation between MOI and wind stress curl is observed in the most parts of the Adriatic Sea. The scatter plots of the average wind stress curl and MOI in the main sites of the deep water formation show the lowest correlation in the SAG (Fig. 3-39a). However, the average vorticity in SAG is not much affected by the MO due to the high positive and negative correlation revealed in the eastern and western coasts of the South Adriatic Sea, respectively. Net heat loss is slightly stronger during the MOI+ compared to the negative mode while the temperature and salinity are not much affected by the index fluctuation. This suggests the additional impact of the internal forcing on the thermohaline of the basin.

Furthermore, precipitation rate is strongly out of phase with the index in this area which, therefore, increases the net evaporation (E-P) in the positive mode.

– **Aegean Sea**

The stronger pressure gradient during the positive MOI results in the different wind pattern compared to the negative phase in the Aegean Sea. More specifically, during the MOI+, strong north-easterlies are dominant in the basin which produce a west-east dipole of the negative-positive vorticity. In addition, the cooling effect associated with the strong evaporation and resulted latent heat loss reduce temperature and subsequent intensification of vertical mixing gives a rise to the increase of salinity. On the other hand, in the negative mode, the wind magnitude diminishes and the wind pattern reveals a weak cyclonic vorticity. Therefore, the due to the less heat loss and weakening of the winter convection, the higher temperature is revealed in this phase.

Moreover, no influence of the MO on the precipitation is evidenced in the Aegean Sea.

– **Levantine Sea**

Positive MOI is associated with the strong north-westerly winds producing the positive vorticity in the Levantine basin. In other words, lower atmospheric pressure and the associated stronger north-westerlies in the Levantine Sea during the MOI+ generates more cyclonic vorticity. Evaporation rate increases due to the enhancement of wind magnitude and the consequent heat loss reduces the temperature of the basin in this phase. The lower atmospheric pressure and intensification of the cyclonic vorticity give a rise to the precipitation rate but due to the dominant effect of evaporation, the net evaporation is also in phase with the index. In addition, the stronger heat loss during the positive mode reduces the surface buoyancy in the basin and therefore, stronger

winter convection takes place during MOI+. In contrast, westerly winds are evidenced during the MOI- due to the weakening of the pressure gradient which gives a rise to basin temperature and reduces the evaporation rate.

Negative correlation between salinity and MOI is evidenced in the Levantine basin (particularly in the intermediate layer) as well as in some small areas in the south Ionian Sea (Fig. 3-33). Nevertheless, as in the case of the Ionian and NAO, any cause-effect relationship can be excluded. In other words, the higher salinity during MOI- (and lower salinity in the positive phase) cannot be explained in terms of air-sea exchanges. This suggests the prevalence of the internal mechanisms in determining the salinity of the eastern basin which may be independent from the external forcing. More specifically, the salt content in the Levantine Sea is mainly controlled by the North Ionian circulation (e.g. Gačić et al., 2011). During the anticyclonic circulation of the NIG, the AW pathway is diverged northward in the Ionian Sea. This results in a variation of salt content of the water flowing toward the Levantine basin and increases the salinity. On other hand, the cyclonic phase causes a more direct inflow of AW into the Levantine and the consequent decrease of upper layer salinity.

Chapter 4

Conclusions

Conclusions

The aim of this research is to describe the impacts of the low frequency modes of the atmospheric variability on the thermohaline properties of the Mediterranean Sea during the winter periods.

The Mediterranean Sea is an almost isolated oceanic system and the site of occurrence of the fundamental processes to the general oceanic circulation. It exchanges the water, salt, heat and the other properties with the North Atlantic Ocean, which is the important location of deep- and bottom-water formation for the global conveyor belt. The air-sea interaction in terms of the heat, fresh water and momentum fluxes represents an essential factor determining the dynamic behavior of ocean and atmosphere. It plays an important role in the global climate system by affecting key processes such as thermohaline circulation and large scale atmospheric flows. Therefore, due to the importance of the air-sea exchanges in climate of the basin, the connection between large scale climate patterns (as the best illustrative of the physical and meteorological conditions of the system) and oceanography of the Mediterranean is well worth studying.

The climate patterns considered in this study are North Atlantic Oscillation (NAO), East Atlantic (EA) pattern and Mediterranean Oscillation (MO). Two first indices are known as the first and second independent modes of the atmospheric variability, respectively, while the last one is recognized as the combination of the other independent modes illustrating the variability of the SLP over the Mediterranean basin.

Although the climate of the Mediterranean Sea has been widely studied in recent years, many questions still remain unanswered on this subject. This work has attempted to answer some of the following questions:

- How are the basin characteristics affected by NAO, EA patterns, and MO? What are differences between Mediterranean sub-regions in terms of the response to these climate indices?
- What is the relative importance of the climatic modes in different Mediterranean sub-regions?
- To what extent are the sites of the deep water formation influenced by the external forcing? Should the internal mechanisms also be taken into consideration?

– Which mechanisms are responsible for the long-term variation of the intensity of some important gyres? What is the relative importance of each factor?

Here we will summarize the main findings of the study concerning the research questions and provide the synthesis of the results discussed in the previous chapters. Furthermore, strengths and limitations of the work are identified and the recommendations for future research are outlined.

The time-series of the temperature and salinity in the upper and intermediate layers of the Mediterranean basin, wind stress velocity and vorticity, sea level height as well as heat, water and buoyancy flux components, were compared with these indices calculating the correlation coefficients. In addition, the average fields of these parameters associated with the positive and negative modes of the climatic indices were calculated and compared. Temperature and salinity fields in the upper layer respond immediately to the atmospheric forcing while in the intermediate layer they are lagging the climate indices by about one year.

The spatial distribution of the correlation coefficients between NAOI and temperature time-series for the winter periods from January to March (JFM) reveals a dipole structure. In other words, the temperature in the west of the basin is in phase with NAOI while it is out of phase in Eastern Mediterranean (EMED). Salinity is anti-correlated with the index in both sub-basins but this effect is more evident in the upper layer of the Western Mediterranean (WMED) as well as in the intermediate layer of the EMED. Therefore, in the western sub-basin, the positive NAO mode is associated with the warmer and less saline water compared to the negative phase.

This can be explained by the difference in the heat exchanges between two modes of the climate index. During the negative NAOI, the enhancement of the wind magnitude is evidenced over the WMED and the resulting strong heat loss is responsible for the intensification of the vertical mixing and, therefore, the presence of the colder and saltier water in the upper and, to a lesser extent, intermediate layer. The opposite condition is evidenced in the positive mode. This implies that the negative phase of NAO is associated with the more favorable conditions for the Western Mediterranean Deep Water Formation (WMDWF).

The eastern basin, more specifically the Levantine Sea, reveals the different response to this climate index. The reinforcement of the heat loss due to the stronger northerly winds and the subsequent rise in evaporation in the positive phase decreases the temperature of the basin. In addition, the lower salinity is evidenced in the EMED during the positive NAOI. It can be explained by the fact that during NAOI+, western basin and Atlantic jet are characterized by the

lower salinity. The inflow of the less saline Atlantic Water (AW) into EMED through the Strait of Sicily reduces the salinity of the eastern basin. It should be stressed that the pathway of the AW inflow into the eastern basin depends on the phase of Adriatic-Ionian Bimodal Oscillating System (BiOS). More specifically, during the anticyclonic mode of the North Ionian Gyre (NIG) circulation, AW deviates toward the North Ionian and it has the longer path and residence time to reach the Levantine basin. Therefore, the Levantine basin is characterized by the higher salinity. Conversely, in the cyclonic phase of BiOS, AW spreads directly into the Levantine Sea and reduces the salinity of the basin. Therefore, the variation of the surface salinity in the eastern basin is not only the function of the external forcing but the effect of the Ionian circulation should also be considered.

In addition, in the negative NAO mode, lower pressure and the associated westerly winds intensify the cyclonic atmospheric circulation and precipitation rate over the northern areas of the basin. More specifically, higher precipitation is evidenced in the major parts of WMED as well as in the Adriatic, North Ionian and the Aegean seas during the NAOI-. On the contrary, the lower precipitation rate is revealed in the basin over the periods characterized by the positive NAO mode due to the reinforcement of the Azores high pressure.

Sea level in the major portion of the basin is mainly out of phase with NAOI. This might be related to the rise of atmospheric pressure over Mediterranean during the positive mode. Nevertheless, in the NIG and some other circulation features such as Mersa-Matruh, Ierapetra and Algerian gyres, weak influence of NAO on the sea surface height is evidenced. This shows that the internal oceanic processes are the factors mainly determining the circulation in these areas. Particularly in the NIG, the absence of a relation between sea level and NAOI confirms that BiOS mechanism is not affected by climatic patterns.

Due to the combined effects of the heat and water exchanges, the net surface buoyancy flux was found to be in phase with NAOI in the western basin particularly in the Gulf of Lion. This asserts that the negative phase of NAO is associated with the lower surface buoyancy, and therefore, intensification of the dense water formation process in the WMED.

Some differences in the relationship between NAOI and oceanographic conditions in the Mediterranean sub-basins have also been evidenced. More specifically, temperature and salinity along the eastern coasts of Sicily are more affected by the horizontal advection from the WMED, and there is no evidence of the variation of the heat fluxes by changing the index. Temperature

and salinity in the WAG have the opposite response to NAO compared to the rest of western basin. This can be explained by the upwelling mechanism in the north-western Alboran induced by the strengthening of the westerlies during the NAOI- which transports the warmer and fresher surface water to the gyre.

Inter-annual variability of the intensity of the South Adriatic Gyre (SAG) has also been studied. According to the vorticity equation the intensity of the gyre depends on the local forcing and the vorticity advection from the adjacent area, i.e. the northern Ionian.

The maximum correlation between the wintertime wind-stress curl and the geostrophic vorticity tendency in the SAG coincides with the maximum of the current vorticity average. It indicates that the current vorticity tendency can partially be explained in terms of the local wind vorticity input. The vorticity variations in the SAG lag those in the NIG by about 14 months, suggesting an advection speed of about 1 cm/s. Stronger impact of the advection term is evidenced during the anti-cyclonic mode of BiOS, originating from the northern area of the NIG. It implies that the importance of the advective term in the vorticity equation depends on the BiOS circulation mode.

Comparison between the NAOI and the wind-stress curl shows that the higher vorticity in the wind field coincides with the negative NAO mode. Therefore, to a certain extent, the inter-annual variations of the strength of the SAG are associated with the large-scale climatic variations via the wind-stress curl forcing. However, due to the rather important contribution of the vorticity advection from the Ionian, characterized by the prevalent decadal variability, there is no clear evidence of the direct effect of large-scale atmospheric circulation over the North Atlantic (NAO) on the inter-annual variability of the intensity of the SAG.

Contrary to NAO, the influence of EA on the temperature and salinity is much weaker. However, the WMED is more affected by this index. The temperature in the western basin is in phase with EAI while the salinity is out of phase. In other words, during EAI+ the temperature in the WMED increases and conversely, while the colder water in the upper and intermediate layer is associated with EAI-. This can be explained in terms of the variation of the heat exchanges due to the change in EA modes.

More specifically, in both phases of EA, the north-westerly wind blows over the WMED with the maximum magnitude in the Gulf of Lion but stronger wind speed is evidenced during the negative mode. This is related to the higher atmospheric pressure over the western basin during the EAI- and the associated rise in the wind magnitude which result in the increase of the

evaporation rate and heat loss. Therefore, stronger winter convection takes place during the negative mode as the consequence of the surface buoyancy loss, while WMED in the EAI+ is characterized by the warmer and less salty water. Therefore, favorable conditions for the dense water formation are present in the western basin over the periods characterized by the negative phase of EA. The same mechanism in the Ionian Sea, especially the southern parts, associated with the advective effects is responsible for the decrease of temperature in this area during EAI-.

The stronger effect of heat fluxes is evidenced in the Adriatic and in the Aegean seas. In the Adriatic, the temperature doesn't reveal any noticeable change between two modes of this climate index. This emphasizes the importance of the internal processes in the thermohaline conditions of the Adriatic Sea which compensates the impact of the meteorological forcings. The role of the EA pattern on the temperature variation of the Aegean Sea through the heat fluxes is more clear, although it is not comparable with its effects on the WMED.

The influence of the EA on the sea level height is limited to the area in the north-western part of the basin including the Gulf of Lion. Positive EAI is associated with the higher sea level due to the lower atmospheric pressure in this area during this mode. Similar to NAO, EA doesn't have any impact on the sea level of the NIG which again confirms that the BiOS mechanism is not driven by the atmospheric forcing. In addition, EA pattern doesn't have any considerable impact on the precipitation in the basin.

On the other hand, MO reveals stronger impact on the eastern basin. Temperature in the EMED is negatively correlated to MOI. By intensification of the pressure gradient during the positive mode of the index, stronger northerlies are evidenced over EMED. The wind pattern reveals the local speed maximum over the Aegean and Levantine seas during MOI+ which coincides with the location of the maximum heat loss during the positive mode. This strongly highlights the importance of the MO in determining the characteristics of the eastern basin. The increase of the evaporation rate and the consequent heat and buoyancy loss is related to this configuration of the wind which reduces the temperature of this region. Conversely, negative MOI is associated with the weaker westerlies over the eastern parts and therefore, the higher temperature is observed.

Furthermore, it should be emphasized that the salinity of the Levantine basin is mainly controlled by the Ionian circulation modes. Therefore, the variations of the salt content of this basin cannot be well explained in terms of external forcing. In addition, the configuration of the atmospheric surface pressure associated with this climate pattern implies the higher precipitation

rate over the eastern part and drier conditions in the western basin during its positive phase. Furthermore, MOI+ is characterized by the lower sea level height, particularly in the eastern portion of the basin.

In the Adriatic Sea, north-easterly winds are present during MOI+ while the negative phase reveals the presence of southerlies in the south and north-easterlies in the north of the basin. Hence, the cyclonic atmospheric circulation is intensified during this mode which gives a rise to the precipitation rate in this area. However, similar to the other two indices, the temperature and salinity in the Adriatic are not much influenced by this index.

The only area of the western basin which is considerably influenced by MO is the north-western part of the Alboran Sea. The noticeable increase of salinity is evidenced in this area during the negative mode of MO which can be explained by the presence of the rather strong westerlies which induce the off shore upwelling in the Spanish coasts of the Alboran Sea and increase the salinity in the area.

Therefore, it is evident that the large-scale climatic patterns have an important effect on the Mediterranean Sea. In general, the change in the atmospheric pressure pattern and the subsequent variations in the pressure gradient axis and the resulted wind configuration are responsible for the variability of the air-sea heat and water exchanges. This can consequently explains the variation of the temperature and the salinity of the basin, or in other words, the thermohaline properties of the Mediterranean Sea.

To summarize, the effect of each index differs from one sub-region to another. In other words, NAO affects both western and eastern sub-basins while the effects of the EA and MO are limited to smaller areas. The stronger impact of the EA is evidenced on the WMED, whereas the effect of the MO on the EMED is more pronounced. In addition, it seems that the contribution of the meteorological conditions in determining the oceanic characteristics is more visible in the western basin while it is sometimes less clear in the EMED, particularly in the Adriatic Sea, due to the additional contribution of the internal oceanic processes, although this part of the basin is strongly affected by the atmospheric forcing through the wind effects.

This research has faced some limitations. For instance, the analysis has been carried out for the time period covering the available data-sets of the atmospheric and oceanic variables when the climate conditions were on average characterized by a rather persistent positive phase of NAO and MO. In addition, reanalysis temperature and salinity time-series obtained from OGCM have been

increasingly used in Mediterranean Sea studies and the accuracy of the data-sets has been validated. However, in the case that continuous high-resolution observational temperature and salinity data-sets which spatially cover the entire basin were available, the level of confidence of the analyses concerning the inter-annual variability of oceanic processes would increase.

Further research on the following subjects would add to the current knowledge:

- The long-term variability of the Mediterranean gyres and its relation with climatic patterns.
- The role of the internal processes in the characteristics of the Adriatic Sea. More specifically, since the significant heat flux variation due to the changes in the modes of climate patterns is evidenced in the Adriatic Sea, it would be interesting to study the manner in which the effects of the atmospheric forcing compete with the internal mechanisms in this area.
- The role of the large-scale climatic patterns on the extreme conditions of the Mediterranean basin. For instance, how the extreme events of sea level height are related to the climate indices.

References

Atlas, R., Ardizzone, J. V., Hoffman, R., Jusem, J. C. and Leidner, S. M.: Cross-calibrated, multi-platform ocean surface wind velocity product (MEaSUREs Project). Guide Document. Physical Oceanography Distributed Active Archive Center (PO.DAAC). JPL, Pasadena, California, 18 May 2009, Version 1.0., 26p, 2009.

Barnston, A. G. and Livezey, R. E.: Classification, seasonality and persistence of low- frequency atmospheric circulation patterns. Mon.Wea. Rev. 115, 1083–1126, 1987.

Bignami, F., Mattietti, G., Rotundi, A. and Salusti, E.: On a Sugimoto-Whitehead effect in the Mediterranean Sea: Sinking and mixing of a bottom current in the Bari Canyon, southern Adriatic Sea. Deep Sea Research Part A 37, 657–665, 1990.

Borzelli, G. L. E., Gačić, M., Cardin, V. and Civitarese, G.: Eastern Mediterranean transient and reversal of the Ionian Sea circulation. Geophys. Res. Lett., 36, L15108, 2009, doi:10.1029/2009GL039261.

Brunetti, M., Maugeri, M. and Nanni, T.: Atmospheric circulation and precipitation in Italy for the last 50 years. International Journal of Climatology, vol. 22, no. 12, 1455–1471, 2002.

Castellari, S., Pinardi, N. and Leaman, K.: Simulation of water mass formation processes in the Mediterranean Sea: Influence of the time frequency of the atmospheric forcing. J. Geophys. Res., 105(C10), 24,157–24,181, 2000, doi:10.1029/2000JC900055.

Cheney, R. E. and Doblar, R. A.: Structure and variability of the Alborán Sea frontal system. J. Geophys. Res. 87 (C1), 585–594, 1982.

Civitarese, G., Gačić, M., Borzelli, G. L. and Lipizer, M.: On the impact of the Bimodal Oscillating System (BiOS) on the iogeochemistry and biology of the Adriatic and Ionian Seas (eastern Mediterranean). Biogeosciences, 7, 3987–3997, 2010, doi:10.5194/bg-7-3987-2010.

Conte, M., Giuffrida, S. and Tedesco, S.: The Mediterranean oscillation: impact on precipitation and hydrology in Italy. In Proceedings of the Conference on Climate and Water, Vol. 1. Publications of Academy of Finland: Helsinki; 121–137, 1989.

Crepon, M.: Influence de la pression atmospherique sur le nivau moyen de la Mediterranee Occidentale et sur le flux a travers le detroit de Gibraltar. Cah. Oceanogr. 1 (7), 15–32, 1965.

Criado-Aldeanueva, F., Del Río, J. and García-Lafuente, J.: Steric and mass induced Mediterranean Sea level trends from 14 years of altimetry data. Global and Planetary Change, 60, 563-575, 2008.

Criado-Aldeanueva, F. and Soto-Navarro, F. J.: The Mediterranean oscillation teleconnection index: station-based versus principal component paradigms. Advances in Meteorology, vol. 2013, Article ID 738501, 10 pages, 2013. doi:10.1155/2013/738501.

Criado-Aldeanueva, F., Soto-Navarro, F. J, García-Lafuente, J.: Climatic indices influencing the long-term variability of Mediterranean heat and water fluxes: The North Atlantic and Mediterranean oscillations. Atmosphere-Ocean, 52, Iss. 2, 2014a.

Criado-Aldeanueva, F., Soto-Navarro, F. J. and García-Lafuente, J.: Large-scale atmospheric forcing influencing the long-term variability of Mediterranean heat and freshwater Budgets: Climatic Indices. J. Hydrometeor, 15, 650–663, 2014b, doi: http://dx.doi.org/10.1175/JHM-D-13-04.1

Cronin, M. F. and Sprintall, J.: Wind and buoyancy-forced upper ocean. In: J. Steele, S. Thorpe, and K. Turekian (eds.) Encyclopedia of Ocean Sciences, Vol. 6, 3219-3227, Academic Press, London, UK, 2001.

Cushman-Roisin, B., Gačić, M., Poulain, P. M., and Artegiani, A.: physical oceanography of the Adriatic Sea; Past, present and future. 126 pp, Kluwer Academic Publishers, Dordrecht, 2001.

deCastro, M., Gomez-Gesteira, M., Alvarez, I., Cabanas, J.M. and Prego, R.: Characterization of fall-winter upwelling recurrence along the Galician western coast (NW Spain) from 2000 to 2005: dependence on atmospheric forcing. Journal of Marine Systems 72, 145–148. 2008, doi:10.1016/ j.jmarsys.2007.04.005.

Demirov, E. and Pinardi, N.: Simulation of the Mediterranean Sea circulation from 1979 to 1993: Part I. The interannual variability, J. Mar. Syst., 33–34, 23–50, 2002, doi: 10.1016/S0924-7963(02)00051-9.

Ezer, T. and Mellor G. L.: Diagnostic and prognostic calculations of the North Atlantic circulation and sea level using a sigma coordinate ocean model, J. Geophys. Res., 99, 14159-14171, 1994.

Gačić, M., Civitarese, G., Miserocchi, S., Cardin, V., Crise A. and Mauri, E.: The open-ocean convention in the Southern Adriatic: a controlling mechanism of the spring phytoplankton bloom, Cont. Shelf Res., 22, 1897-1908, 2002.

Gačić, M., Borzelli G. L. E., Civitarese G., Cardin V. and Yari S.: Can internal processes sustain reversals of the ocean upper circulation? The Ionian Sea example, Geophys. Res. Lett., 37, L09608, 2010, doi:10.1029/ 2010GL043216.

Gačić, M., Civitarese, G., Eusebi Borzelli, G. L., Kovačević, V., Poulain, P. M., Theocharis, A., Menna, M., Catucci, A. and Zarokanellos, N.: On the relationship between the decadal oscillations of the Northern Ionian Sea and the salinity distributions in the Eastern Mediterranean, J. Geophys. Res., 116, C12002, 2011, doi:10.1029/2011JC007280.

Gačić, M., Schroeder, K., Civitarese, G., Cosoli, S., Vetrano, A., and ´Eusebi Borzelli, G. L.: Salinity in the Sicily Channel corroborates the role of the Adriatic-Ionian Bimodal Oscillating System (BiOS) in shaping the decadal variability of the Mediterranean overturning circulation, Ocean Sci., 9, 83–90, 2013, doi:10.5194/os-9-83-2013.

Gačić, M., Civitarese, G., Kovačević, V., Ursella, L., Bensi, M., Menna, M., Cardin V., Poulain, P. M., Cosoli, S., Notarstefano, G. and Pizzi, C: Extreme winter 2012 in the Adriatic: an example of climatic effect on the BiOS rhythm. Ocean Sci., 10, 513-522, 2014, doi:10.5194/os-10-513-2014.

Giorgi, F.: Variability and trends of subcontinental scale surface climate in the twentieth century. Part I: observatorios. Climate Dynamics 18: 675–691, 2002.

Giorgi, F.: Regional climate modeling: status and perspectives. Journal de Physique, IV, 139, 101-118, 2006.

Giorgi, F. and Lionello, P.: Climate Change Projections for the Mediterranean Region Global and Planetary Change, 63:90-104, 2008, doi: 10.1016/j.gloplacha.2007.09.005.

Gomis, D., Tsimplis, M. N., Martín-Míguez, B., Ratsimandresy, A. W., García-Lafuente, J. and Josey, S. A.: Mediterranean Sea level and barotropic flow through the Strait of Gibraltar for the period 1958–2001 and reconstructed since 1659. Journal of Geophysical Research C, 111, 11, Article ID C11005, 2006.

Gomis, D., Ruiz, S., Sotillo, M. G. et al: Low frequency Mediterranean sea level variability: the contribution of atmospheric pressure and wind. Global Planet Change 63:215–229, 2008, doi:10.1016/j.gloplacha.2008.06.005.

Grancini, G. F. and Michelato, A.: Current structure and variability in the Strait of Sicily and adjacent area, Ann. Geophys., Ser. B., 5, 75–88, 1987.

Grignon, L., Smeed, D. A., Bryden, H. L. and Schroeder, K.: Importance of the variability of hydrographic preconditioning for deep convection in the Gulf of Lion, NW Mediterranean. Ocean Sci. 6, 573–586, 2010.

Grisogono, B. and Belušić, D.: A review of recent advances in understanding the meso- and microscale properties of the severe Bora wind, Tellus A, 61, 1-16, 2009.

Hendershott, M. C. and Malanotte-Rizzoli, P.: The winter circulation of the Adriatic Sea. Deep Sea Res., 23, 353-370, 1976.

Herbaut, C., Martel, F. and Crepon, M.: A sensitivity study of the general circulation of the western Mediterranean Sea. Part II: The response to atmospheric forcing. J. Phys. Ocean., 27, 10, 2126-2145, 1997.

Hurrell, J. W.: Transient eddy forcing of the rotational flow during northern winter. J. Atmos. Sci. 52, 2286–2301, 1995.

Hurrell, J. W.: Influence of variations in extratropical wintertime teleconnections on northern hemisphere temperature. Geophys. Res. Lett. 23, 665–668, 1996.

Jerez, S., Jimenez-Guerrero, P., Montávez J. P. and Trigo R. M.: Impact of the North Atlantic Oscillation on European aerosol ground levels through local processes: a seasonal model-based assessment using fixed anthropogenic emissions, Atmos. Chem. Phys., 13, 11195-11207, 2013.

Josey, S. A.: Changes in the heat and freshwater forcing of the eastern Mediterranean and their influence on deep water formation, J. Geophys. Res., 108, 3237, 2003, doi:10.1029/2003JC001778.

Josey, S. A, Somot, S. and M. Tsimplis: Impacts of atmospheric modes of variability on Mediterranean Sea surface heat exchange. J. Geophys. Res., 116, C02032, 2011, doi:10.1029/2010JC006685.

Kalnay, E., Kanamitsu, M., Kistler, R., Collins, W., Deaven, D., Gandin, L., Iredell, M., Saha, S., White, G., Woollen, J., Zhu, Y., Leetmaa, A., Reynolds, R., Chelliah, M., Ebisuzaki, W., Higgins, W., Janowiak, J., Mo, K. C., Ropelewski, C., Wang, J., Roy Jenne, and Dennis Joseph: The NCEP/NCAR 40-year reanalysis project. Bull. Amer. Meteor. Soc., 77, 437–471, 1996, doi: http://dx.doi.org/10.1175/1520-0477(1996)077<0437:TNYRP>2.0.CO;2

Köhl, A.: Detecting processes contributing to interannual halosteric and thermosteric sea level variability. Journal of Climate, 27, 2417-2426, 2014, doi:10.1175/JCLI-D-13-00412.1.

Krichak, S. O., Kishcha, P. and Alpert, P.: Decadal trends of main Eurasian oscillations and the Eastern Mediterranean precipitation. Theor. Appl. Climatol., 72, 209–220, 2002.

Kushnir, Y.: Europe's winter prospects. Nature 398: 298–299, 1999.

Lamb, P. J. and Peppler, R. A: North Atlantic Oscillation: concept and an application, B. Am. Meteorol. Soc. 68: 1218-1225, 1987.

Larnicol, G., Ayoub, N. and Le Traon P. Y.: Major changes in Mediterranean Sea level variability from 7 years of TOPEX/Poseidon and ERS-1/2 data, J. Mar. Syst., 33–34, 63–89, 2002, doi:10.1016/S0924-7963 (02)00053-2.

Lascaratos, A.: Estimation of deep and intermediate water formation rates in the Mediterranean Sea, Deep-Sea Res. II, 40(6), 1327-1332, 1993.

Leaman, K. D., and Schott F.: Hydrographic structure of the convection regime in the Golfe du Lion, J. Phys. Oceanogr., 21, 575-598, 1991.

Lionello, P., Bhend, J., Buzzi, A., et al. : Cyclones in the Mediterranean region: climatology and effects on the environment, Mediterranean climate variability, Elsevier B. V., 325–372, 2006.

Lionello, P. (Ed.): The Climate of the Mediterranean Region, from the past to the future. Elsevier, pp 502, 2012, ISBN: 9780124160422

Luterbacher, J., Xoplaki, E., Casty, C., Wanner, H., Pauling, A., Küttel, M., et al.: Mediterranean climate variability over the last centuries: a review. In: Lionello, P., Malanotte-Rizzoli, P., Boscolo, R. (Eds.), The Mediterranean Climate: An overview of the main characteristics and issues. Elsevier, Amsterdam, pp. 27–148, 2006.

Madec, G., Lott, F., Delecluse, P. and Crepon, M.: Large-scale preconditioning of deep-water formation in the Northwestern Mediterranean Sea. J. Phys. Oceanogr. 26, 1393–1408, 1996.

Madec, G., Delecluse P., Imbard M. and Levy C.: OPA 8.1 ocean general circulation model reference manual. Institut Pierre-Simon Laplace, Note du Pole de Modelisazion, No. 11, 91 pp, 1998.

Malanotte-Rizzoli, P., Manca, B. B., Ribera, d'Alcala M., Theocharis, A., Brenner, S., Budillon, G. and Ozsoy, E.: The Eastern Mediterranean in the 80s and in the 90s: the big transition in the intermediate and deep circulation. Dynamics of Atmosphere and Oceans, 29 (2–4), pp. 365–395, 1999.

Malanotte-Rizzoli P.: The Northern Adriatic Sea as a prototype of convection and water mass formation on the continental shelf. In: Chu P.C. and Gascard J.C. (eds), Deep convection and deep water formation in the oceans, Elsevier Ocean. Series, 57, 229-239, 1991.

Malanotte-Rizzoli, P.: Introduction to special section: Physical and biochemical evolution of the Eastern Mediterranean in the 1990s (PBE), J. Geophys. Res., 108(C9), 8100, 2003, doi:10.1029/2003JC002063.

Malanotte-Rizzoli, P. and Eremeev, V. E.: The Eastern Mediterranean as a laboratory basin for the assessment of contrasting ecosystems. eds., Kluwer Academic Publishers, NATO Science Series, vol. 51, 521 pp., 1999.

Manca, B. B., Kovačević, V., Gačić, M., and Viezzoli, D.: Dense water formation in the Southern Adriatic Sea and spreading into the Ionian Sea in the period 1997-1999, J. Marine Syst. 33-34, 133-154, 2002.

Mantziafou, A. and Lascaratos, A.: Deep-water formation in the Adriatic Sea: Interannual simulation for years 1979–1999, DeepSea Res. Pt. 1, 55(11), 1403–1426, 2008.

Manzella, G. M. R., Hopkins, T. S., Minnett, P. J. and Nacini, E.: Atlantic water in the Strait of Sicily. Journal of Geophysical Research, 95, 1569-1575, 1990: doi: 10.1029/89JC00268. issn: 0148-0227.

Marcos, M. and Tsimplis, M. N.: Coastal sea level trends in southern Europe. Geophys. J. Int., 175(1), 70-82, 2008.

Mariotti, A., Struglia, M., Zeng, N. and Lau, K.: The hydrological cycle in the Mediterranean region and implications for the water budget of the Mediterranean Sea, J. Climate, 15, 1674–1690, 2002, DOI: 10.1175/1520-0442(2002)0152.0.CO;2.

Mariotti, A. and Arkin P.: The North Atlantic Oscillation and oceanic precipitation variability. Climate Dyn., 28(1), 35-51, 2007, DOI: 10.1007/s00382-006-0170-4.

Mariotti, A. and Dell'Aquila, A.: Decadal climate variability in the Mediterranean region: roles of large-scale forcings and regional processes. Clim. Dyn., 2011, doi:10.1007/s00382-011-1056-7.

Martínez-Asensio, A., Marcos, M., Tsimplis, M. N., Gomis, D., Josey, S., Jordà, G.: Impact of the atmospheric climate modes on Mediterranean sea level variability. Global and Planetary Change 118, 1-15, 2014.

Marullo, S., Napolitano, E., Santoleri, R., Manca, B. and Evans, R.: Variability of Rhodes and Ierapetra Gyres during Levantine intermediate water experiment: Observations and model results. J. Geophys. Res., 108, 2003, doi: 10.1029/2002JC001393. issn: 0148-0227.

Mertens, C. and Schott F.: Interannual variability of deep convection in the northwestern Mediterranean, J. Phys. Oceanogr., 28, 1410-1424, 1998

Mihanović, H., Vilibić, I., Carniel, S., Tudor, M., Russo, A., Bergamasco, A., Bubić, N., Ljubešić, Z., Viličić, D., Boldrin, A., Malačič, V., Celio, M., Comici, C. and Raicich, F: Exceptional dense water formation on the Adriatic shelf in the winter of 2012, Ocean Sci., 9, 561–572, 2013, doi:10.5194/os-9-561.

Millot, C.: Circulation in the western Mediterranean Sea, Oceanol. Acta, 10(2), 143-149, 1987.

Moretti, M., Sansone, E., Spezie, G., and De Maio, A.: Results of investigations in the Sicily Channel (1986–1990). Deep-Sea Research II, 40, 1181–1192, 1993.

Oddo, P., Adani, M., Pinardi, N., Fratianni, C., Tonani, M., Pettenuzzo, D.: A nested Atlantic-Mediterranean Sea general circulation model for operational forecasting. Ocean Sciences 5, 461-473, 2009.

Ovchinnikov, I. M., Zats, V. I., Krivosheia, V. G. and Udodov, A. I.: Formation of deep Eastern Mediterranean waters in the Adriatic Sea. Oceanology, 25: 704-707, 1985.

Ovchinnikov, I. M., Zats, V. I., Krivosheya, V. G., Nemirosky, M. S. and Udodov, A. I.: Winter convection in the Adriatic and formation of deep eastern Mediterranean waters, Ann. Geophysicae, 5B, 89–92, 1987.

Palutikof, J. P.: Analysis of Mediterranean climate data: measured and modelled, in Mediterranean climate: Variability and trends, Bolle, H. J., Ed., Springer, Berlin, Germany, 2003.

Pandžić, K. and Likso, T.: Eastern Adriatic typical wind field patterns and 699 large scale atmospheric conditions. Int. J. Climatol., 25, 81–98, 2005.

Papadopoulos, V. P., Kontoyiannis, H., Ruiz, S. and Zarokanellos, N.: Influence of atmospheric circulation on turbulent air-sea heat fluxes over the Mediterranean Sea during winter. J. Geophys. Res., C, 117, 3, Article ID C03044, 2012b.

Papadopoulos, V. P., Josey, S., Bartzokas, A., Somot, S., Ruiz, S. and Drakopoulou, P.: Large-scale atmospheric circulation favoring deep –and intermediate- water formation in the Mediterranean Sea. Journal of Climate, 25, pp. 6079–6091, 2012c.

Parrilla, G.: Mar de Alboran. Situación del giro anticiclónico en Abril de 1980. Bol. Inst. Esp. Oceanogr. 1 (2), 106–113, 1984.

Pedlosky, J.: Geophysical fluid dynamics. 2nd ed., 710 pp., Springer, New York, 1987.

Pettenuzzo, D., Large, W. G. and Pinardi, N.: On the corrections of ERA-40 surface flux products consistent with the Mediterranean heat and water budgets and the connection between basin surface total heat flux and NAO. J. Geophys. Res., 115, C06022, 2010, doi:10.1029/2009JC005631.

Pickart, R. S., Spall M. A., Ribergaard, M. H., Moore, G. W. K. and Milliff, R. F.: Deep convection in the Irminger Sea forced by the Greenland tip jet. Nature, 424, 152 – 156, 2003.

Pirazzoli, P. A. and Tomasin, A.: Recent near-surface wind changes in the Central Mediterranean and Adriatic areas, Int. J. Climatol., 23, 963-973, 2003.

POEM Group: General circulation of the eastern Mediterranean. Earth Science Reviews 32, 285–309, 1992.

Pujol, M. I. and Larnicol G.: Mediterranean Sea eddy kinetic energy variability from 11 years of altimetric data, J. Mar. Syst., 58, 121–142, 2005, doi:10.1016/j.jmarsys.2005.07.005.

Rio, M. H., Pascual, A., Poulain, P. M., Menna, M., Barcelò, B. and Tintoré, J.: Computation of a new mean dynamic topography for the Mediterranean Sea from model outputs, altimeter measurements and oceanographic in situ data, Ocean Sci., 10, 731-744, 2014.

Rixen, M., Beckers, J., Levitus, S., Antonov, J., Boyer, T., Maillard, C., Fichaut, M., Balopoulos, E., Iona, S., Dooley, H., Garcia, M., Manca, B., Giorgetti, A., Manzella, G., Michailov, N., Pinardi, N. and Zavatarelli, M.: The Western Mediterranean deep water: a proxy for climate change, Geophys. Res. Lett., 32, L12608, 2005, doi:10.1029/2005GL022702.

Robinson, A., Leslie, W., Theocharis, A. and Lascaratos, A.: Mediterranean Sea circulation, in Encyclopedia of Ocean Sciences, 3, 1689–1705, Elsevier, New York, 2001.

Rogers, J. C.: Atmospheric circulation changes associated with the warming over the northern North Atlantic in the 1920s. Journal of Climate and Applied Meteorology 24: 1303–1310, 1985.

Rogers, J. C.: Patterns of low-frequency monthly sea level pressure variability (1899–1986) and associated wave cyclone frequencies. J. Climate, 3, 1364–1379, 1990.

Romanou, A., Tselioudis, G., Zerefos, C., Clayson, C., Curry, J. and Andersson, A.: Evaporation-precipitation variability over the Mediterranean and the Black Seas from satellite and reanalysis estimates, J. Climate, 23, 5268–5287, 2010, DOI: 10.1175/2010JCLI3525.1.

Rosenzweig, C., et al. in Climate Change 2007: Impacts, adaptation and vulnerability (eds Parry, M. L. et al.) 79–131 (Cambridge Univ. Press, 2007).

Sáenz, J., Zubillaga, J. and Rodríguez-Puebla, C.: Interannual winter temperature variability in the north of the Iberian Peninsula. Clim Res 16(3):169–179, 2001.

Sarhan, T, Lafuente, J. G., Vargas, M., Vargas J. M. and Plaza, F.: Upwelling mechanisms in the northwestern Alboran Sea. Journal of Marine Systems, 23, 317–331, 2000.

Schott, F.et al. Observations of deep convection in the Gulf of Lions, Northern Mediterranean, during the winter of 1991/92. J. Phys. Oceanogr. 26, 505–524, 1996.

Schroeder, K., Josey, S., Herrmann, M., Grignon, L., Gasparini, G. and Bryden, H.: Abrupt warming and salting of the Western Mediterranean deep water after 2005: atmospheric forcing and lateral advection., J. Geophys. Res., 2010, doi:10.1029/2009JC005850.

Schwab, D. J. and Beletsky D.: Relative effects of wind-stress curl, topography, and stratification on large-scale circulation in Lake Michigan, J. Geophys. Res., 108(C2), 3044, 2003, doi: 10.1029/2001JC001066.

Shabrang, L., Menna, M., Pizzi, C., Lavigne, H., Civitarese, G. and Gačić, M.: Long-term variability of the Southern Adriatic circulation in relation to North Atlantic Oscillation. Ocean Sci., 12, 233–241, 2016, doi:10.5194/os-12-233-2016.

Skliris, N., Sofianos, S., Gkanasos, A., Mantziafou, A., Vervatis, V., Axaopoulos, P. and Lascaratos, A.: Decadal scale variability of sea surface temperature in the Mediterranean Sea in relation to atmospheric variability. Ocean Dyn. , 2011, http://dx.doi.org/10.1007/ s10236-011-0493-5.

Snedecor, G. W. and Cochran, W. G.: Statistical Methods, 7th Edn. Ames: Iowa State University Press, 1980.

Solomon, S., Qin, D., Manning, M., Alley, R. B., Berntsen, T., Bindoff, N. L., Chen, Z., Chidthaisong, A., Gregory, J. M., Hegerl, G. C., Heimann, M., Hewitson, B., Hoskins B. J., Joos, F., Jouzel, J., Kattsov, V., Lohmann, U., Matsuno, T., Molina, M., Nicholls, N., Overpeck, J., Raga, G., Ramaswamy, V., Ren, J., Rusticucci, M., Somerville, R., Stocker, T. F., Whetton, P., Wood, R. A. and Wratt, D.: Technical Summary. In: Climate Change 2007: The Physical Science Basis.

Contribution of Working Group I to the Fourth Assessment Report of the Intergovernmental Panel on Climate Change [Solomon, S., D. Qin, M. Manning, Z. Chen, M. Marquis, K.B. Averyt, M. Tignor and H.L. Miller (eds.)]. Cambridge University Press, Cambridge, United Kingdom and New York, NY, USA, 2007.

Suselj, K. and Bergant, K.: Mediterranean Oscillation Index, Geophysical Research Abstracts 8, 02145 European Geosciences Union, 2006.

Suselj, K., Tsimplis, M. N. and Bergant, K.: Is the Mediterranean Sea surface height variability predictable? Phys. Chem. Earth, 33, 225–238, 2008.

Tonani, M., Pinardi, N., Dobricic, S., Pujol, I. and Fratianni, C.: A high-resolution free-surface model of the Mediterranean Sea". Ocean Sci., 4, 1-14, 2008.

Toreti, A., Desiato, F., Fioravanti, G. and Perconti, W.: Seasonal temperatures over Italy and their relationship with low-frequency atmospheric circulation patterns, Clim. Change, 99, 211–227, 2010.

Trigo, R. M., Osborn, T. J. and Corte-Real, J. M.: The North Atlantic Oscillation influence on Europe: climate impacts and associated physical mechanisms, Clim. Res., 20, 9-17, 2002.

Trigo, R., M., Pozo-Vazquez, D., Osborn, T. J., Casrto-Diez, Y., Gamiz-Fortis, S. and Esteban-Parra, M., J.: North Atlantic Oscillation influence on precipitation, river flow and water resources in the Iberian peninsula. International Journal of Climatology, Vol. 24, No. 8, p. 925–944, 2004.

Trigo, R., Xoplaki, E., Zorita, E., Luterbacher, J., Krichak, S., Alpert, P., Jacobeit, J., Saenz, J., Fernandez, J., Gonzalez-Rouco, J.F., Garcia-Herrera, R., Rodo, X., Brunetti, M., Nanni, T., Maugeri, M., Turkes, M., Gimeno, L., Ribera, P., Brunet, M., Trigo, I., Crepon, M. and Mariotti A.: Relations between variability in the Mediterranean region and mid-latitude variability. In Lionello P., Malanotte-Rizzoli P. and Boscolo R. (eds): The Mediterranean climate: an overview of the main characteristics and issues. The Netherlands: Elsevier, pp. 179–226, 2006.

Tsimplis, M. N. and Josey, S., A.: Forcing of the Mediterranean Sea by atmospheric oscillations over the North Atlantic. Geophys Res Lett 28:803–806, 2001.

Tsimplis, M. N. and Rixen M.: Sea level in the Mediterranean Sea: The contribution of temperature and salinity changes, Geophys. Res. Lett., 29(23), 2136, 2002, doi:10.1029/2002GL015870.

Tsimplis, M., Zervakis, V., Josey, S. A., Peneva, E., Struglia, M.V., Stanev, E., Lionello, P., Malanotte-Rizzoli, P., Artale, V., Theocharis, A., Tragou, E. and Oguz, T.: Changes in the oceanography of the Mediterranean Sea and their link to climate variability. In, Lionello, P., Malanotte-Rizzoli, P. and Boscolo, R. (eds.) Mediterranean climate variability. Amsterdam, the Netherlands, Elsevier, 227-282, 2006. (Developments in Earth and Environmental Sciences 4).

Tsimplis, M. N. and Shaw, A. G. P.: The forcing of mean sea level variability around Europe. Global and Planetary Change, 63, (2-3), 196-202, 2008, doi:10.1016/j.gloplacha.2007.08.018.

Tsimplis, M. N. and Shaw, A. G. P.: Seasonal sea level extremes in the Mediterranean Sea and at the Atlantic European coasts, Nat. Hazards Earth Syst. Sci., 10, 1457-1475, doi:10.5194/nhess-10-1457-2010, 2010.

Tsimplis, M. N., Spada, G., Marcos, M. and Flemming, N.: Multi-decadal sea level trends and land movements in the Mediterranean Sea with estimates of factors perturbing tide gauge data and cumulative uncertainties, Global Planet. Change, 76, 63–76, 2011.

Tsimplis, M. N., Calafat, F. M., Marcos, M., Jordà, G., Gomis, D., Fenoglio-Marc, L., Struglia, M. V., Josey, S. A. and Chambers, D. P.: The effect of the NAO on sea level and on mass changes in the Mediterranean Sea, J. Geophys. Res. Oceans, 118, 944–952, 2013, doi:10.1002/jgrc.20078.

Türkeş, M. and Erlat, E.: Precipitation changes and variability in Turkey linked to the North Atlantic Oscillation during the period 1930-2000. International Journal of Climatology 23: 1771-1796, 2003.

Türkeş, M. and Erlat, E.: Winter mean temperature variability in Turkey associated with the North Atlantic Oscillation. Meteorology and Atmosphere Physics 105: 211-225, 2009.

Ulbrich, U, Christoph, M., Pinto, J. and Corte-Real, J.: Dependence of winter precipitation over Portugal on NAO and baroclinic wave activity. International Journal of Climatology 19: 379–390, 1999.

Van Loon, H. and Williams, J.: Connection between trends of mean temperature and circulation at surface. 1. Winter. Monthly Weather Reiews 104: 365–380, 1976.

Van Loon, H. and Rogers, J. C.: The Seesaw in Winter Temperatures between Greenland and Northern Europe. Part I: General Description', Mon. Wea. Rev. 106, 296–310, 1978.

Vargas-Yáñez, M., Ramírez, T., Cortés, D., Sebastián, M. and Plaza, F.: Warming trends in the continental shelf of Málaga Bay (Alborán Sea), Geophys. Res. Letters, 29(22), 2082, 2002, doi: 10.1029/2002GL015306.

Vignudelli, S., Gasparini, G. P., Schiano M. E. and Astraldi M.: A possible influence of the North Atlantic Oscillation on the western Mediterranean circulation, Geophys. Res. Lett., 26, 623 – 626, 1999.

Vilibić, I. and Orlić, M.: Least-squares tracer analysis of water masses in the South Adriatic (1967–1990), Deep-Sea Res. I, 48, 2297-2330, 2001.

Wallace, J. M. and Gutzler, D. S.: Teleconnections in the geopotential height field during the Northern Hemisphere winter, Mon. Wea. Rev., 109, 784-812, 1981.

Wallace, J. M., Zhang, Y. and Renwick, J. A.: Dynamic contribution to hemispheric mean temperature trends. Science, 270, 780-783, 1995.

Woollings, T. J., Hannachi, A., Hoskins. B. J. and Turner, A.: A regime view of the North Atlantic Oscillation and its response to anthropogenic forcing. J. Climate, 23, 1291–1307, 2010.

Xoplaki, E.: Climate variability over the Mediterranean. PhD thesis, University of Bern, Switzerland, 2002, Available through: http://sinus.unibe.ch/klimet/docs/phd_xoplaki.pdf

Yan, H., Zhong, M., Zhu, Y.: Determination of the degree of freedom of digital filtered time series with an application to the correlation analysis between the length of day and the Southern Oscillation Index. Chin. Astron. Astrophy. 28 (1), 120–126, 2004.

Yelland, M. and Taylor P. K.: Wind-stress measurements from the open ocean, J. Phys. Oceanogr. 26, 541-558, 1996.

Zervakis, V., Georgopoulos, D., Karageorgis, A. P. and Theocharis, A.: On the response of the Aegean Sea to climatic variability: A review. Int. J. Climatol., 24, 1845–1858, 2004, doi:10.1002/joc.1108.